Convergent margins processes

E. Burov

University of Pierre et Marie Curie

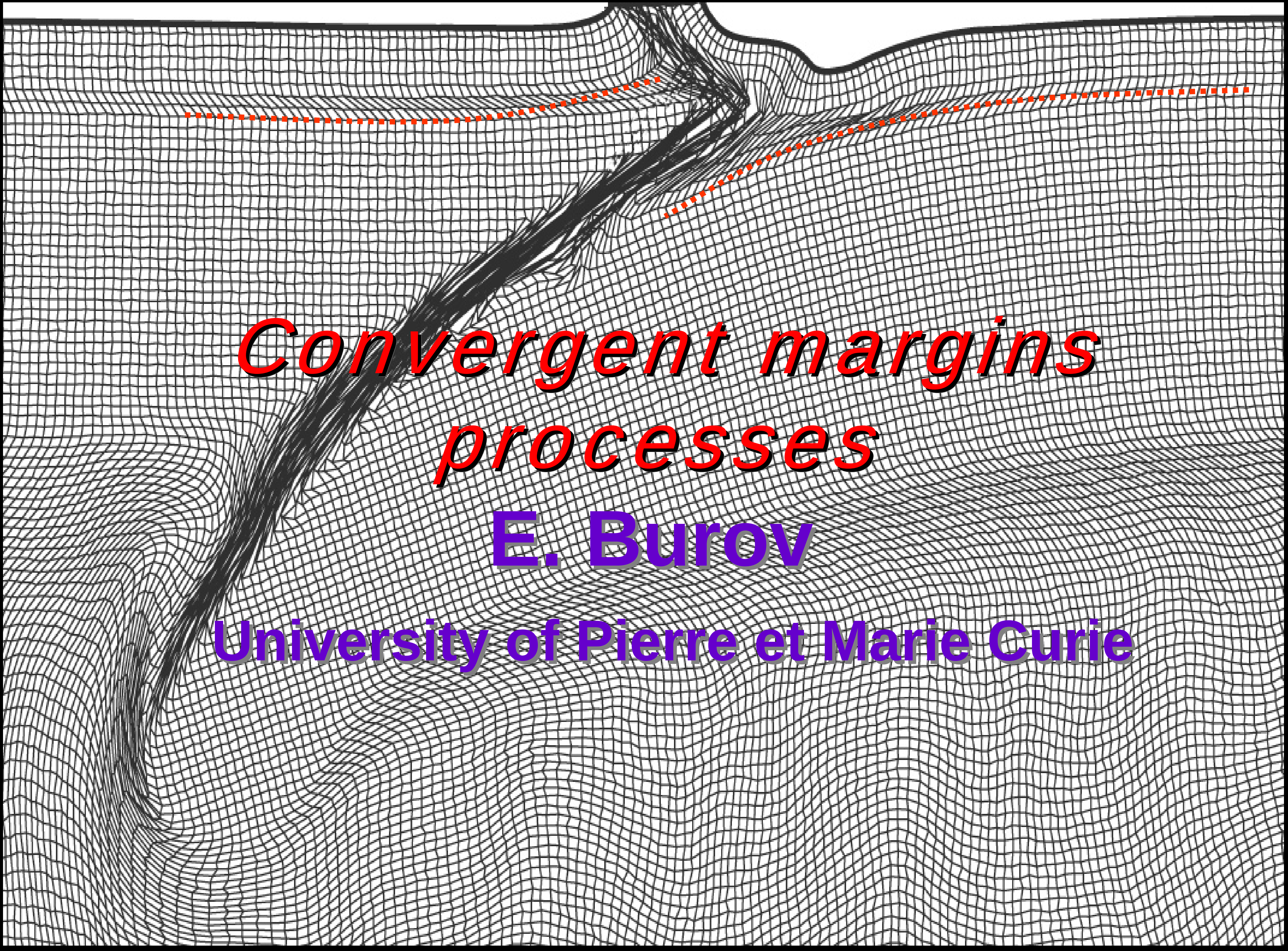

four possible collision modes

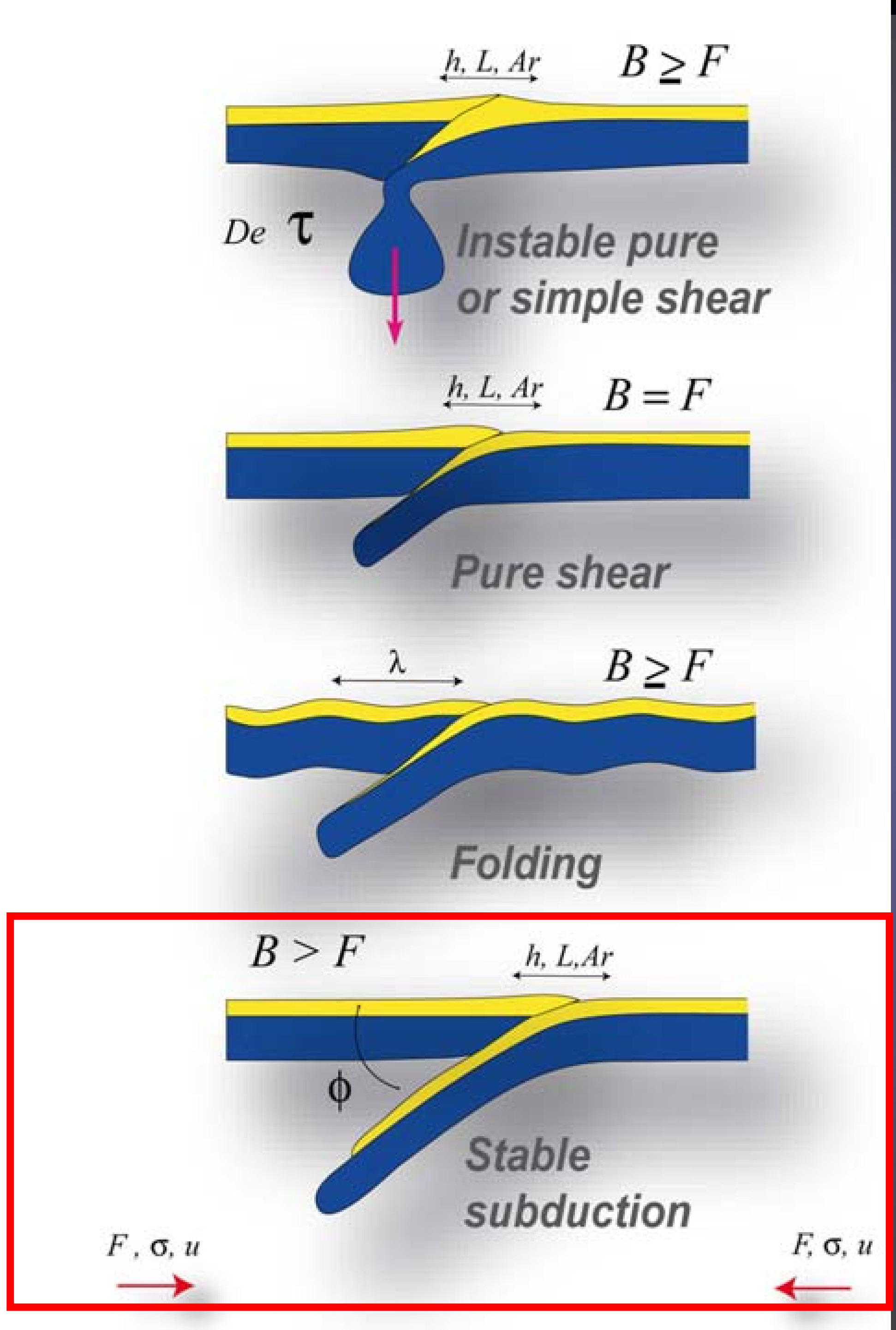

important controlling parameters of subduction

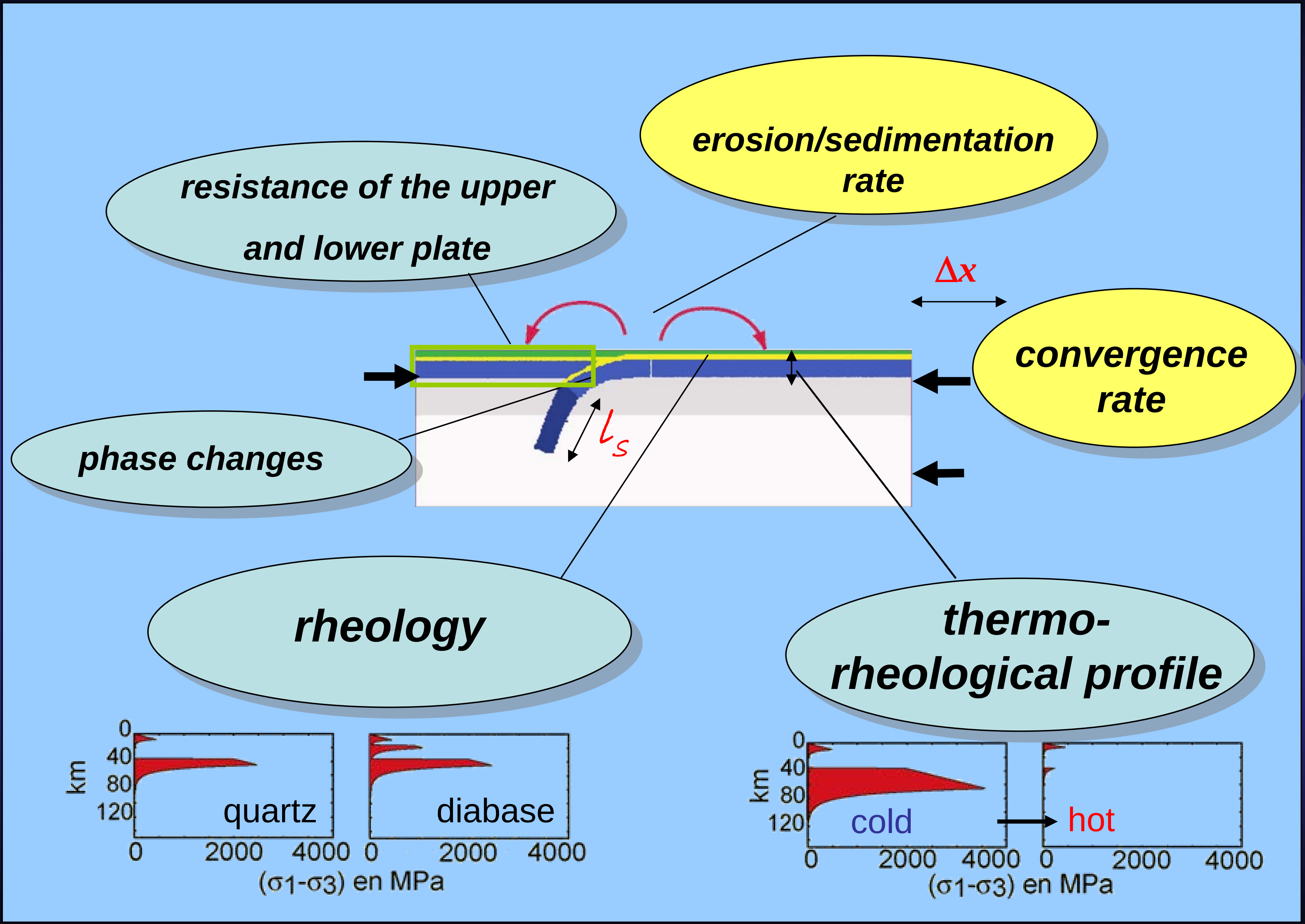

SUBDUCTION NUMBER:

$$S = \frac{\Delta x}{l_s}$$

(subduction length)

SUBDUCTION FEASIBILITY:

Peclet number >> 1

$$Pe = \frac{\text{advection rate}}{\text{diffusion rate}}$$

Numerical method

FLAMAR-PARA(O)VOZ

⇨ $$\rho g_i + \frac{\partial \sigma_{ij}}{\partial x_j} = \rho \frac{\partial V_i}{\partial t}$$

Newton's 2nd law of motion

⇨ $$\frac{DT}{Dt} = \frac{\partial}{\partial x_i}\left(\chi \frac{\partial T}{\partial x_i}\right) + \frac{H_r}{\rho\, C_p} - V_i \frac{\partial T}{\partial x_i}$$

Heat Diffusion, Production, Advection

⇨ $$\frac{D\sigma}{Dt} = F\left(\sigma, \mathbf{u}, \mathbf{V}, \nabla\mathbf{V}, \ldots, T, \ldots\right)$$

Constitutive laws

⇨ $$\rho = f\left(P, T\right)$$ ⇨ $$\partial h_s/\partial t - \nabla(k_e\, (\nabla h)^m\, \nabla h_s) = 0$$

Additional laws

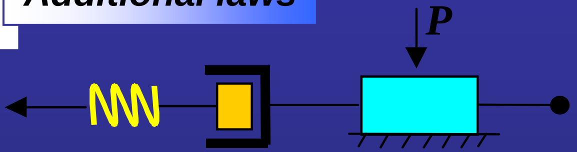

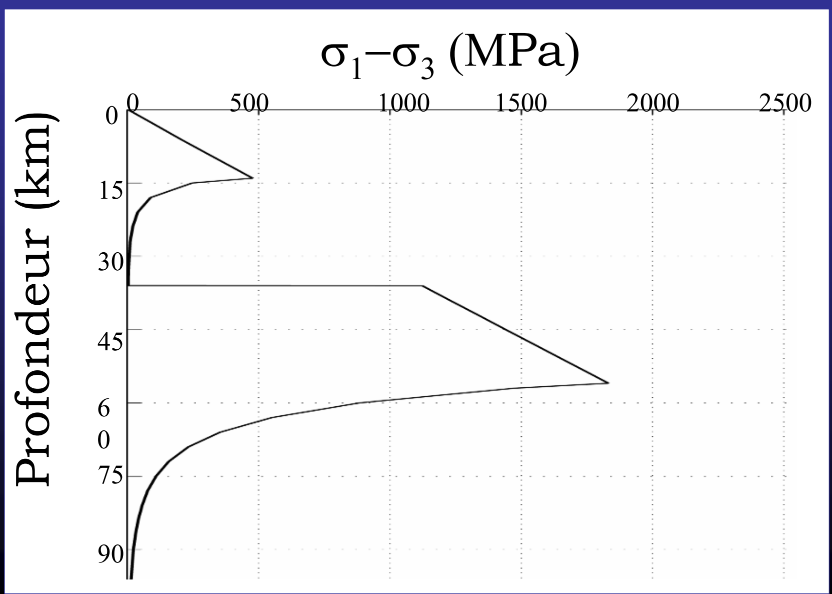

Viscous $$\dot{\varepsilon} = A\ \exp\left(-\frac{E}{RT}\right)\sigma^n$$

Elastic $$\sigma_{ij} = \lambda\, \delta_{ij} \sum_k \varepsilon_{kk} + 2\mu\varepsilon_{ij}$$

Plastic $$\tau = (\tan\varphi)\,\sigma_n + C_0$$

Gaussian difference equations for polygonal elements (Malvern, 1969)

$$\int_s n_i \, f \, ds = \int_A \frac{\partial f}{\partial x_i} \, dA$$

where $\int_s$ is the integral around the boundary of a closed surface;

n_i is the unit normal to the surface, s;

f is a scalar, vector or tensor;

x_i are position vectors;

ds is an incremental arc length; and

$\int_A$ is the integral over the surface area,

The grid

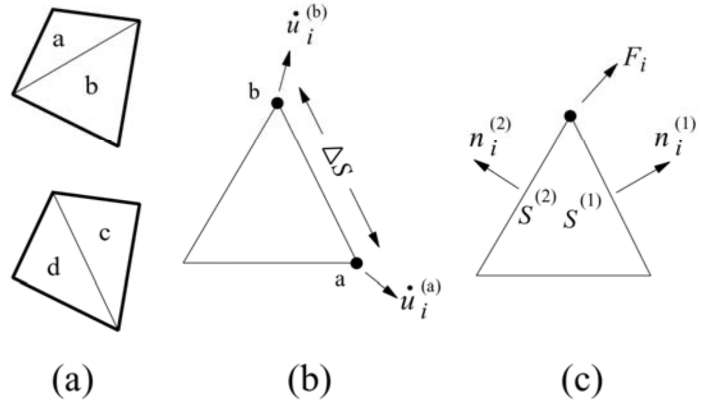

$$< \frac{\partial f}{\partial x_i} > = \frac{1}{A} \int_A \frac{\partial f}{\partial x_i} \, dA$$

$$< \frac{\partial f}{\partial x_i} > = \frac{1}{A} \int_S n_i \, f \, ds$$

Strain – stress – force – velocity increments

$$\Delta\varepsilon_{ij}^{(e)} = \frac{1}{2}\left(\frac{\partial v_i^{(e)}}{\partial x_j} + \frac{\partial v_j^{(e)}}{\partial x_i}\right)\Delta t$$

$$\frac{\partial v_i^{(e)}}{\partial x_1} = \sum_{k=1}^{3} v_i^{(k)} \cdot \beta_k, \qquad \frac{\partial v_i^{(e)}}{\partial x_2} = \sum_{k=1}^{3} v_i^{(k)} \cdot \gamma_k.$$

$$\sigma_{ij}^{(e)} = M(\sigma_{ij}^{(e)}, \Delta e_{ij}^{(e)}, S_i)$$

$$F_i^{(n)} = -\sum \frac{1}{2}\sigma_{ij}^{(e)}(n_j^{(1)}\Delta l^{(1)} + n_j^{(2)}\Delta l^{(2)})$$

$$v_i^{(n)}(t+\Delta t) = v_i^{(n)}(t) + [F_i^{(n)} - \alpha|F_i^{(n)}|sign(v_i)]\frac{\Delta t}{m_{inert}}$$

The damping term

$$dt_{crit} = min\left(\frac{\Delta x}{\sqrt{K/\rho_{inert}}}, \frac{\eta}{G}\right)$$

$$Re = \frac{\rho_{inert} V L}{\eta}$$

Large strain formulation (Jaumann's correction)

$$\sigma_{ij} := \sigma_{ij} + (\omega_{ik}\sigma_{kj} - \sigma_{ik}\omega_{kj})\,\Delta t$$

where

$$\omega_{ij} = \frac{1}{2}\left\{\frac{\partial \dot{u}_i}{\partial x_j} - \frac{\partial \dot{u}_j}{\partial x_i}\right\}$$

Extended Maxwell solid

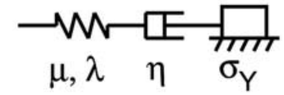

Kelvin solid

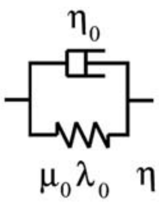

$$\left.\begin{aligned} \bar{e} &= \dot{\varepsilon}_{ii}/3 \\ e_{ij} &= \dot{\varepsilon}_{ij} - \delta_{ij}\bar{e} \\ \bar{\sigma} &= \sigma_{ii}/3 \\ \tau_{ij} &= \sigma_{ij} - \delta_{ij}\bar{\sigma} \end{aligned}\right\}$$

Burgers' solid

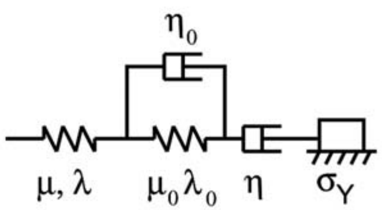

$$\left\{\begin{aligned} & \varepsilon^{\mathrm{elas}} + \varepsilon^{\mathrm{vis}} + \varepsilon^{\mathrm{plast}} - \varepsilon = 0 \\ & e^{\mathrm{elas}} = \dot{\tau}/2G \quad \textit{elastic part} \\ & e^{\mathrm{vis}} = \tau/2\eta \quad \textit{viscous part} \\ & \left.\begin{aligned} & F = \tau^* + \sin\phi\sigma^* - \cos\phi Co \\ & \tau^* = \sqrt{(\tau_{11} - \tau_{22})^2/4 + \tau_{12}{}^2} \\ & \sigma^* = (\sigma_{11} + \sigma_{22})/2 = (\tau_{11} + \tau_{22})/2 + \bar{\sigma} \\ & \frac{F(\lambda) - F^{old}}{dt} = 0 \\ & Q = \tau^* + \sin\psi\sigma^* \\ & \dot{\bar{\sigma}} = 3K(\bar{e} - \lambda\sin\psi/3) \\ & \dot{\varepsilon}_{ij}^{plas} = \lambda\frac{\partial Q}{\partial\sigma_{ij}} \end{aligned}\right\} \textit{plastic part} \end{aligned}\right\}$$

Continental Lithosphere: THICK MULTI-LAYER with EVP rheology

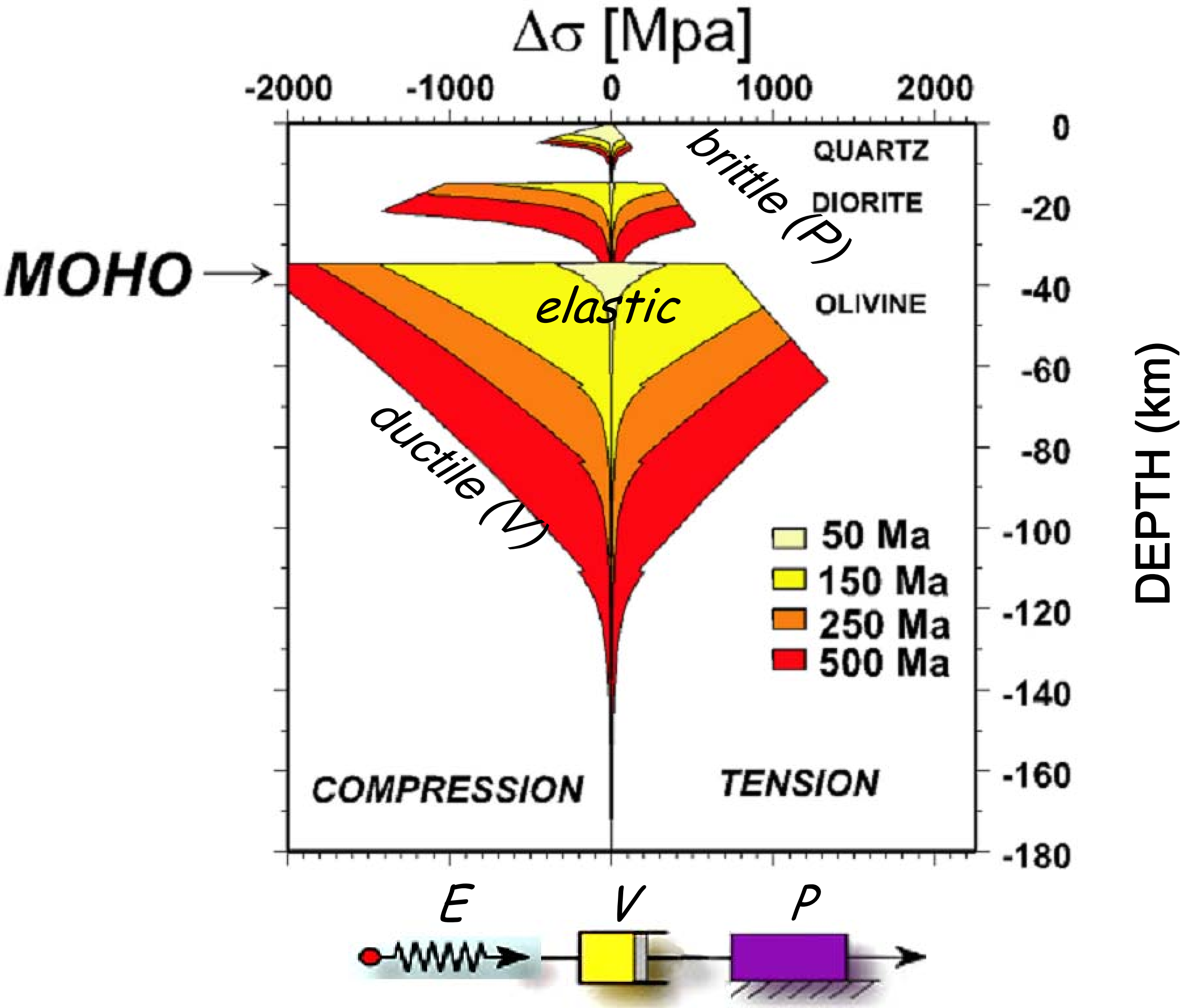

- Erosion – sedimentation
- Progressive phase changes

  Thermodynamic processes
  (THERIAK ; PERPLEX)

$$\rho = f\left(P,T\right) \quad \longrightarrow \quad G = \sum_{i=1}^{n} \mu_i N_i$$

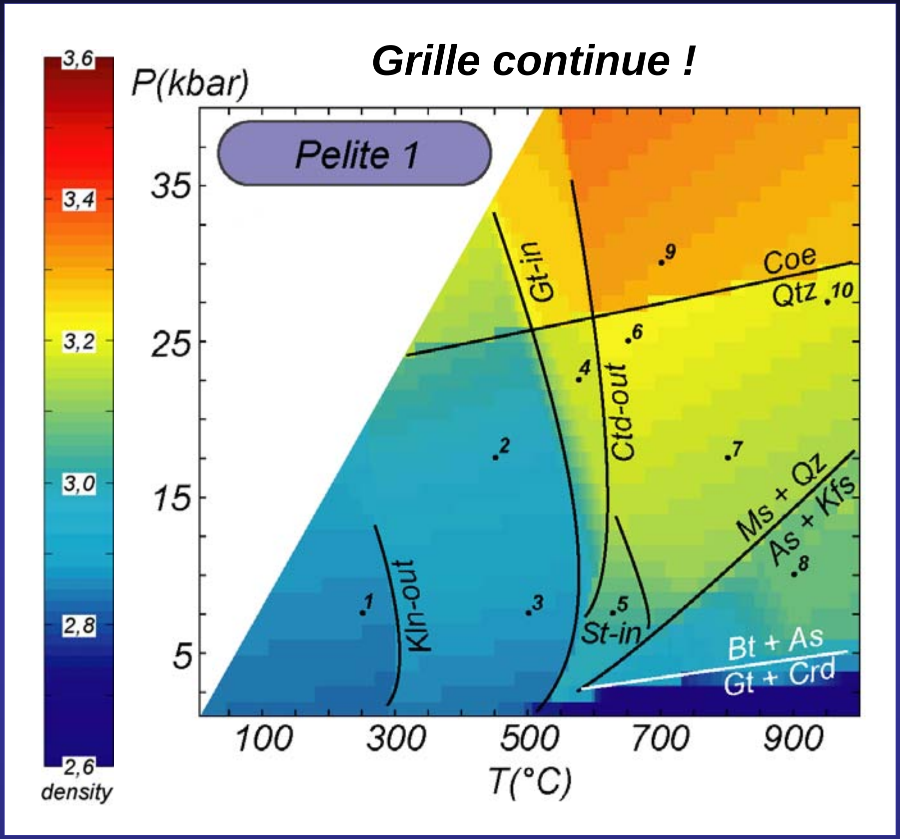

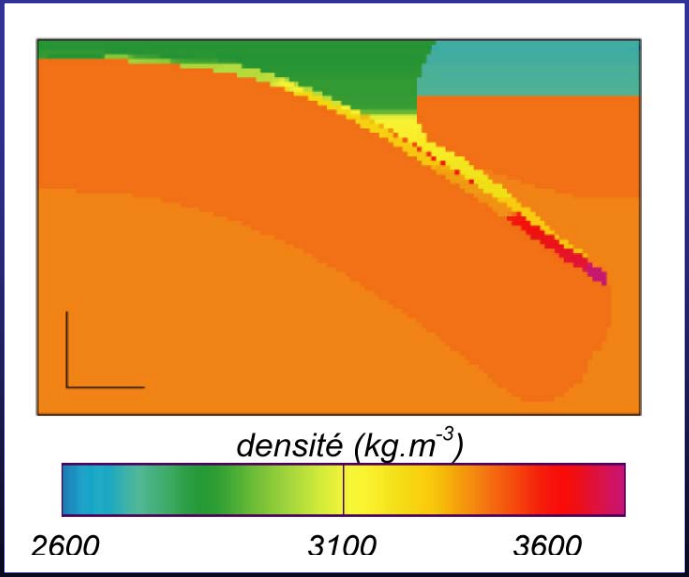

$$\partial h_s / \partial t - \nabla\left(k_e\, (\nabla h)^m\, \nabla h_s\right) = 0$$

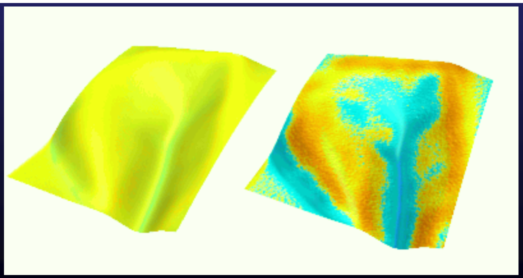

density versus P-T for the mantle part

PerpleX (G. Connolly) data base

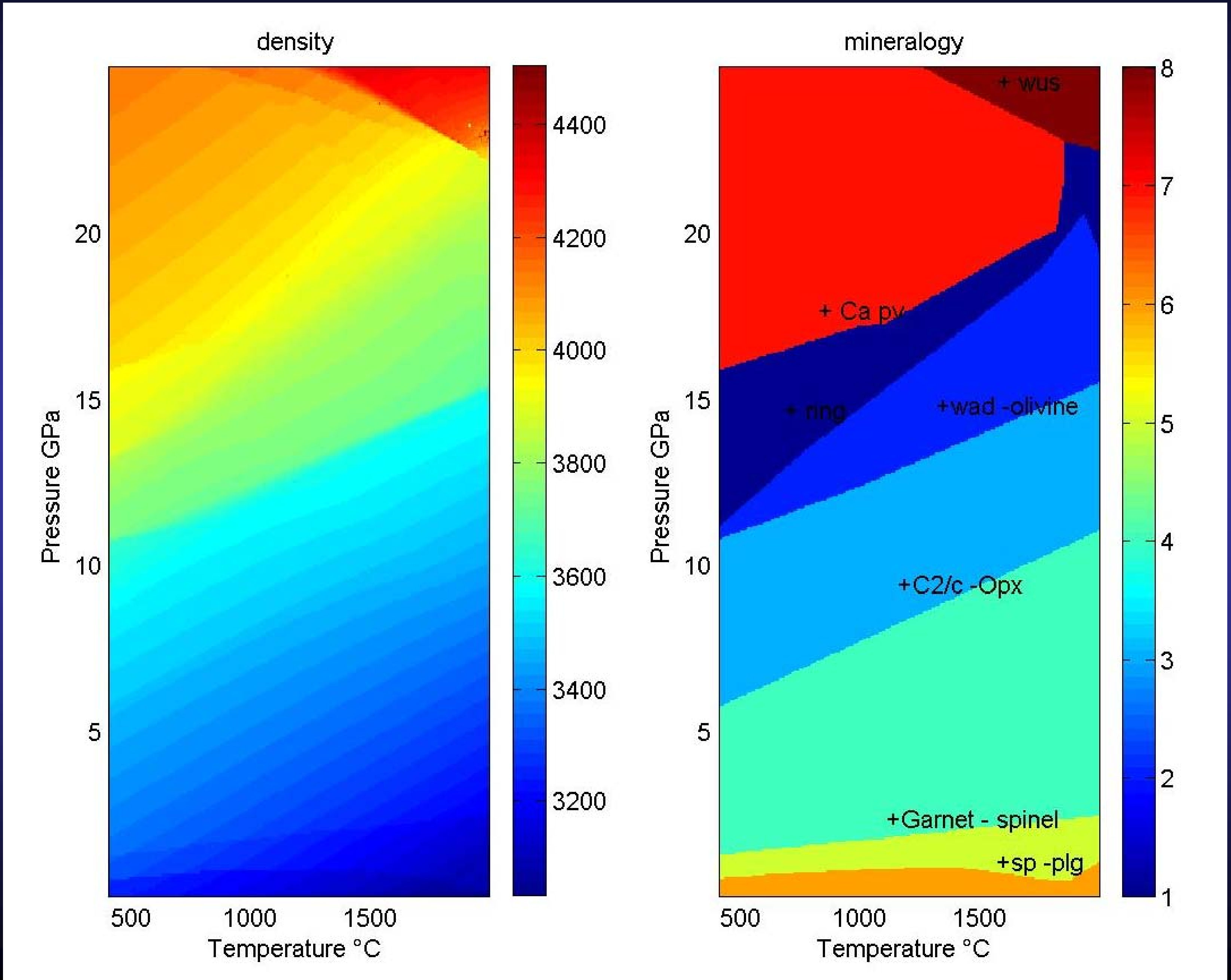

Predicted seismic velocities (m/s)

Vp Vs

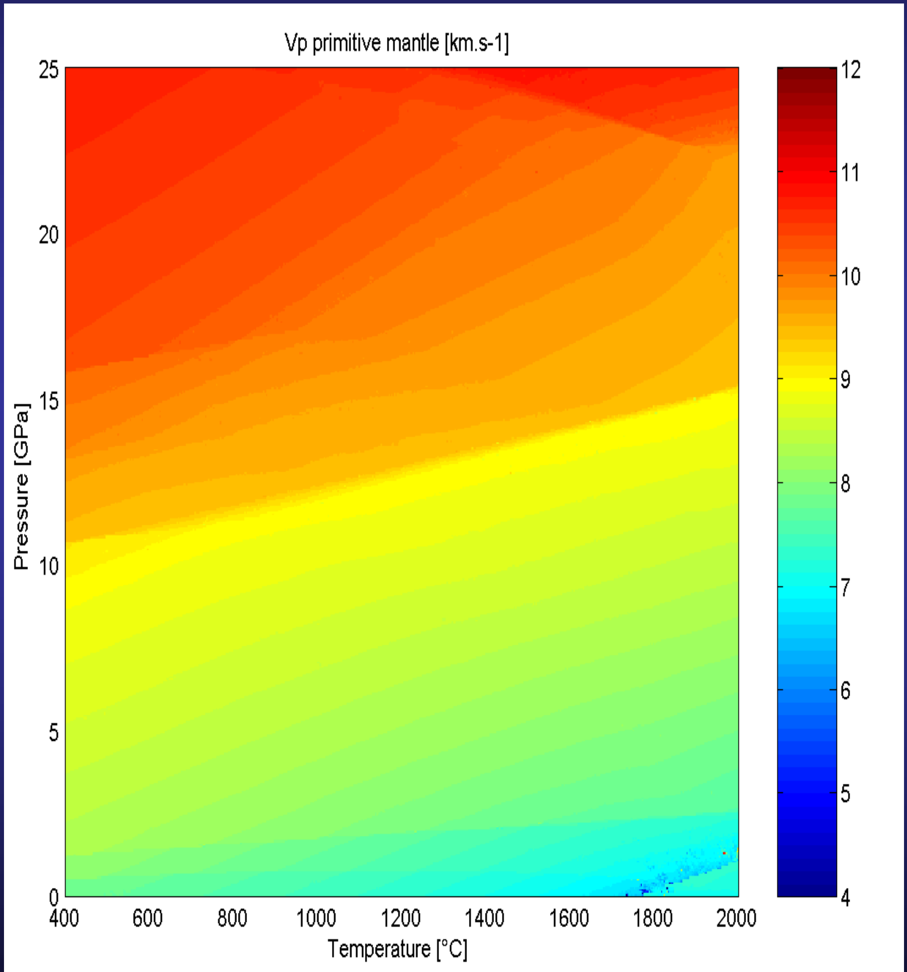

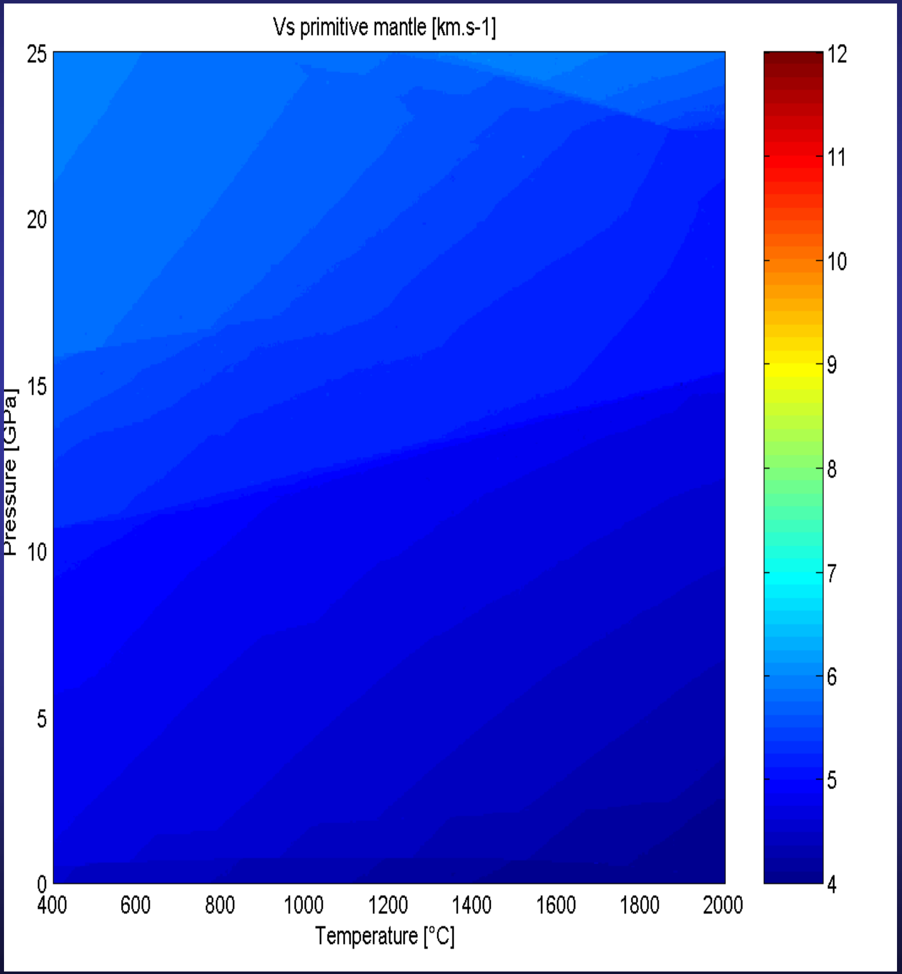

Summary of the numerical method

- *Large strain/transformations*
- *viscous-elastic-plastic rheology:*
  - *Non-associated Mohr-Coulomb law*
  - *Softening-hardening*
  - *Non-linear ductile creep*
- *Thermo-mechanical coupling*
  - *Latent heat sources*
  - *Radiogenic sources*
  - *Frictional dissipation*
- *Thermodynamic coupling*
- *Coupling with surface processes*
- *Free surface as upper boundary condition*
- *Dynamic particle-in-cell remeshing*
- *Inertial mode is possible*

Typical initial setup

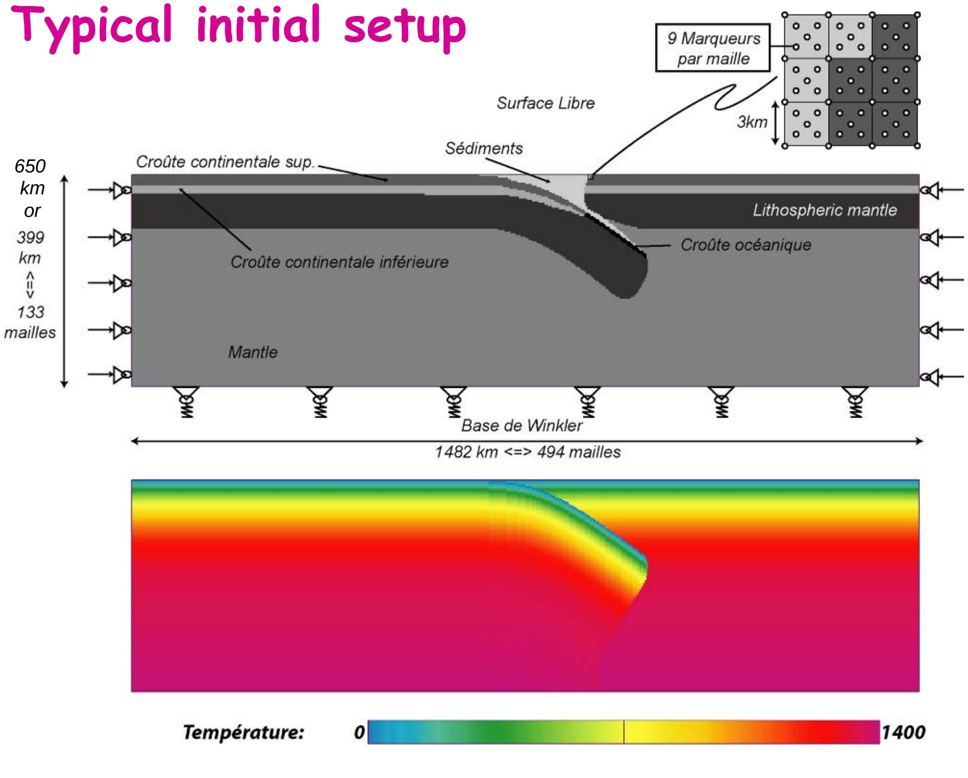

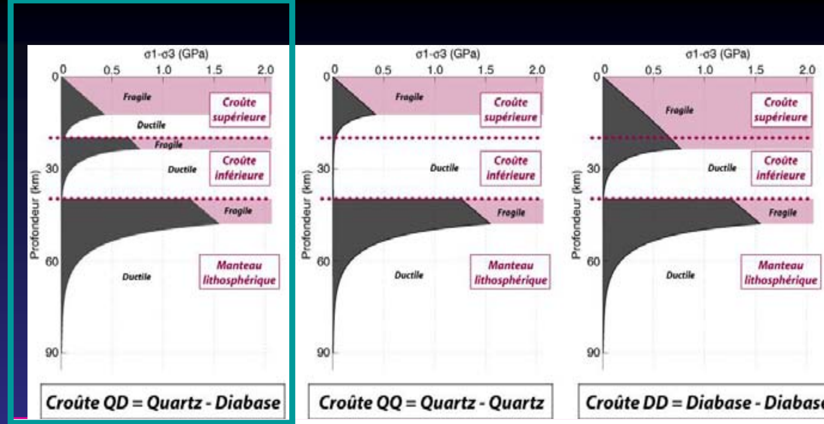

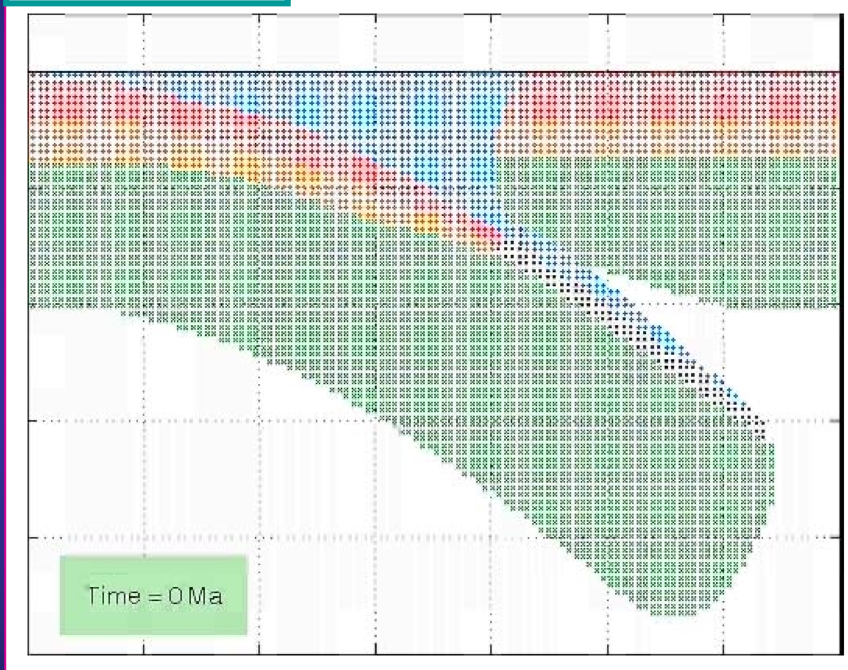

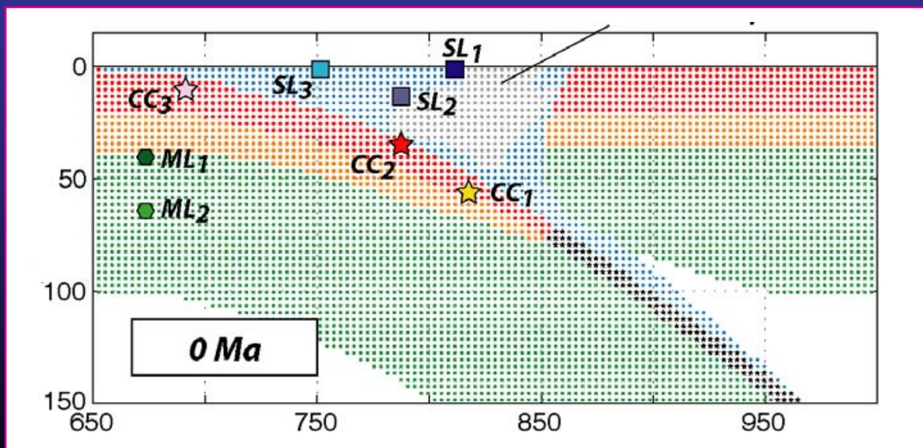

Reference experiment

Collision/Subduction experiments:

1. Influence of the convergence rate

Dependence on shortening rate. Snapshot at Δx = 180 km

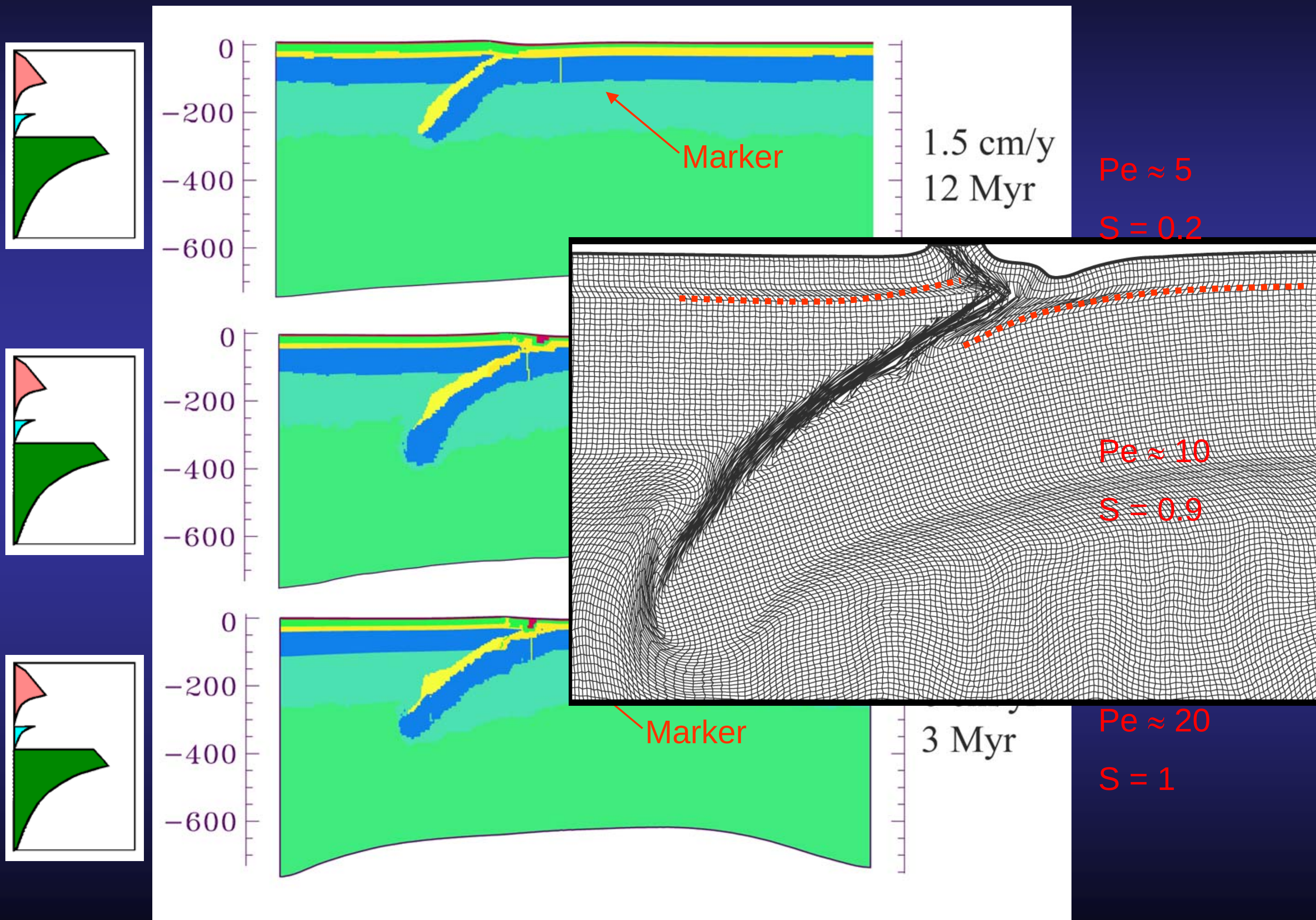

2. Influence of thermo-rheological profile

10 Myr

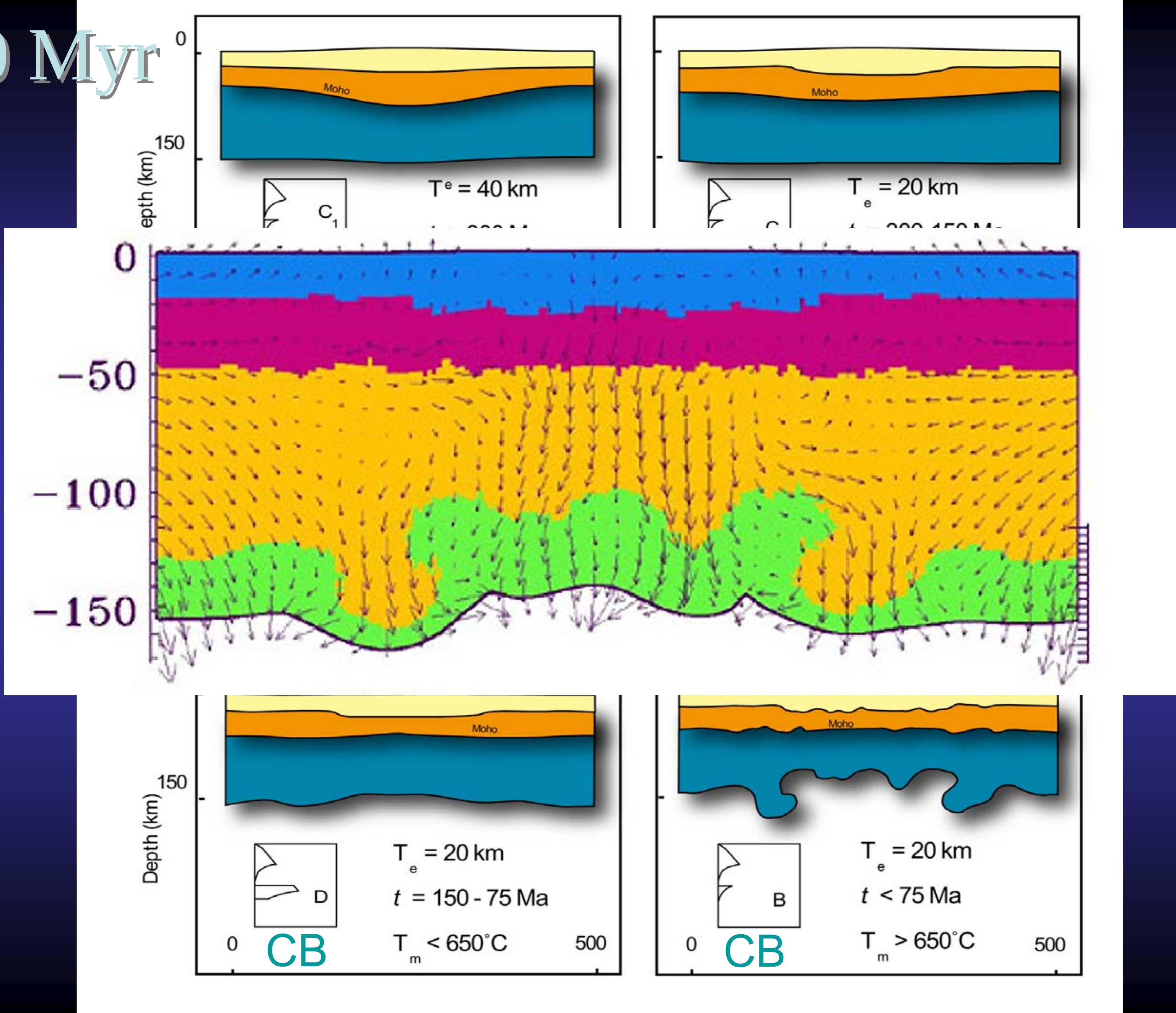

0
150
Depth (km)
Moho
Te = 40 km
C1
Te = 20 km
0
−50
−100
−150
Moho
Moho
150
Depth (km)
D
Te = 20 km
t = 150 - 75 Ma
Tm < 650˚C
0
500
CB
B
Te = 20 km
t < 75 Ma
Tm > 650˚C
0
500
CB

Influence of thermo-rheological age – A1: CREME – BRULEE RHEOLOGY (SOFT)

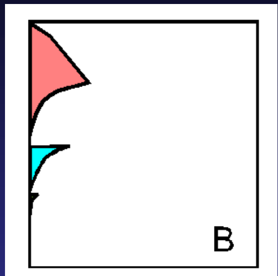

S < 0.1

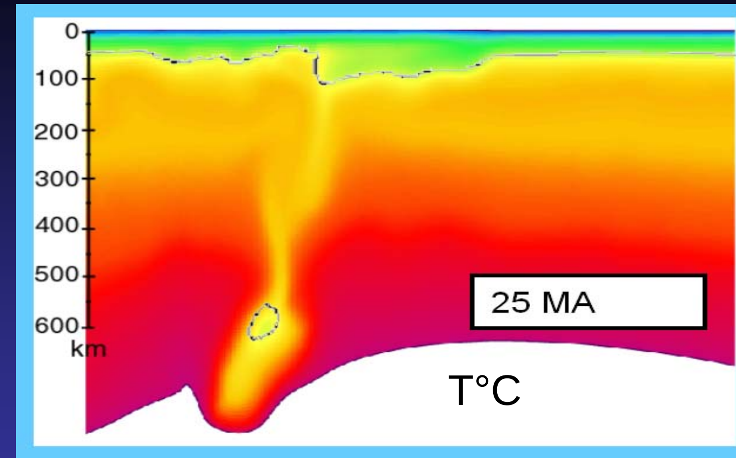

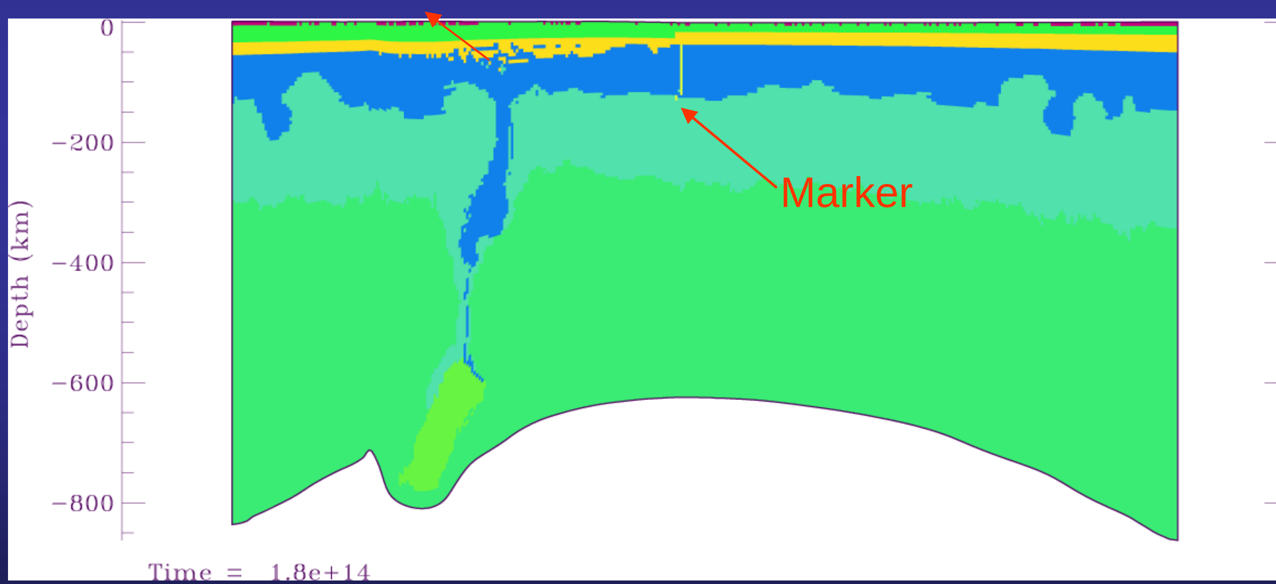

Thermal age of 25 Ma Tm = 850°C, *dx* = 330 km, *t* = 5,5 Ma, 2x3 cm/yr

wait …

Example: Pannonian Basin / Carpathians

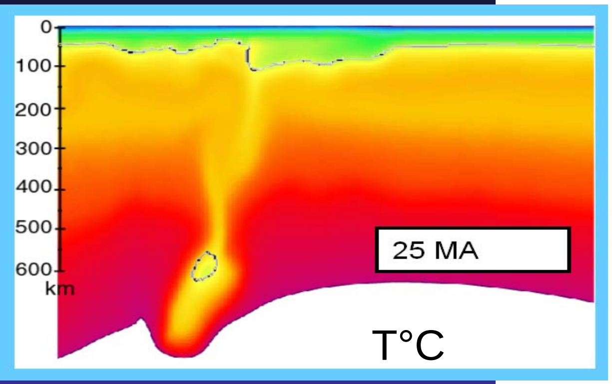

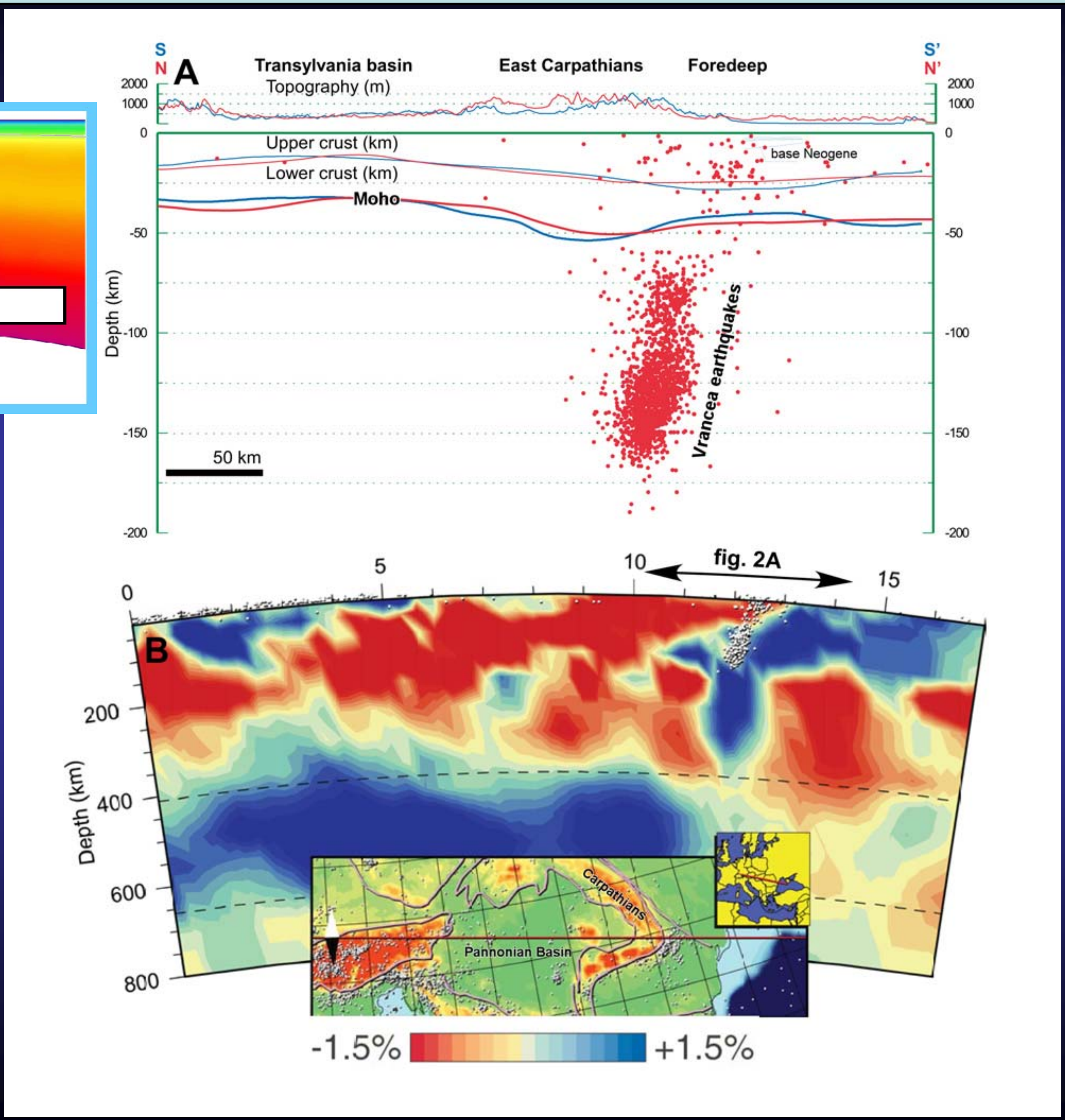

Burov et al, 2007

Figure: *Spakman*

Influence of thermo-rheological age – A2 JELLY SANDWICH (MIDIUM)

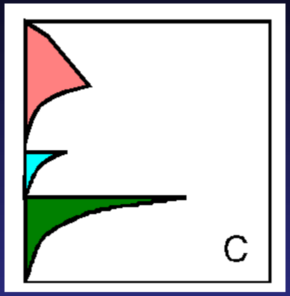

S < 0.3

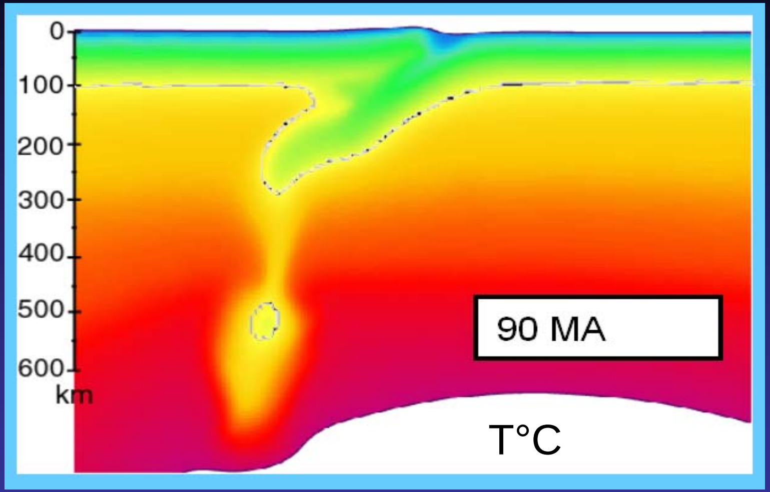

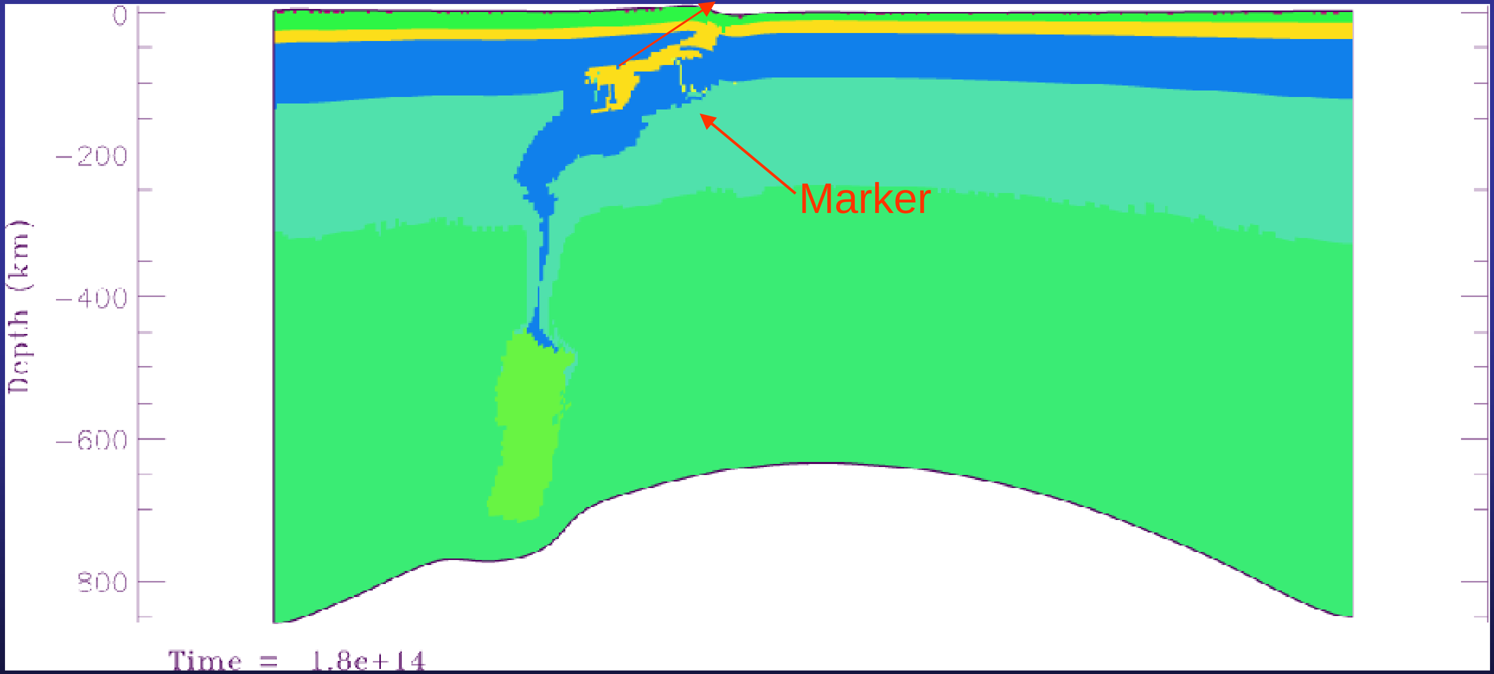

Thermal age of 90 MA, Tm =600°C, *dx* = 330 km, *t* = 5,5 Ma, 2x3 cm/yr

wait …

Influence of thermo-rheological age – B1 JELLY SANDWICH RHEOLOGY

S ~ 0.7

T°C

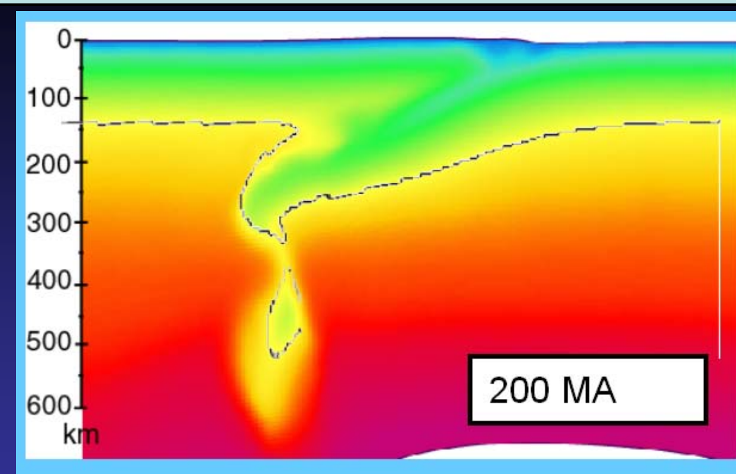

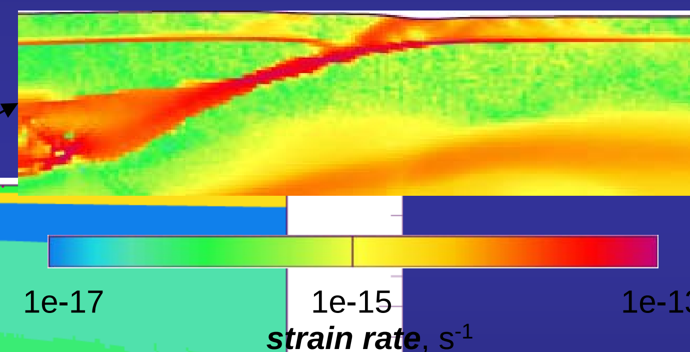

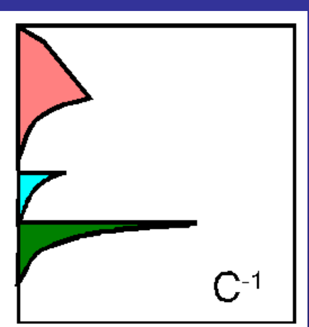

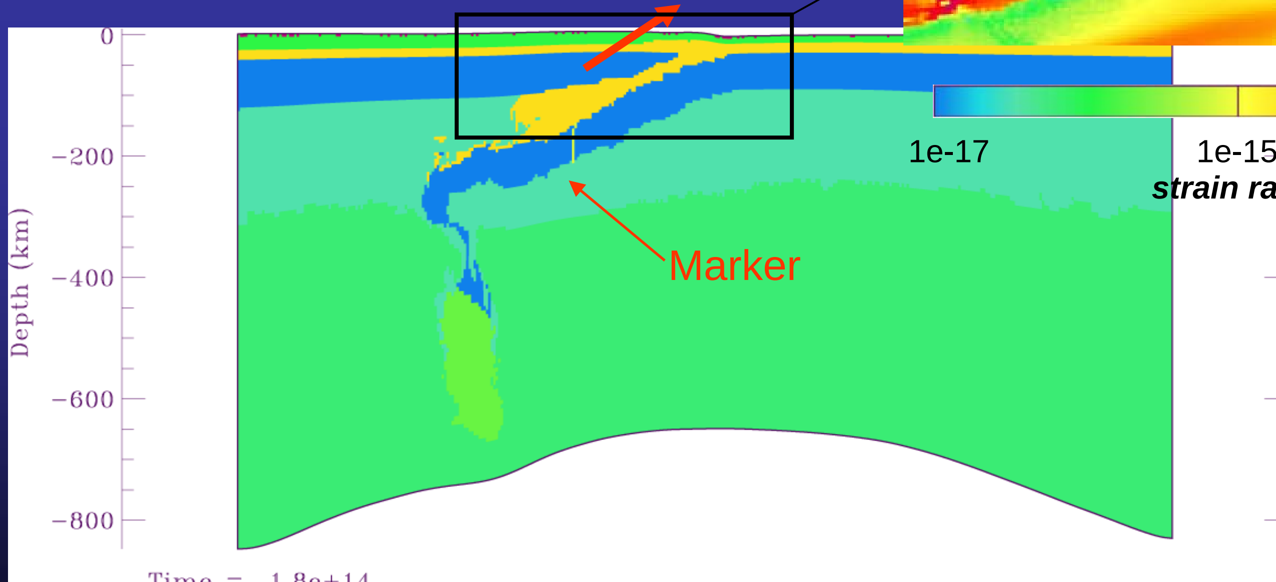

Thermal age of 200MA, Tm =500°C, *dx* = 330 km, *t* = 5,5 Ma, 2x3 cm/yr

wait …

P-T-t PATHS VIA PASSIVE MARKERS

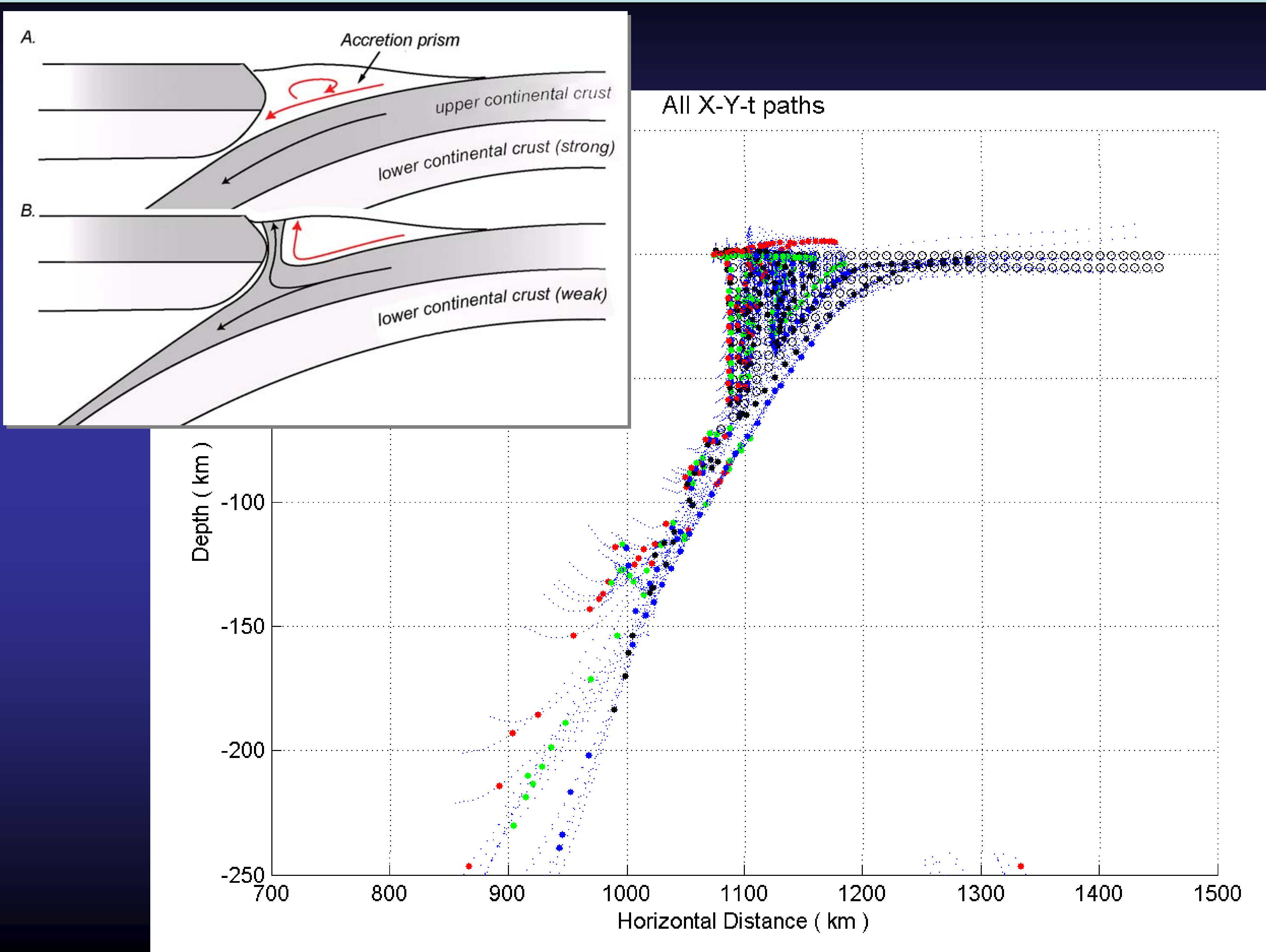

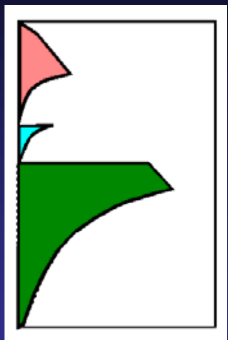

S ~ 1.

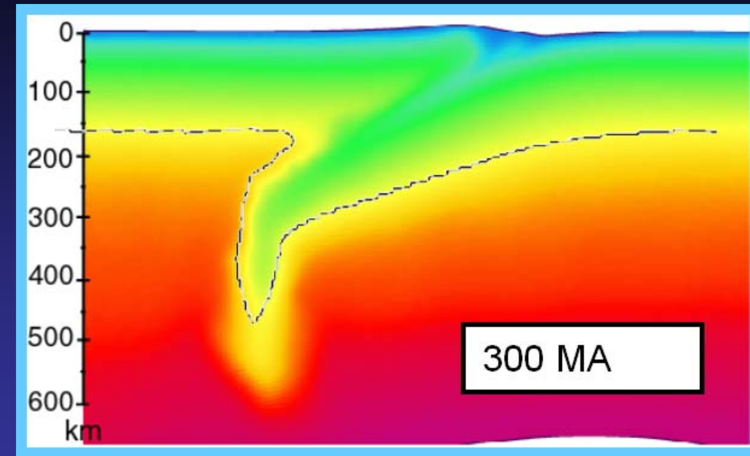

T°C

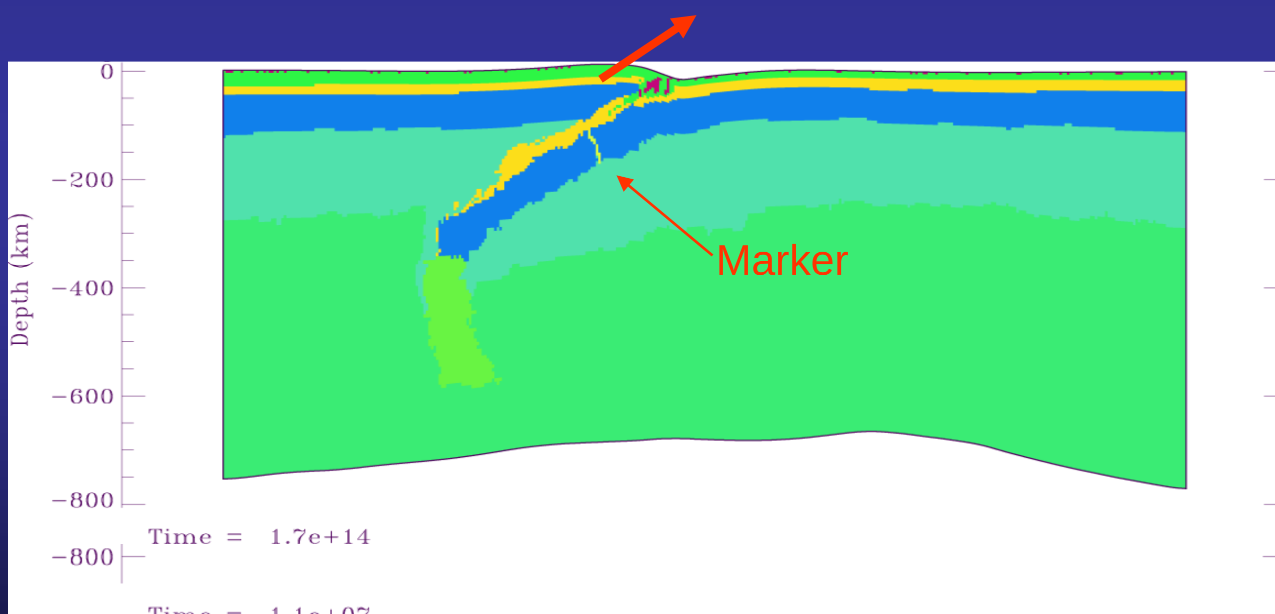

Thermal age of 300MA, Tm =450°C, *dx* = 330 km, *t* = 5,5 Ma, 2x3 cm/yr

wait …

STRONG (Te > 60 km) lithosphere, FAST collision (India-Asia > 5 cm/y)

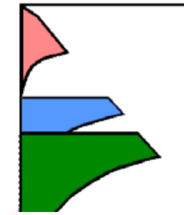

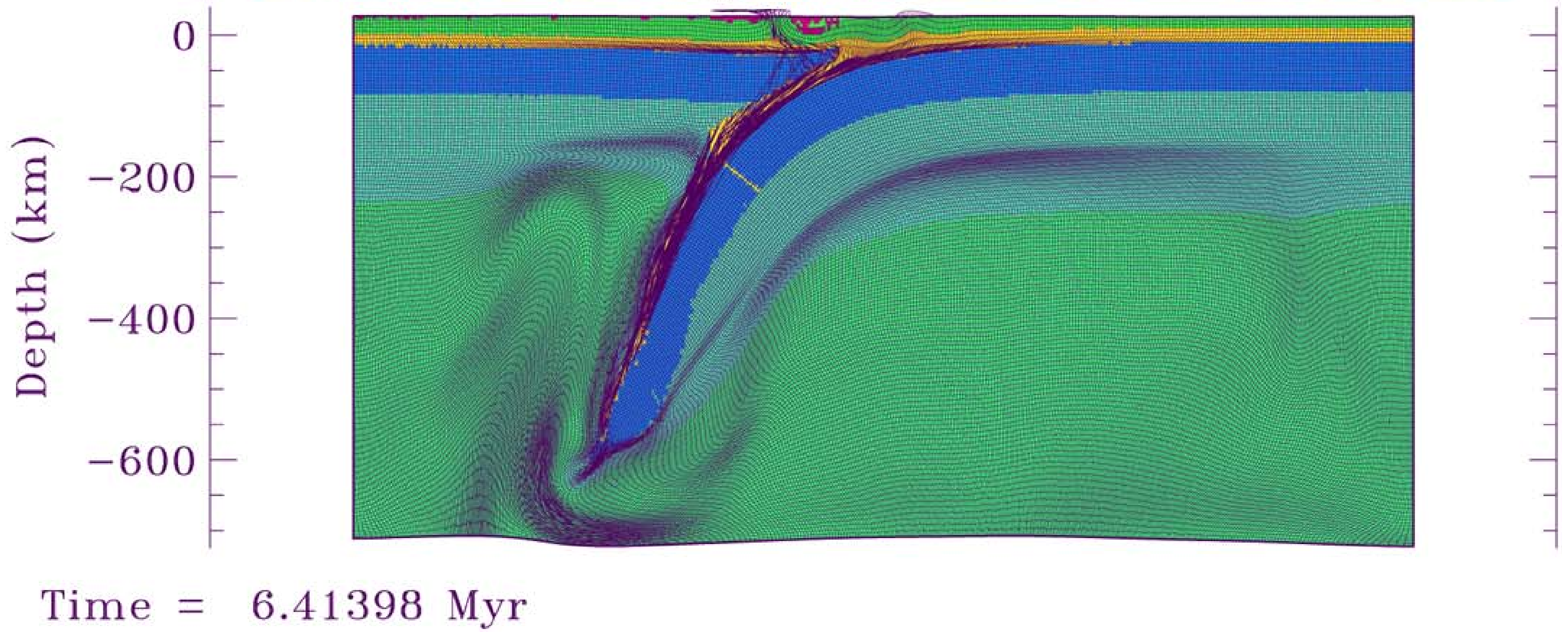

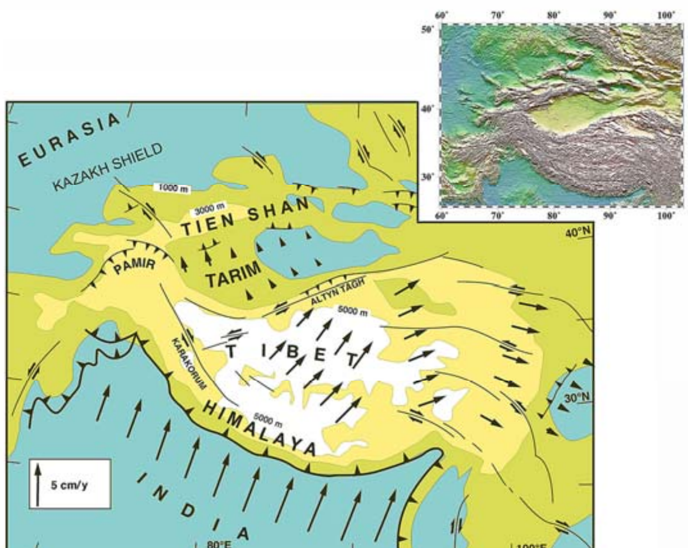

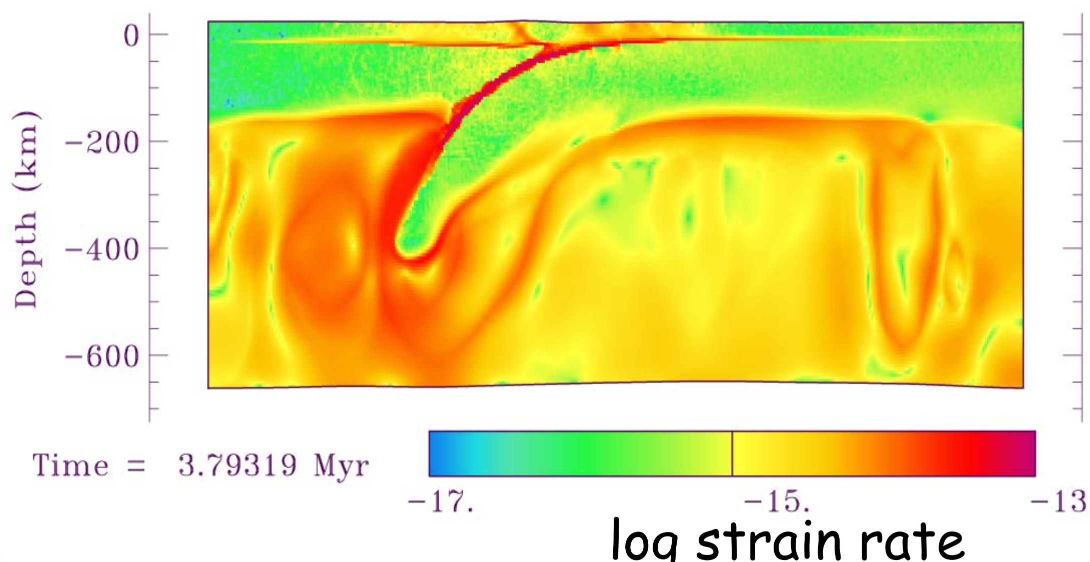

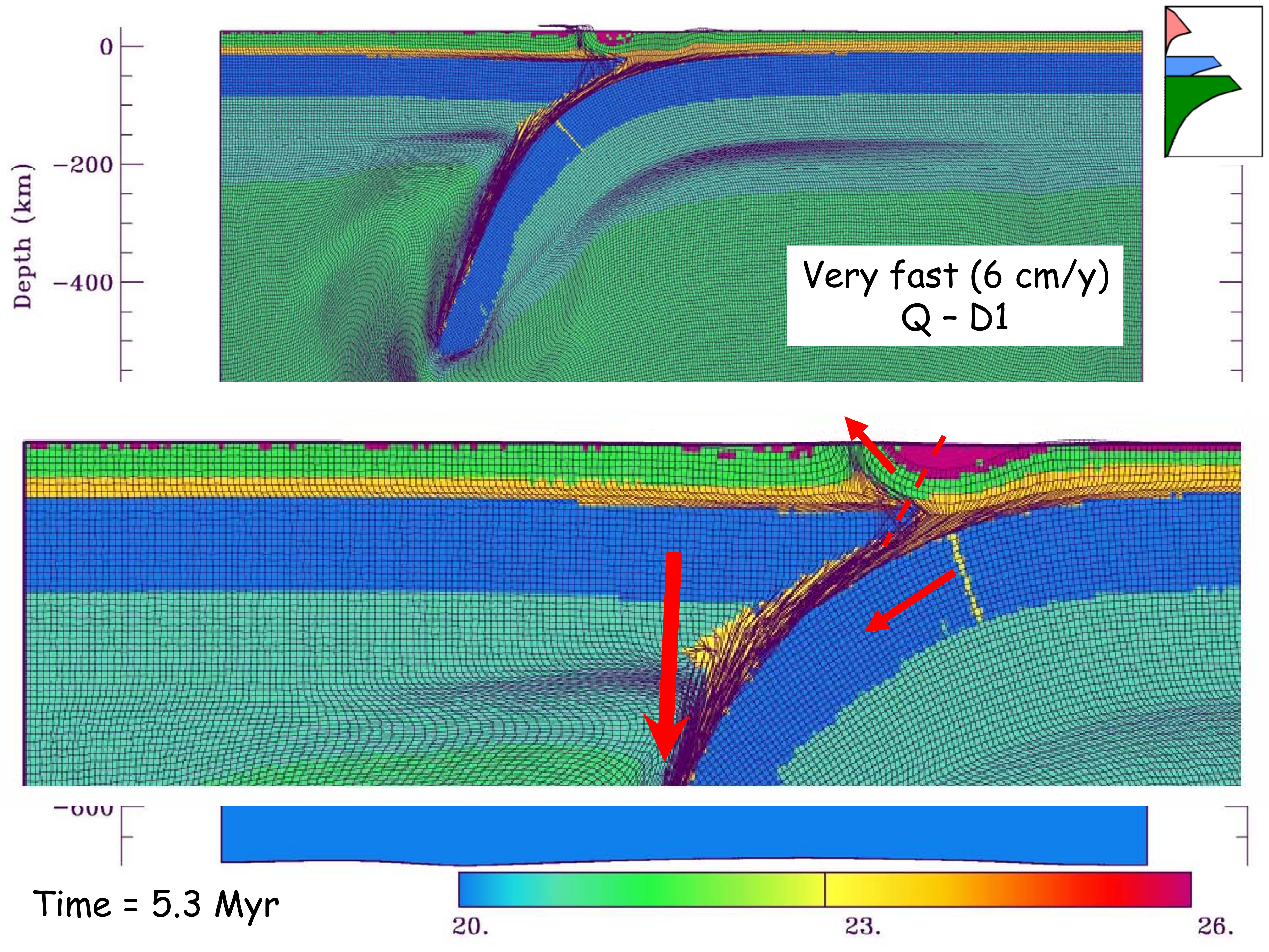

Depth (km)
0
−200
−400
−600
Very fast (6 cm/y)
Q - D1
Time = 5.3 Myr
20.
23.
26.

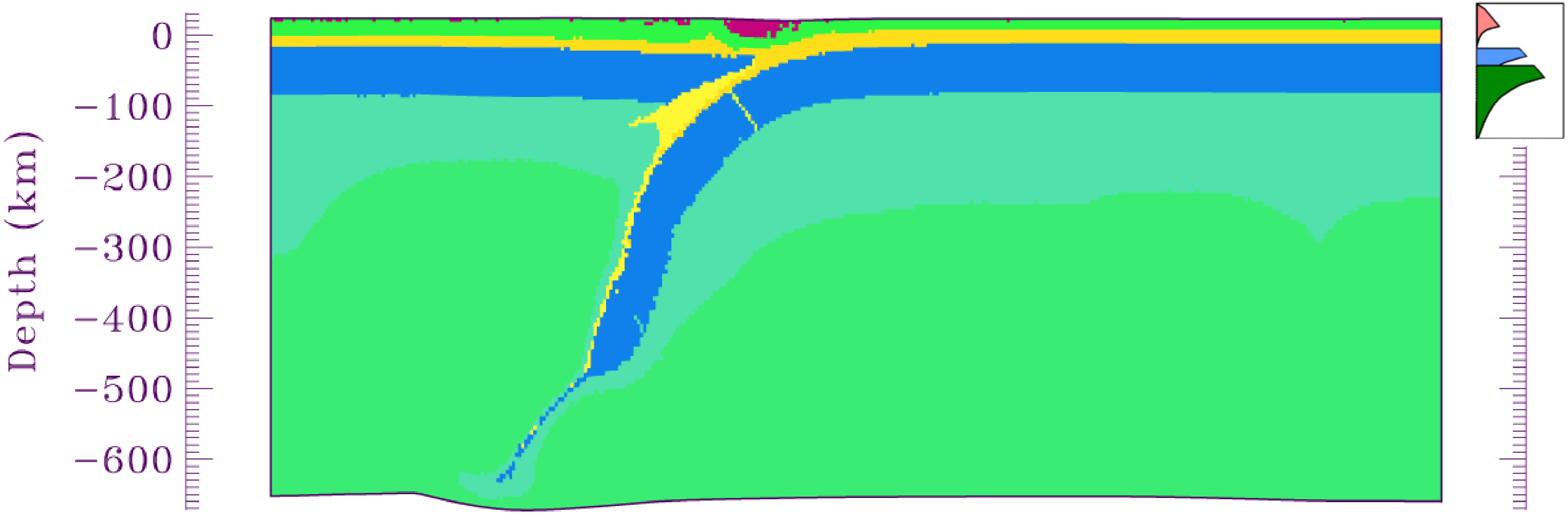

Time = 7.63 Myr

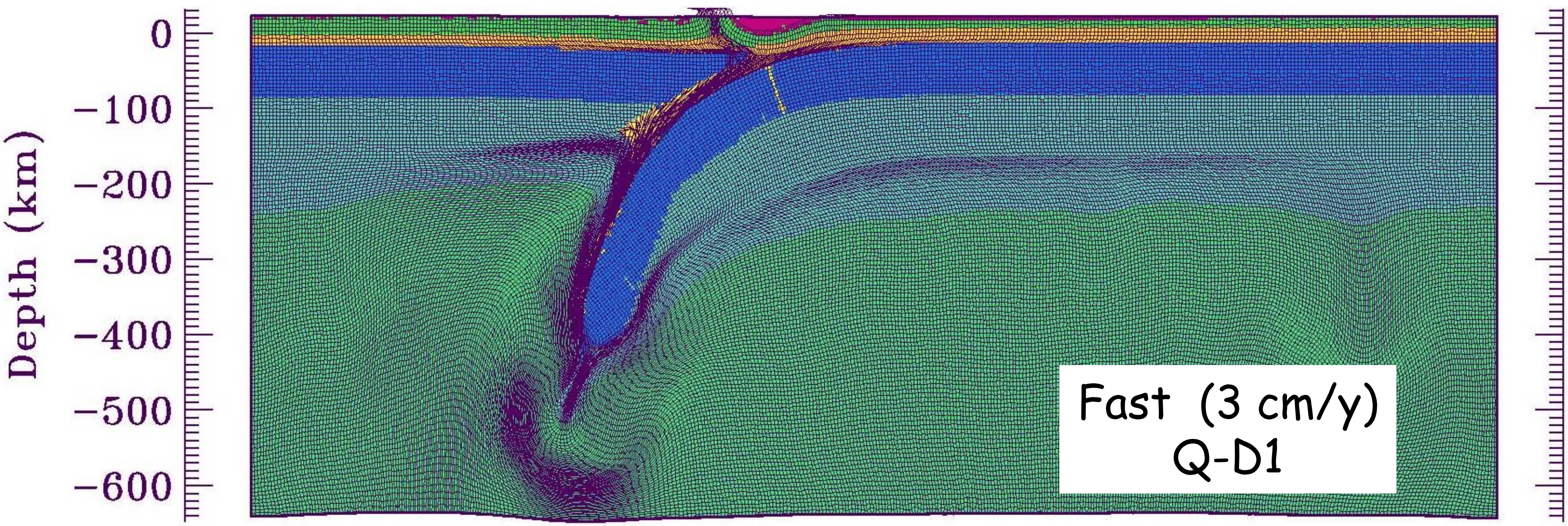

Time = 5.8 Myr

Fast (6 cm/y)
Q-D2

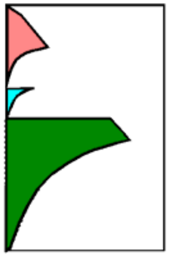

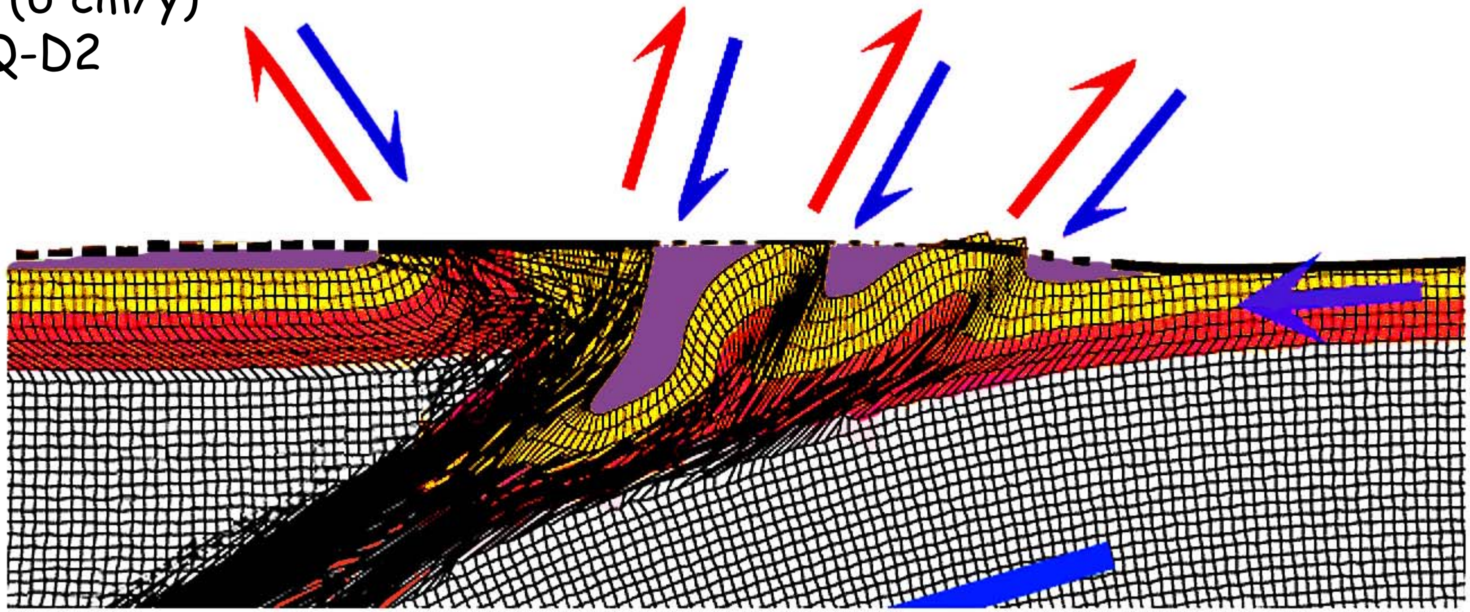

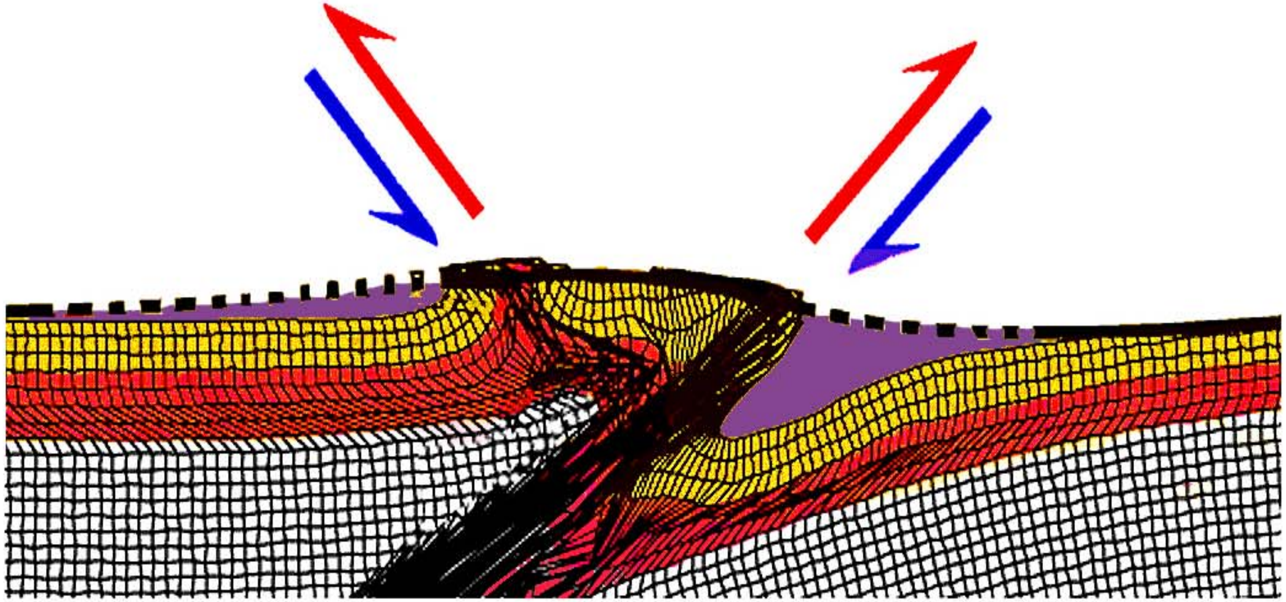

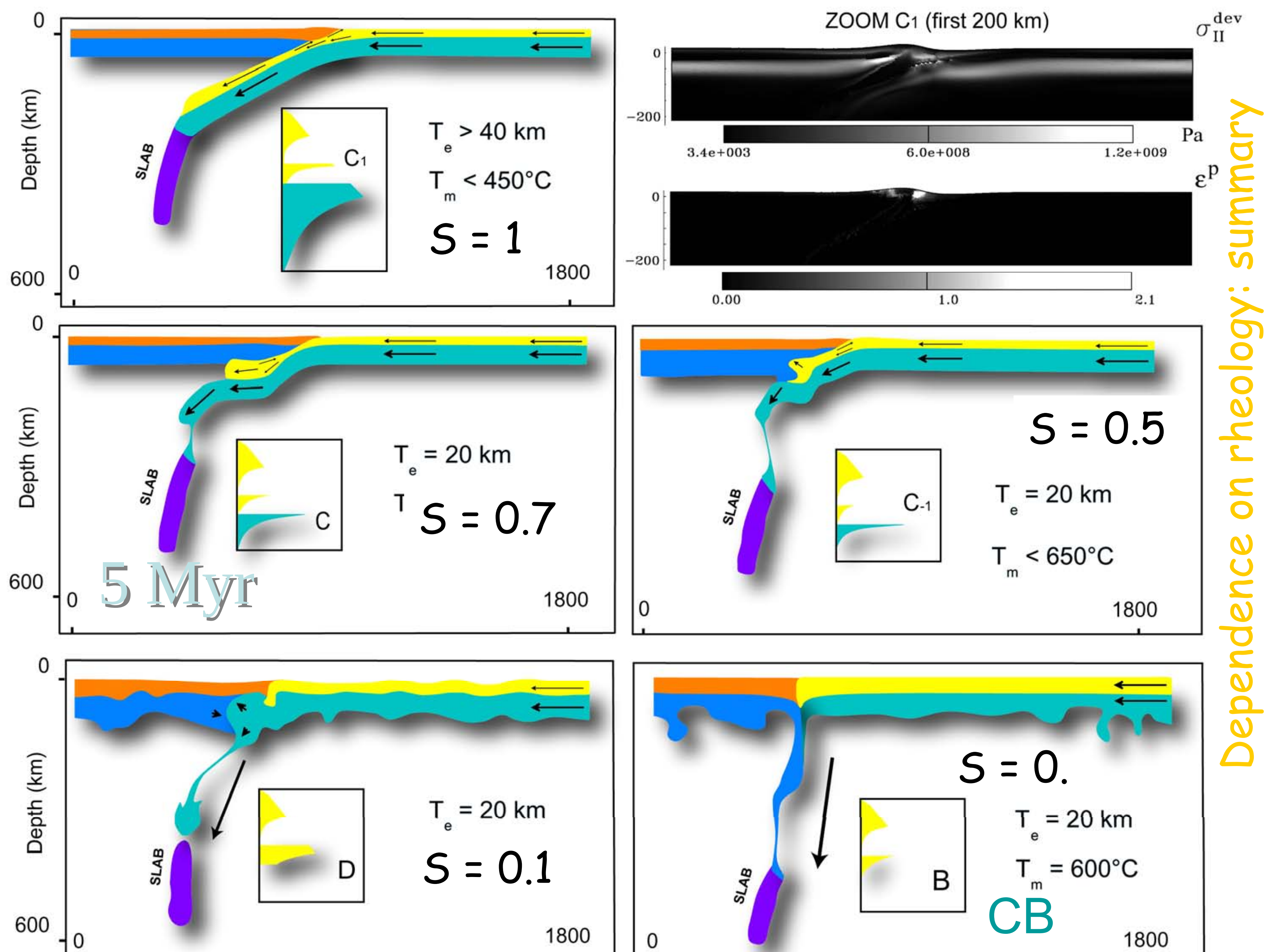

Dependence on rheology: summary
ZOOM C1 (first 200 km)
σ_{II}^{dev}
Pa
3.4e+003
6.0e+008
1.2e+009
ε^p
0.00
1.0
2.1
0
−200
Depth (km)
SLAB
C1
T_e > 40 km
T_m < 450°C
S = 1
0
600
0
1800
C
T_e = 20 km
S = 0.7
5 Myr
C-1
S = 0.5
T_e = 20 km
T_m < 650°C
D
T_e = 20 km
S = 0.1
B
S = 0.
T_e = 20 km
T_m = 600°C
CB

COTRIBUTION TO THE COLLISION STYLE FROM DIFFERENT DEFORMATION MODES

amount of shortening Δx

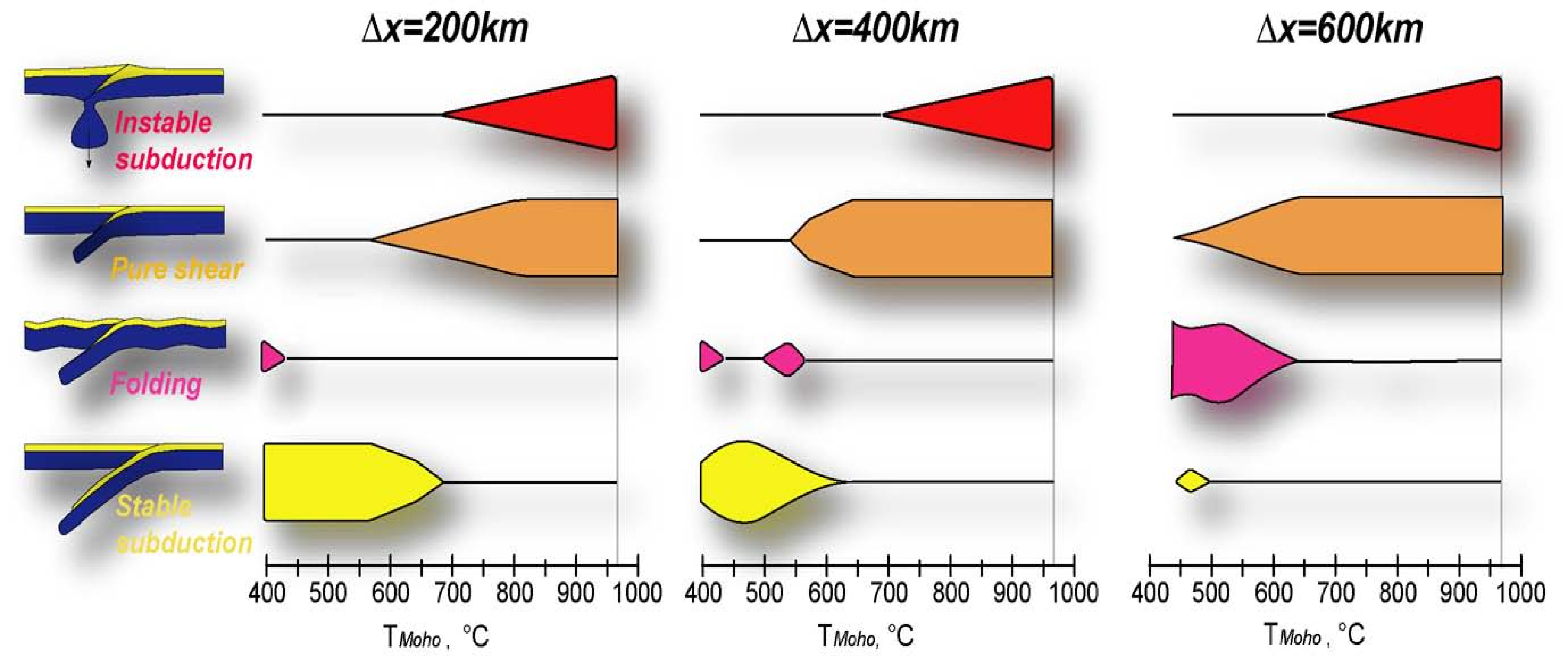

Moho temperature = Thermotectonic Age = thermo-rheological profile

Strong (diabase) lower crust promotes folding

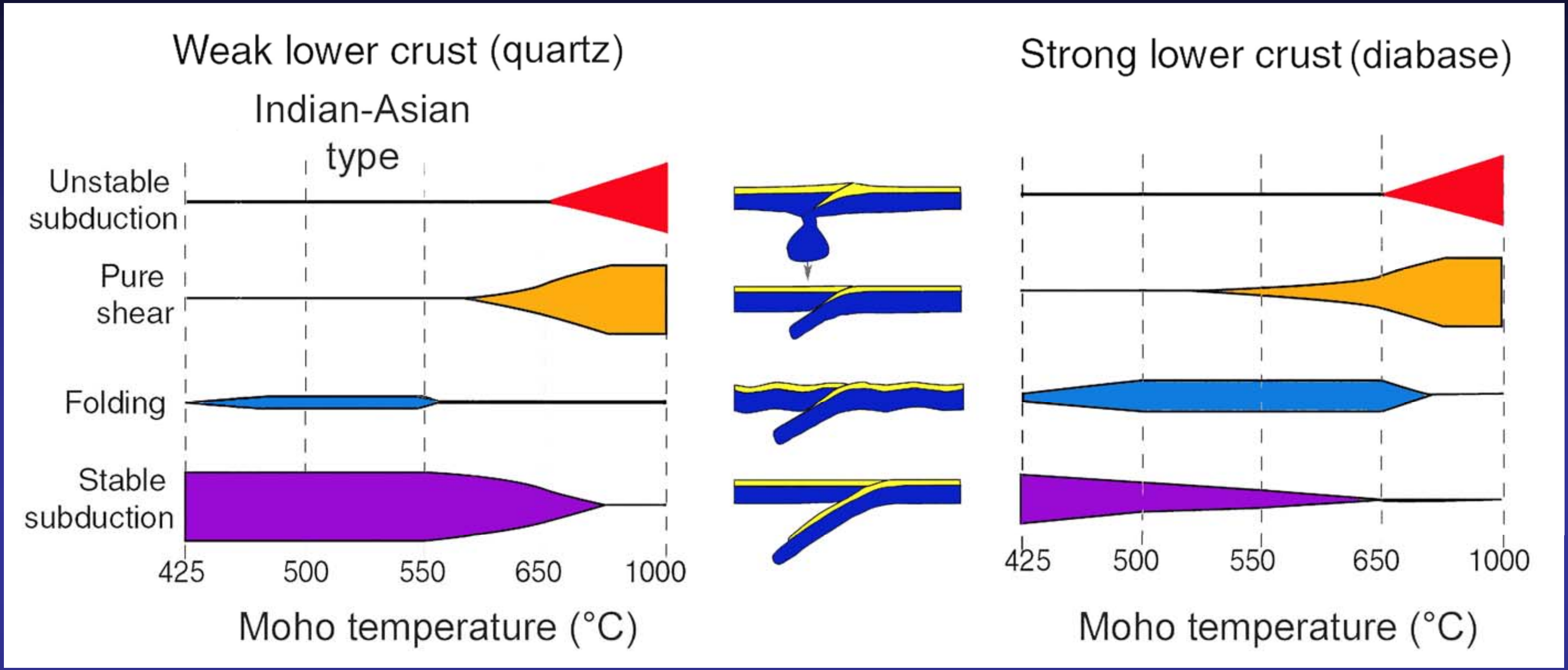

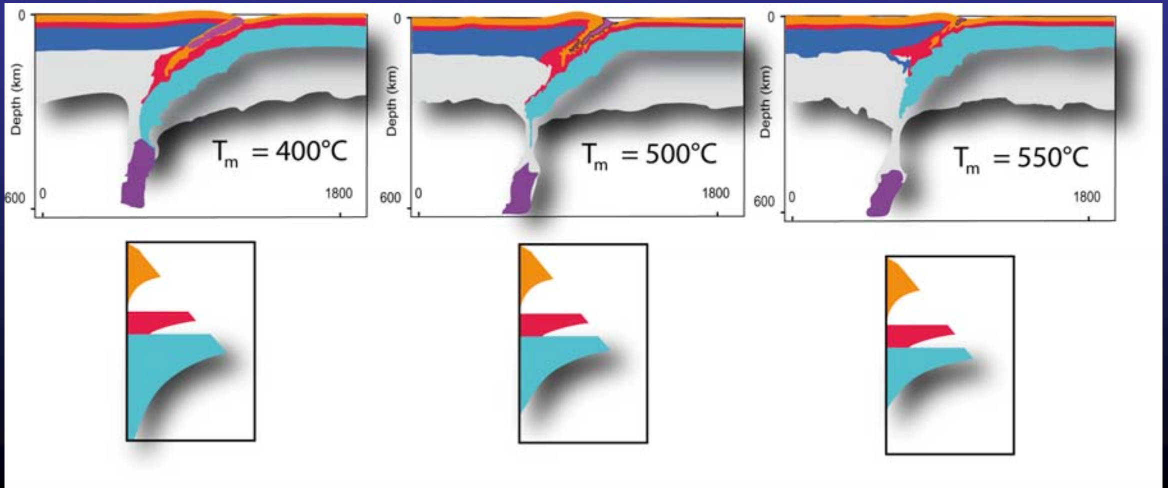

3.Influence of coupling withsurface processes

Final stages of subduction-collision, as function of convergence and erosion rate

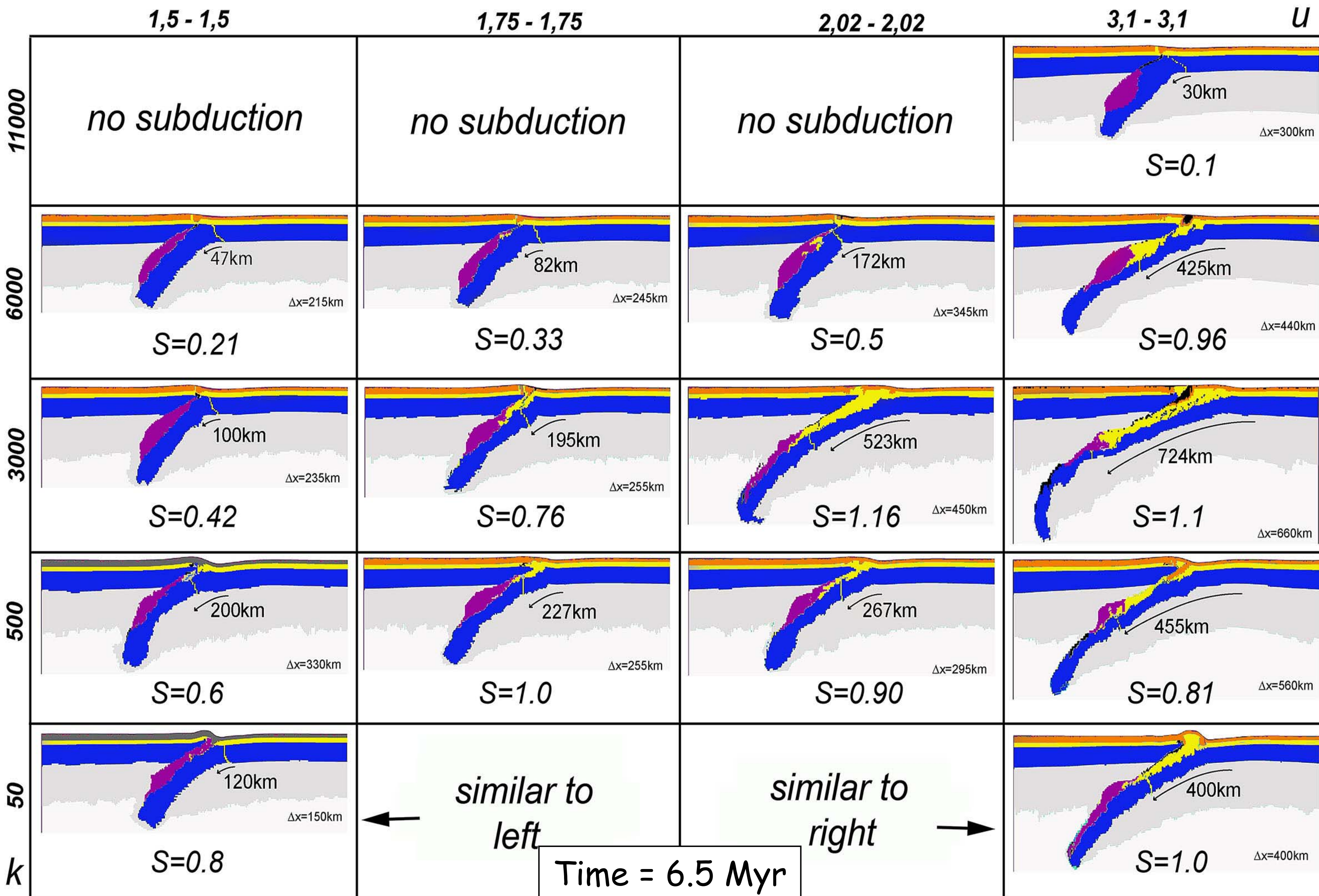

Dependence on efficiency of surface erosion rate (k)

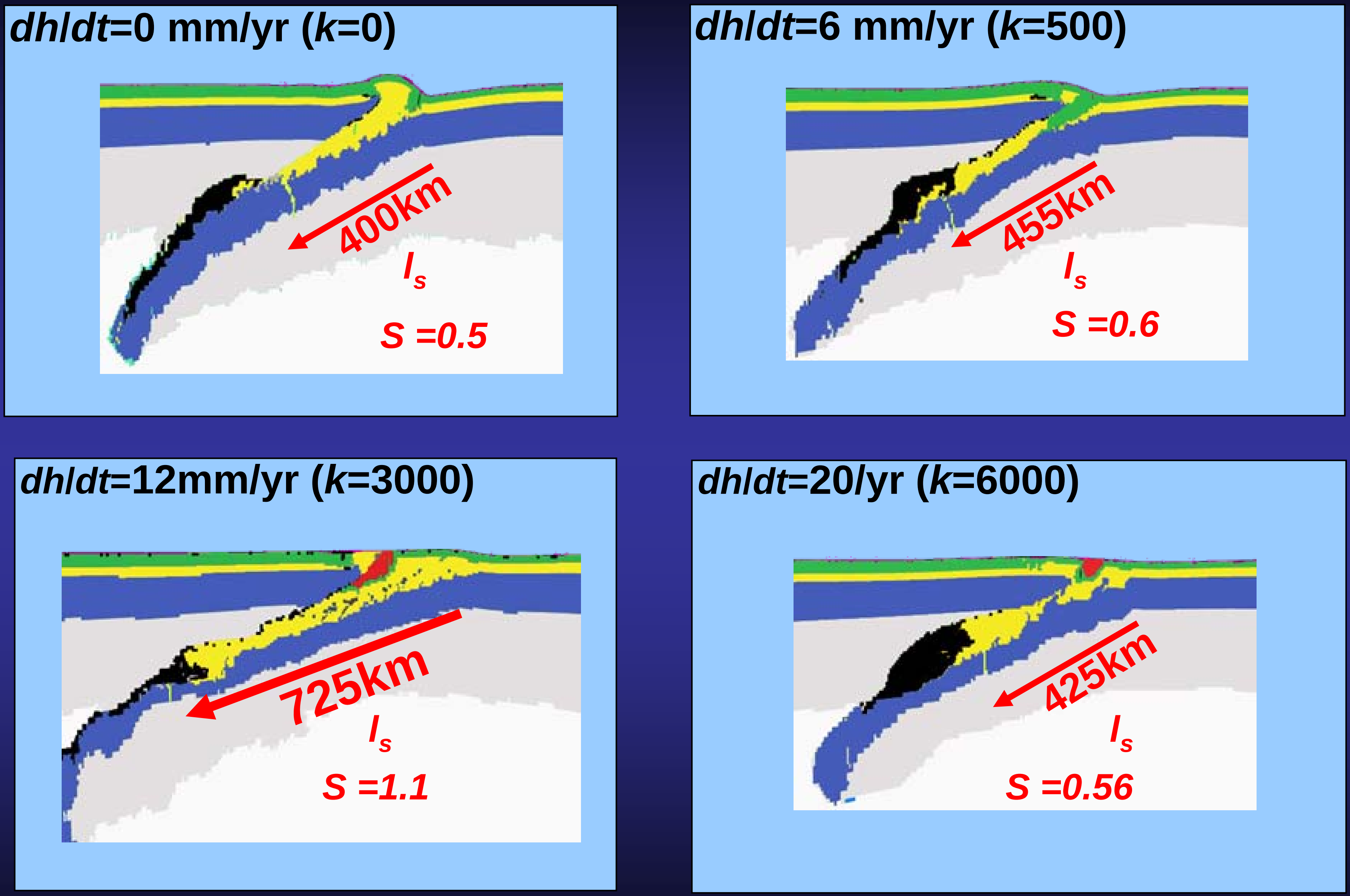

Maximal erosion rate and subduction length as function of k, convergence rate 60 mm/yr

1. First 0 to 5 Myr: similar initial development

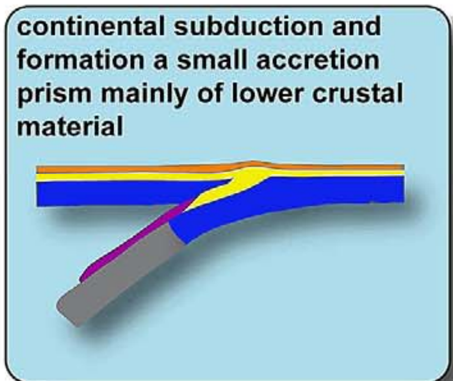

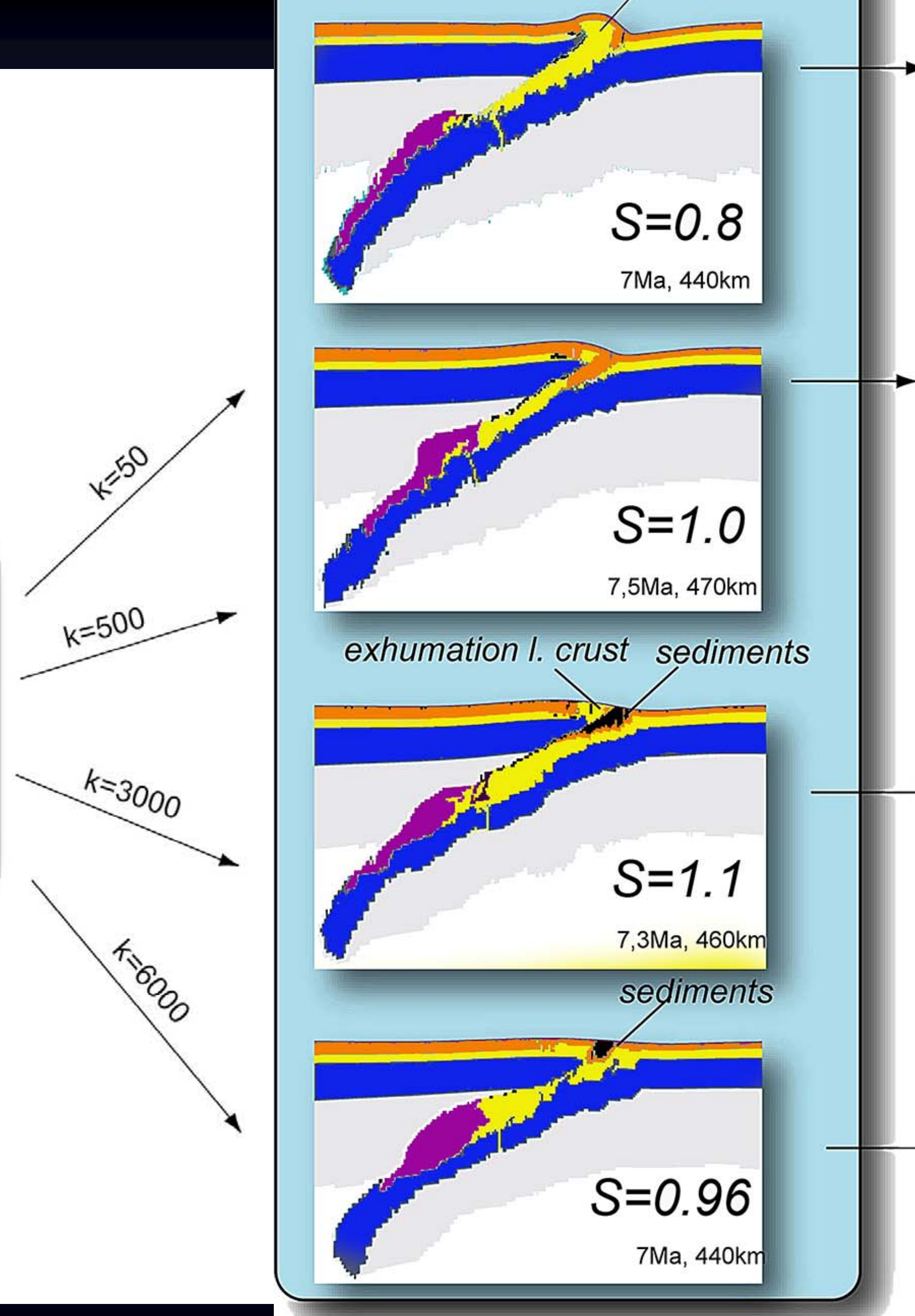

3. After 8 Myr, lution scenarious come different

iment ends up before ', as whole-scale ing with excessively ınrealistic topography ops

raphy becomes gh due to buckling and ɔt be compensated by ɔn

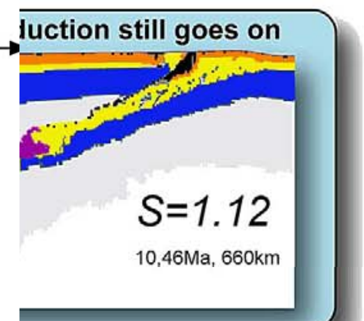

ɔ00 km of subduction, coupling occurs and stem enters into pure collision mode with pography

Topography evolution

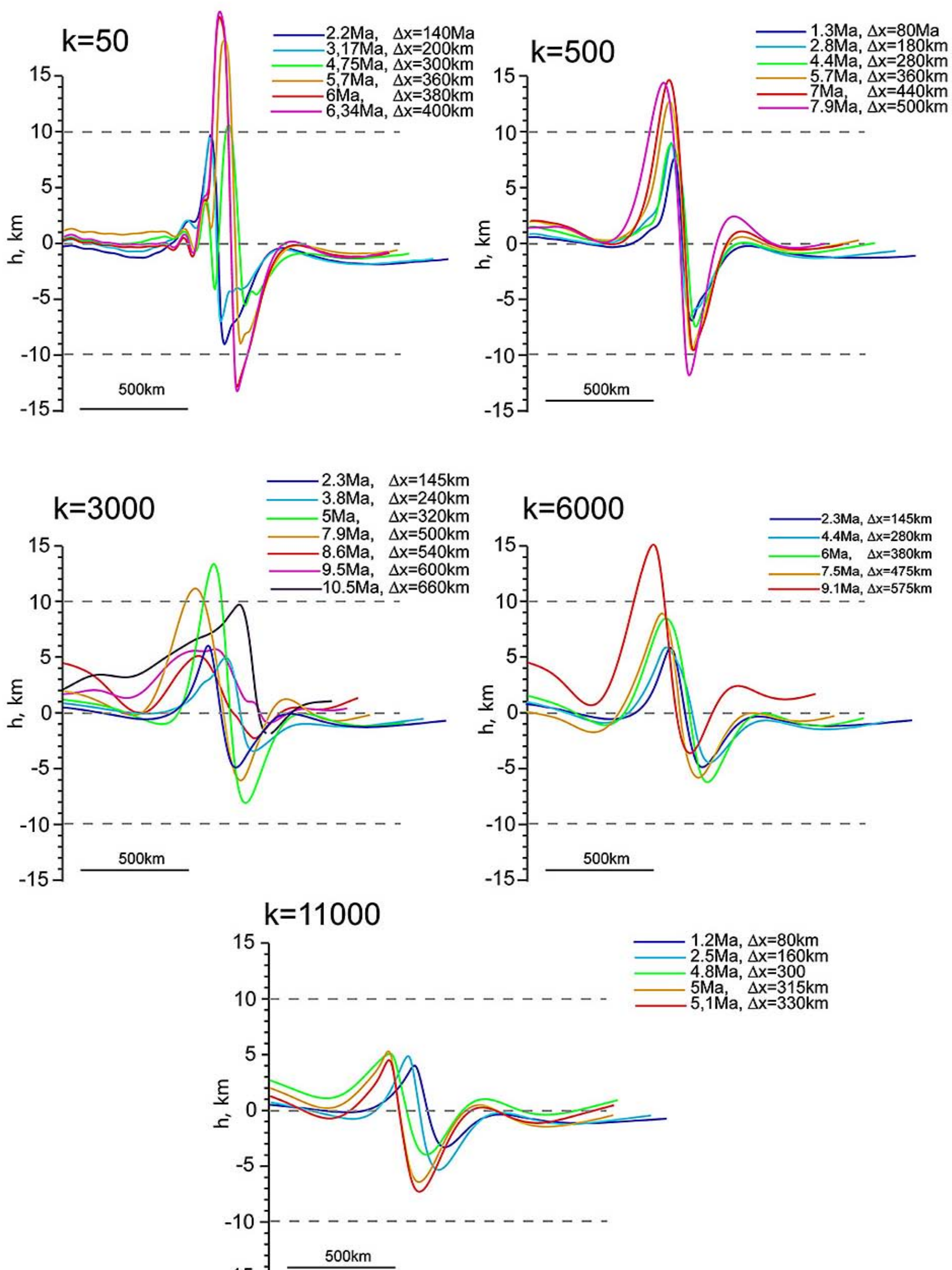

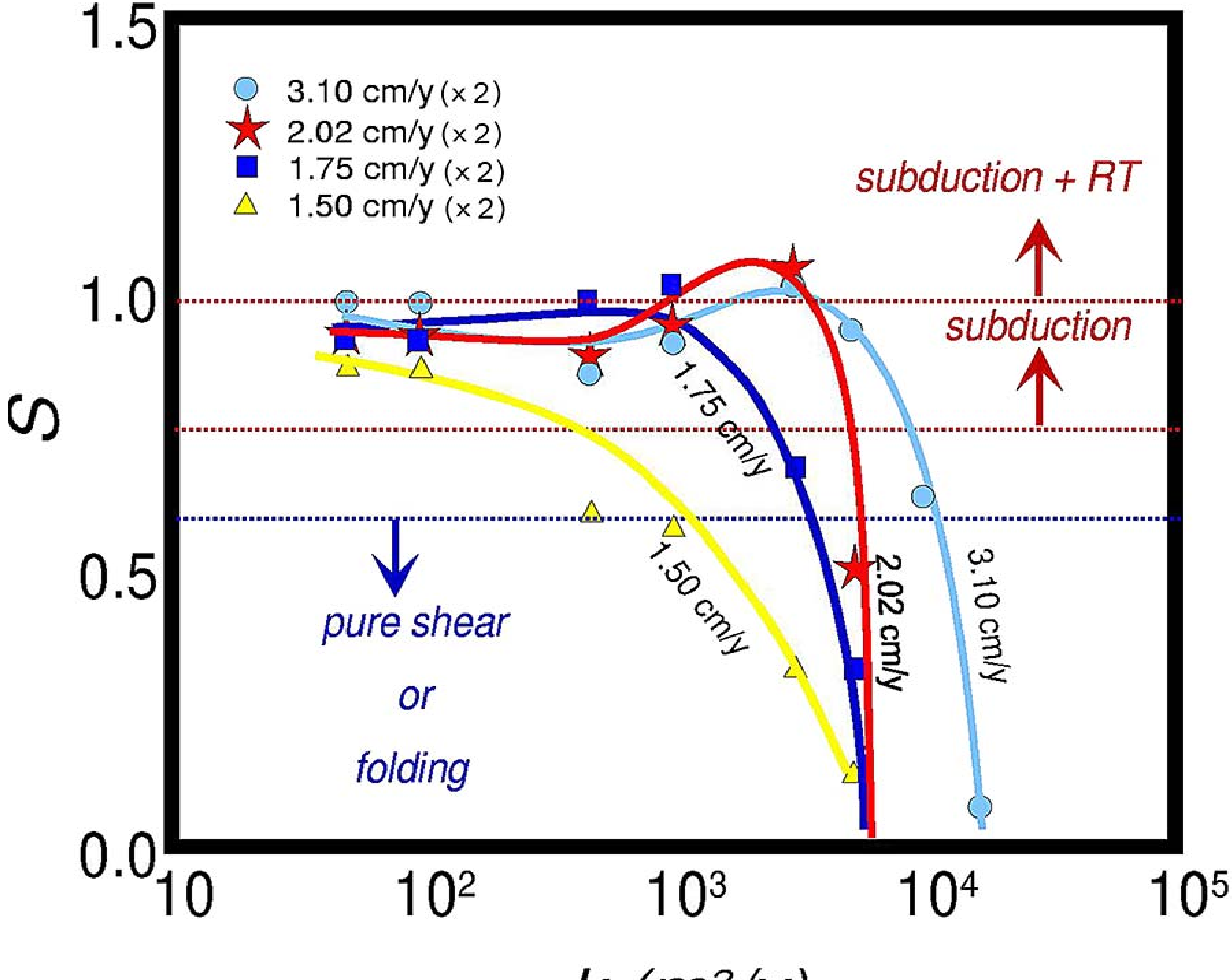

1.5
1.0
0.5
0.0
S
3.10 cm/y (×2)
2.02 cm/y (×2)
1.75 cm/y (×2)
1.50 cm/y (×2)
subduction + RT
subduction
pure shear
or
folding
1.75 cm/y
1.50 cm/y
2.02 cm/y
3.10 cm/y
10
10²
10³
10⁴
10⁵
k (m²/y)

A simulation compatible with Indian -Asian collision

Geotherm 450 Ma (T_{Moho} = 400°C)

High initial convergence rate (6cm/y)

About 700km of subduction

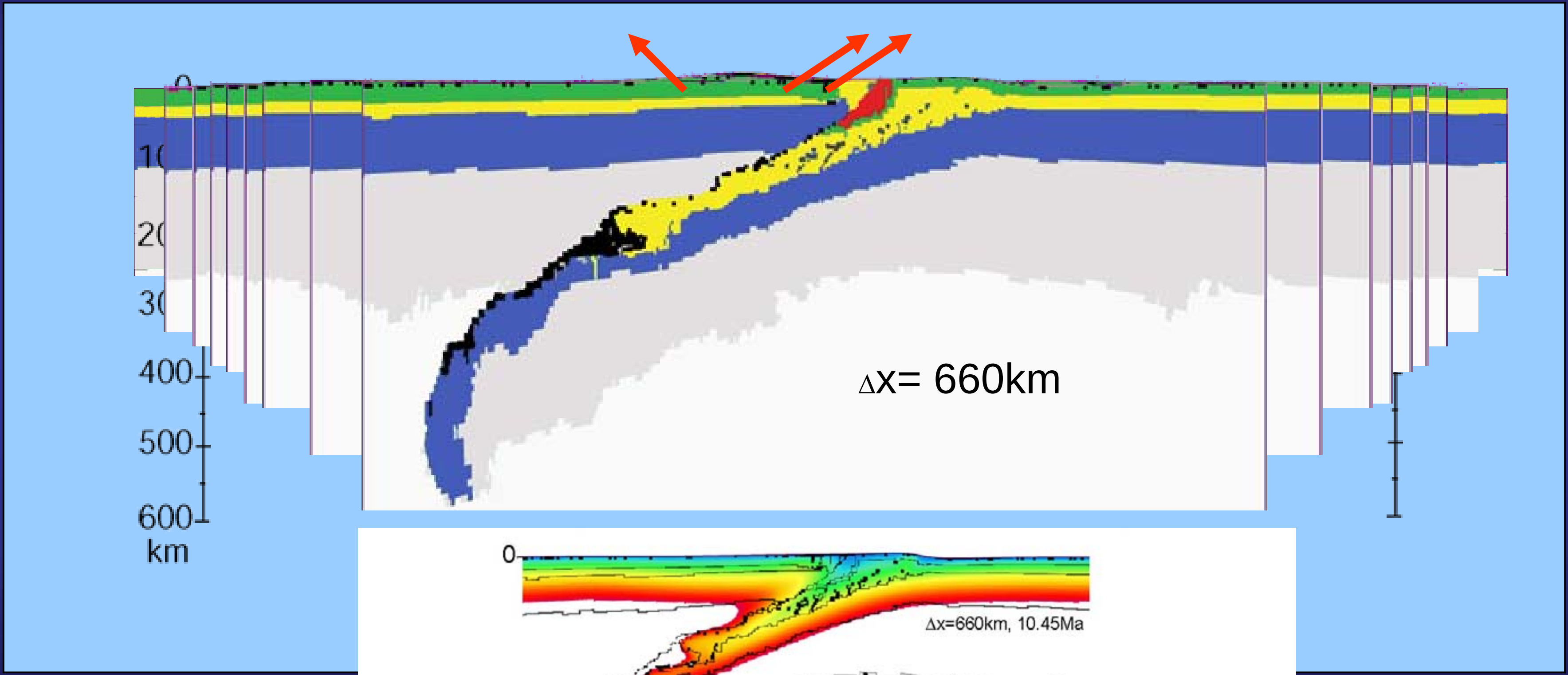

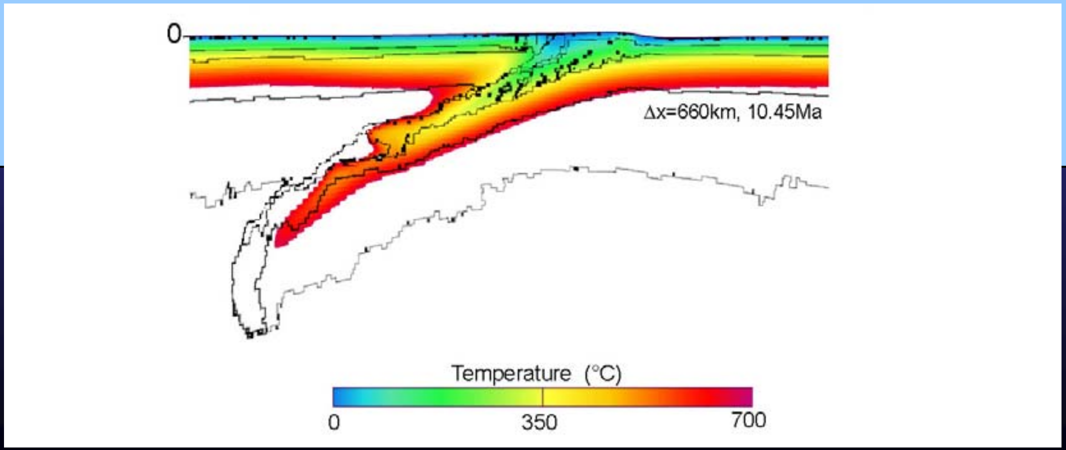

wait ...

Plastic strain

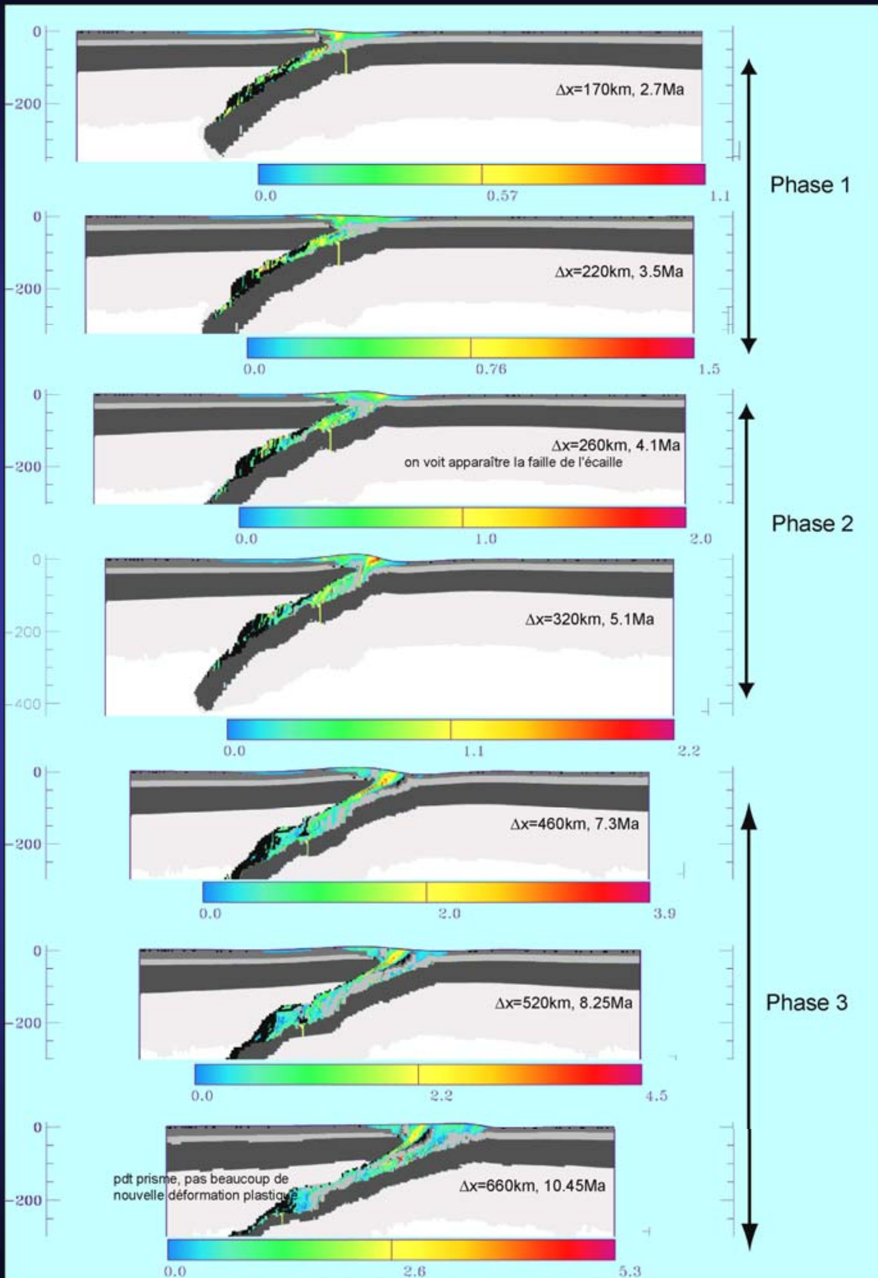

Temperature

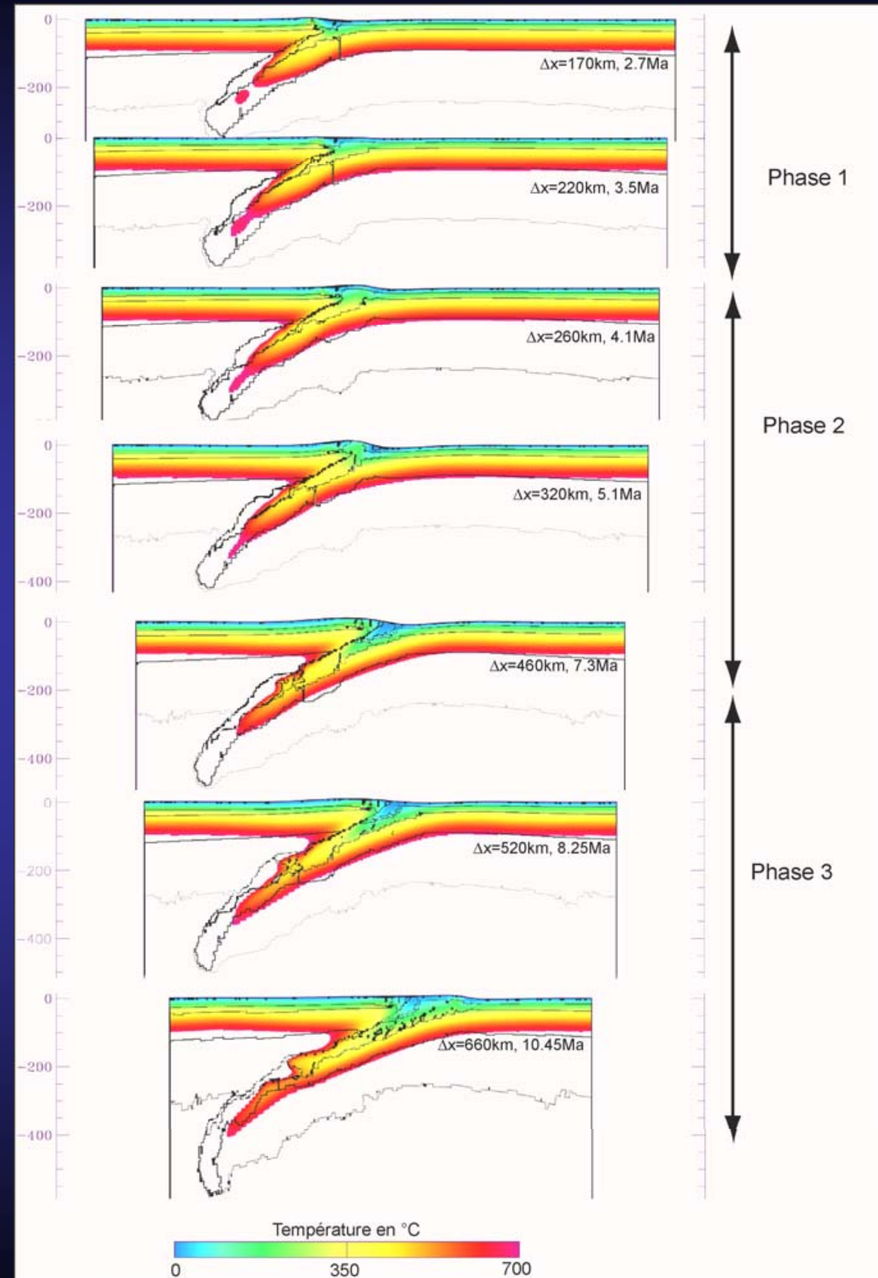

Phase 1 (dx= 0-220km): deformation at suture

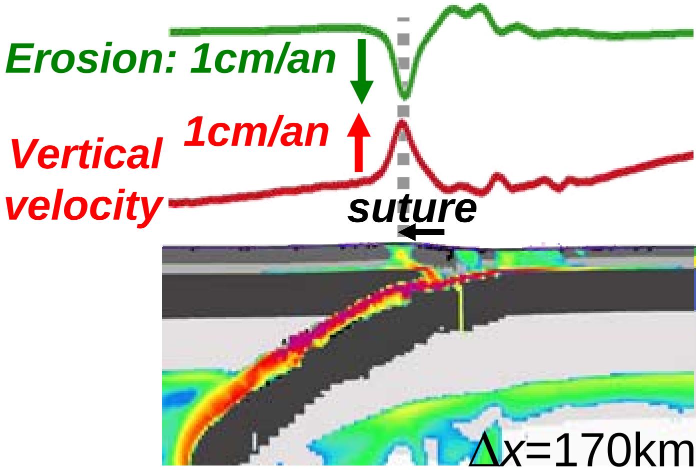

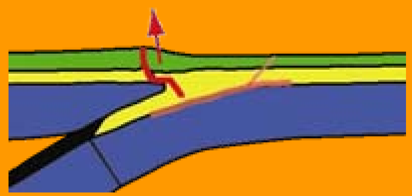

Lower crustal prism

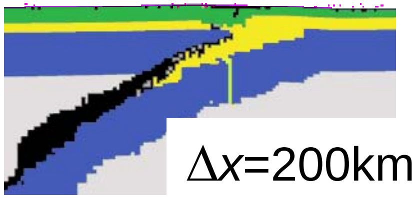

Transitory regime…

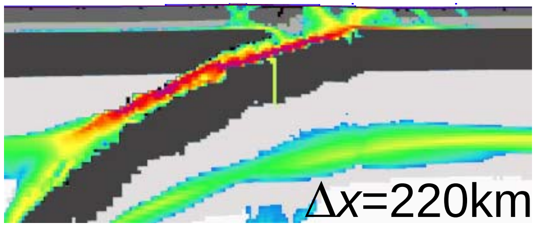

Phase 2: Majour thrust fault activity

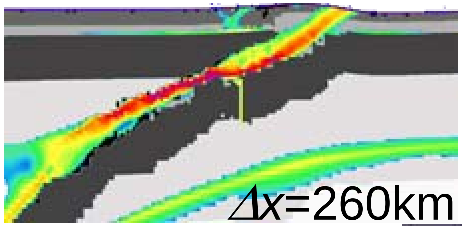

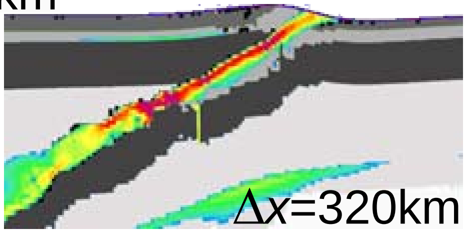

All deformation is concentrated on a single thrust during 250km of shortening

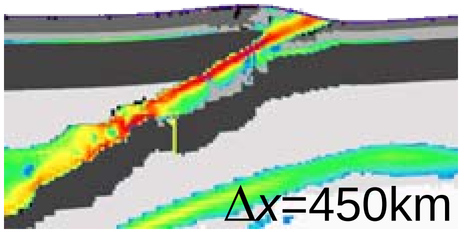

erosion

vertical vel.

horizontal vel.

topography

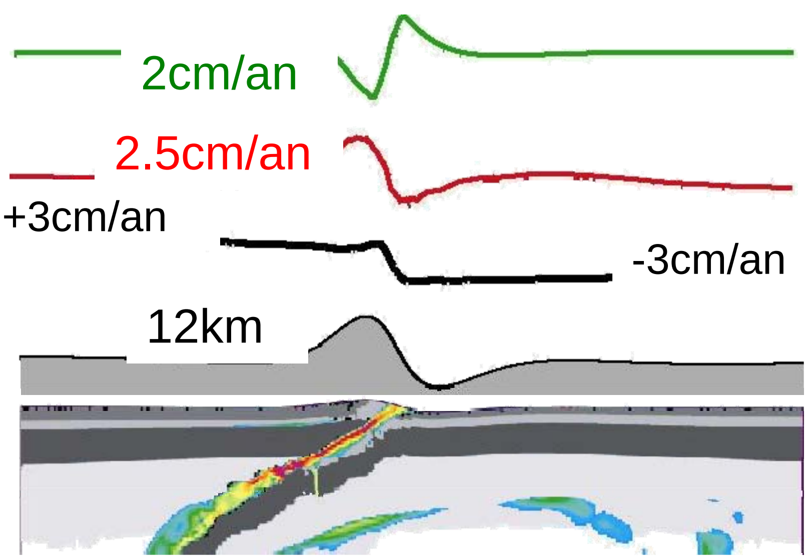

It controlls all surface deformation

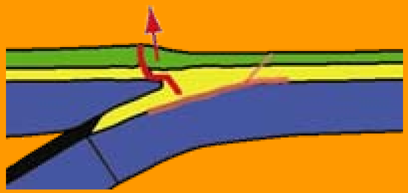

Phase 3: accretion of a large crustal prism

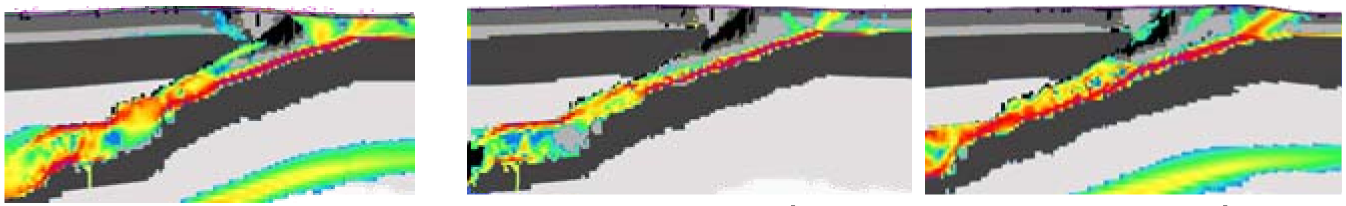

ΔX= 520km ΔX= 600km ΔX= 660km

Successions of frontal thrusts towards South

→ Formation of an assymetric chain above the prism

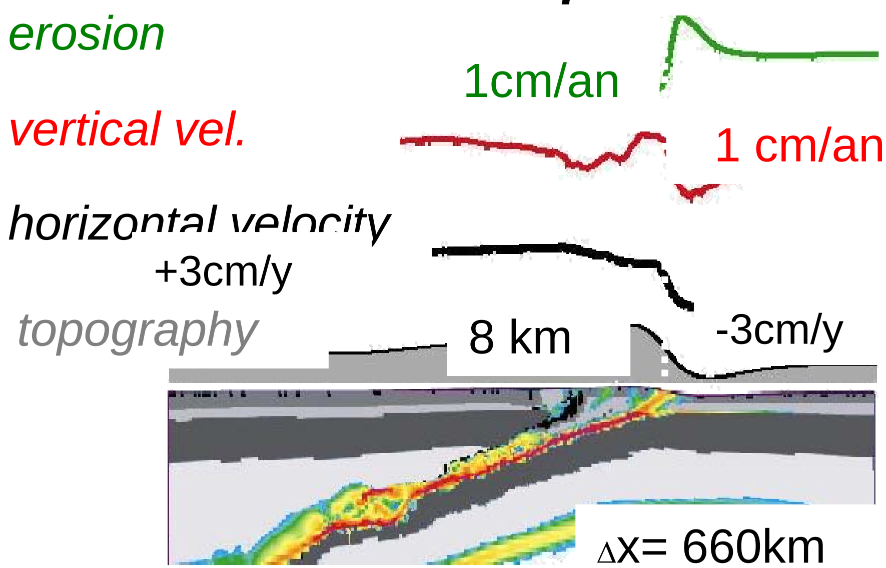

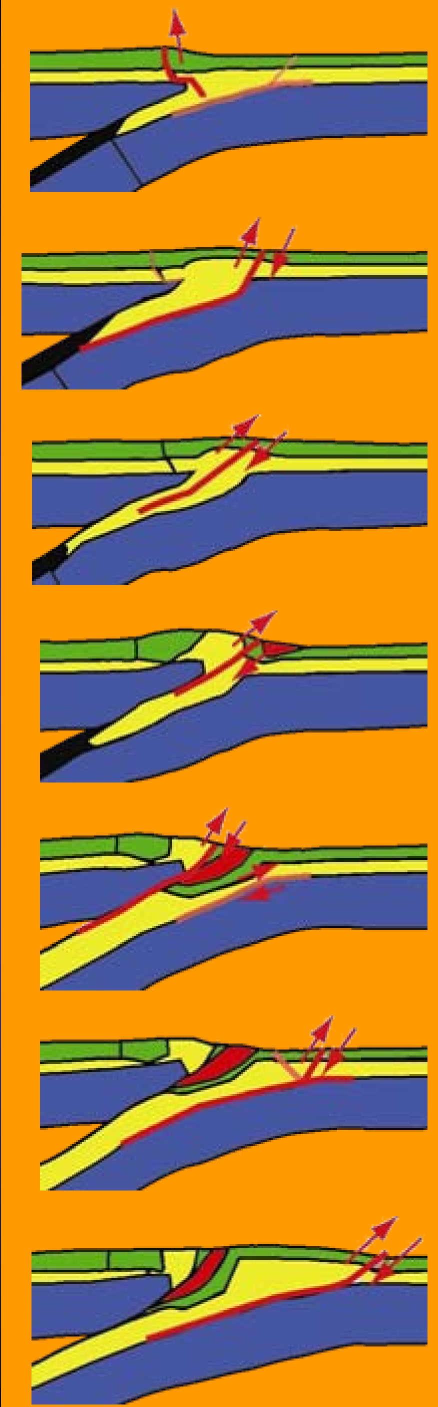

Topography evolution

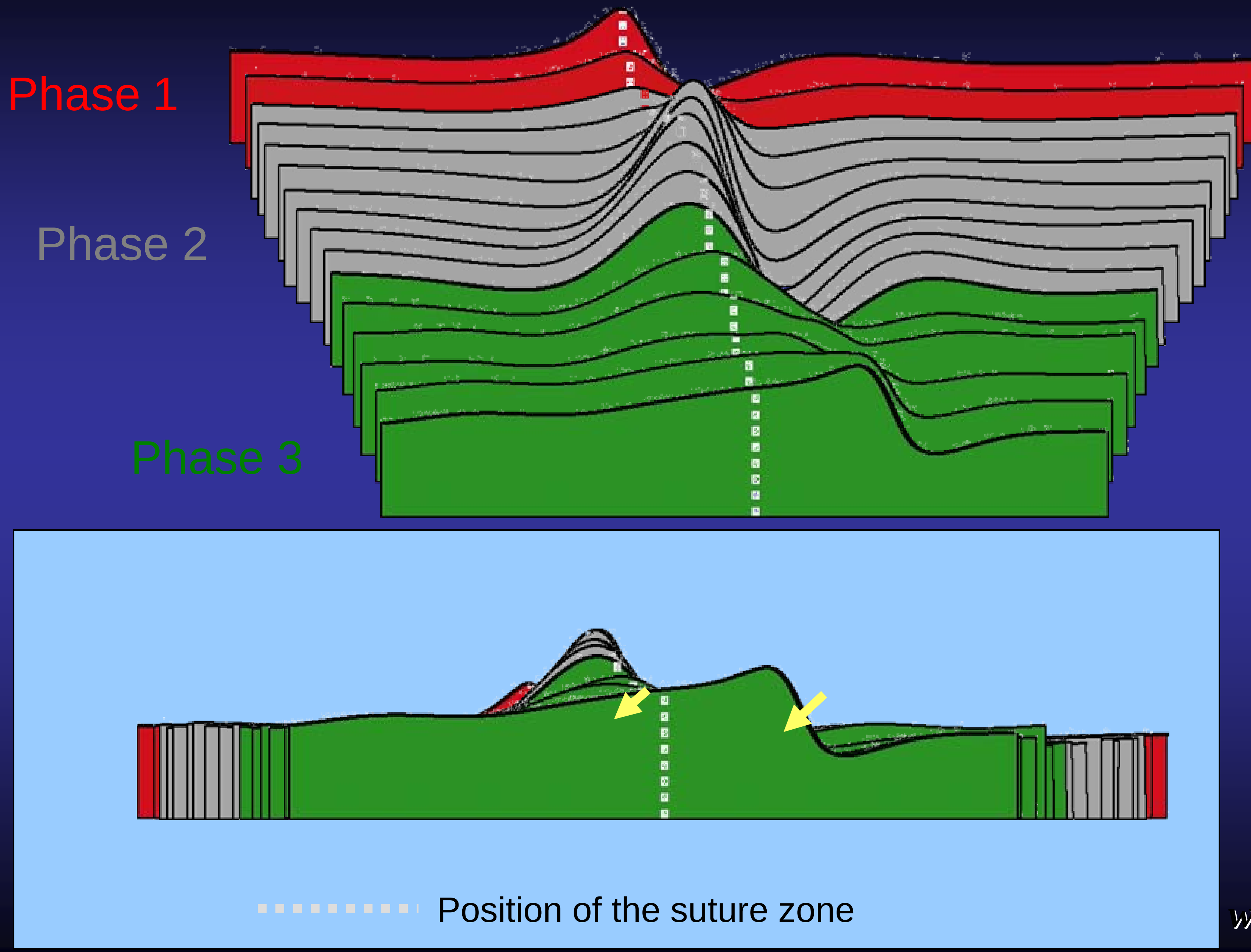

wait …

Δx from 220 to

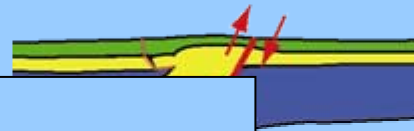

Major Thrust = MCT ?

lower crustal exhumation

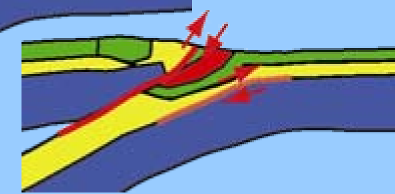

e North of
e Southern
ement STD ?

from Δx = 0 to 220km = Himalaya between 50 and 30Ma?

•Deformation (backthrusting at suture)

Δx=660km = Actual Himalaya ?

- large prism developped at South of suture
- comparable size of the crustal prism
- deformation localized along the Frontal Thrust

End-member case:

Low Pecklet number (i.e. slow)

Convergence

Slow Alpine Collision I:
Oceanic phase

PhD thesis of Ph. Yamato;
Yamato et al., 2007

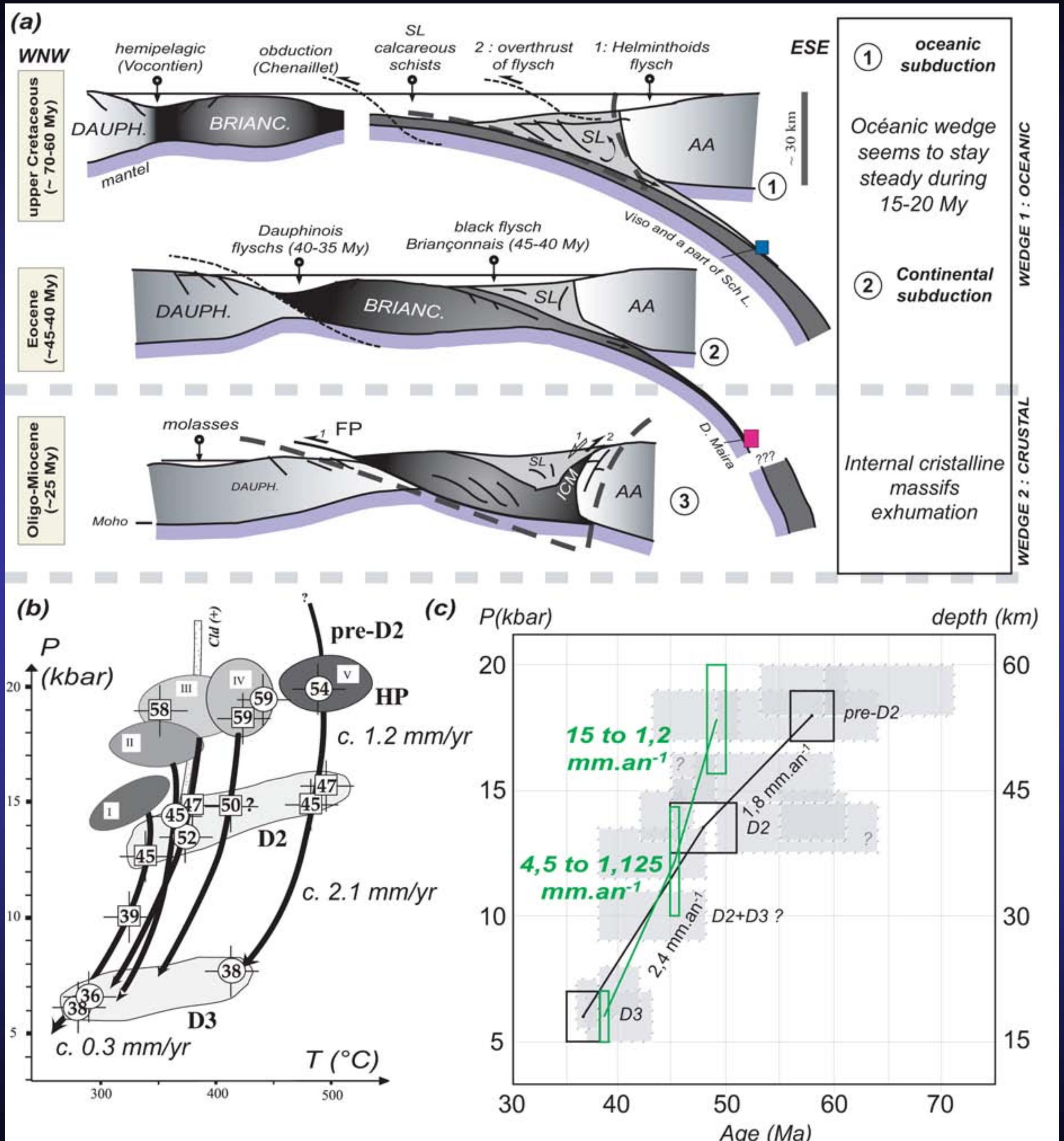

(a)
WNW
ESE
upper Cretaceous (~ 70-60 My)
hemipelagic (Vocontien)
obduction (Chenaillet)
SL calcareous schists
2 : overthrust of flysch
1: Helminthoids flysch
DAUPH.
BRIANC.
SL
AA
mantel
~ 30 km
Viso and a part of Sch L.
Eocene (~45-40 My)
Dauphinois flyschs (40-35 My)
black flysch Briançonnais (45-40 My)
Oligo-Miocene (~25 My)
molasses
FP
ICM
Moho
D. Maira
???
DAUPH.
① oceanic subduction
Océanic wedge seems to stay steady during 15-20 My
② Continental subduction
Internal cristalline massifs exhumation
WEDGE 1 : OCEANIC
WEDGE 2 : CRUSTAL
(b)
P (kbar)
T (°C)
Cld (+)
pre-D2
HP
c. 1.2 mm/yr
D2
c. 2.1 mm/yr
D3
c. 0.3 mm/yr
(c)
P(kbar)
depth (km)
Age (Ma)
pre-D2
15 to 1,2 mm.an-1
4,5 to 1,125 mm.an-1
1,8 mm.an-1
2,4 mm.an-1
D2
D2+D3 ?
D3

Accretion prizm stability

Initial geometry

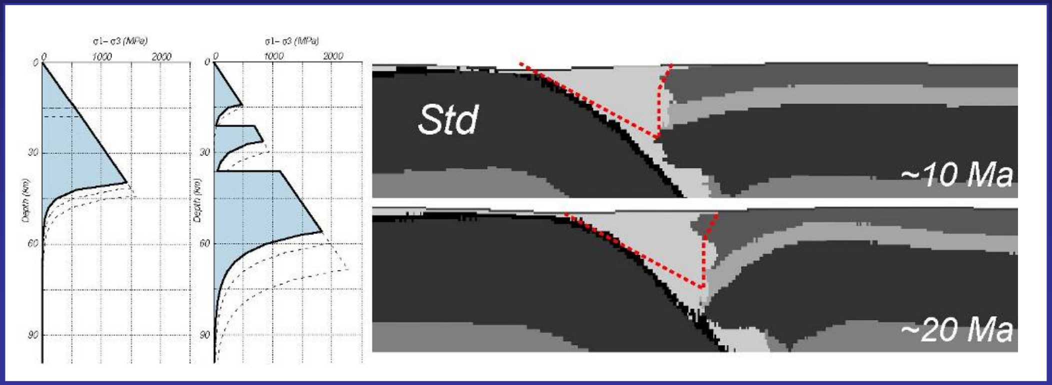

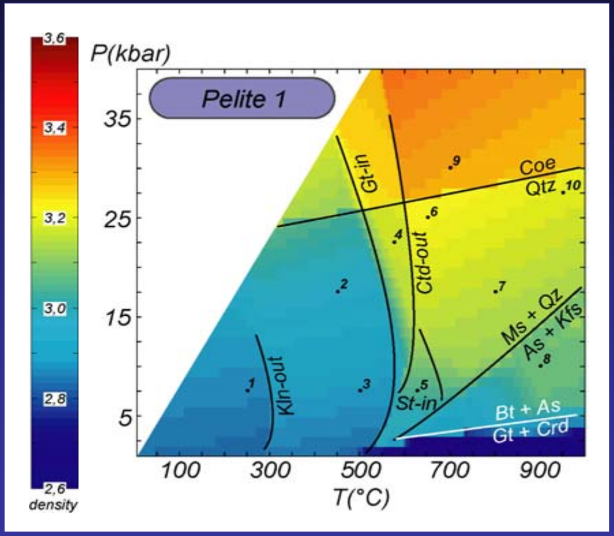

Stable case

Instable case

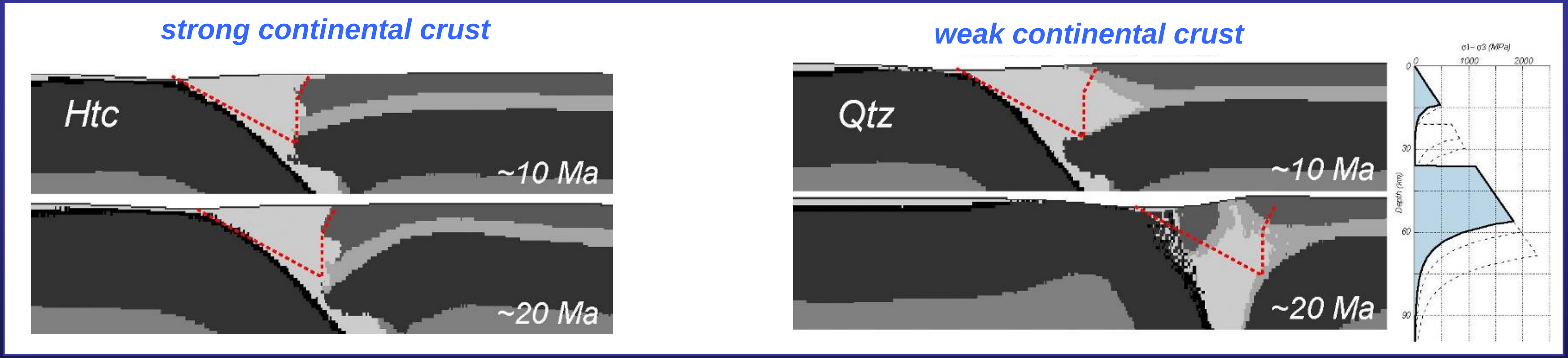

Old upper plate

V = 1,5 cm.an-1; V = 6 cm.an-1
Low sediment viscosity
Schistes go down
Pelite less rich in Al

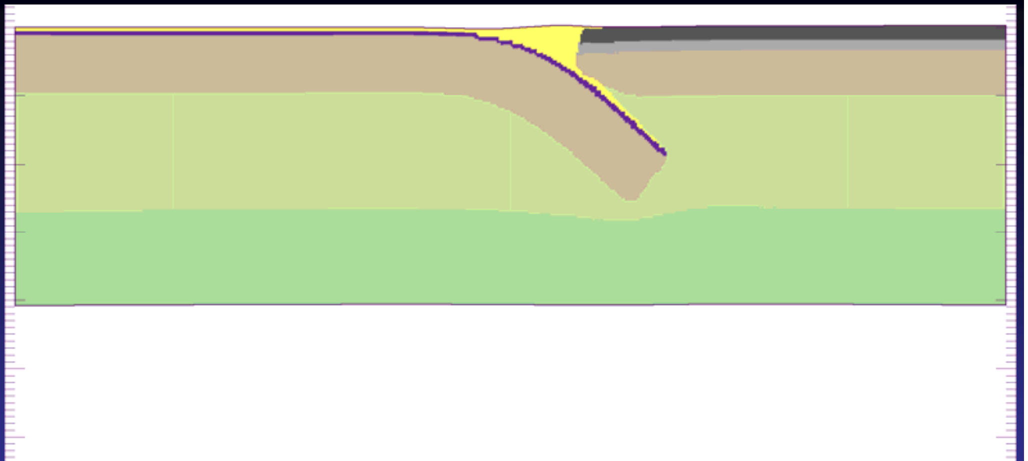

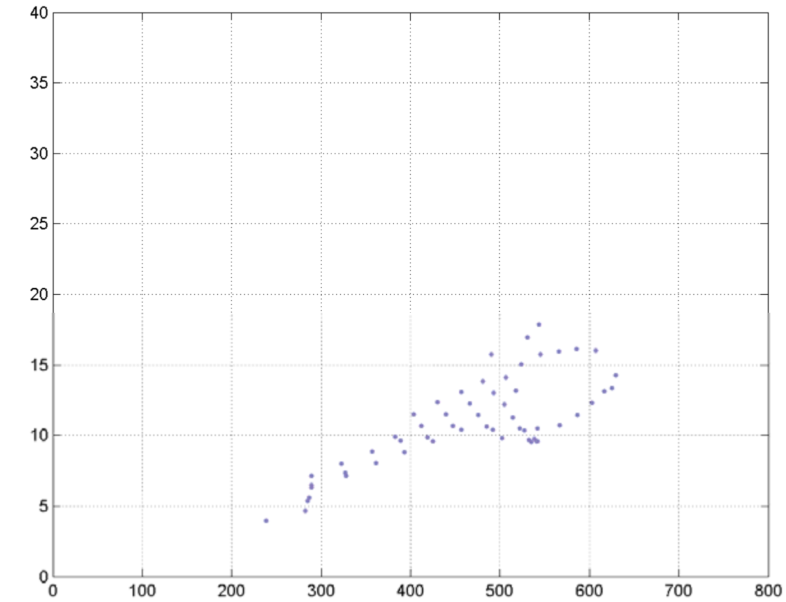

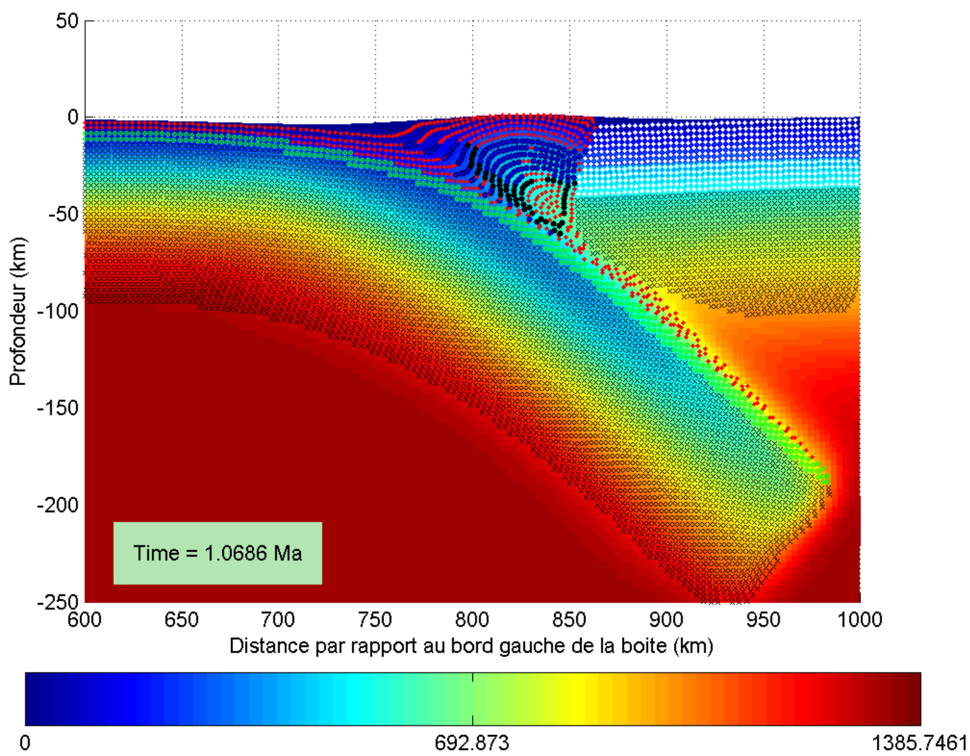

wait …

PhD thesis of Ph. Yamato;
Yamato et al., 2007
Burov and Yamato, 2007

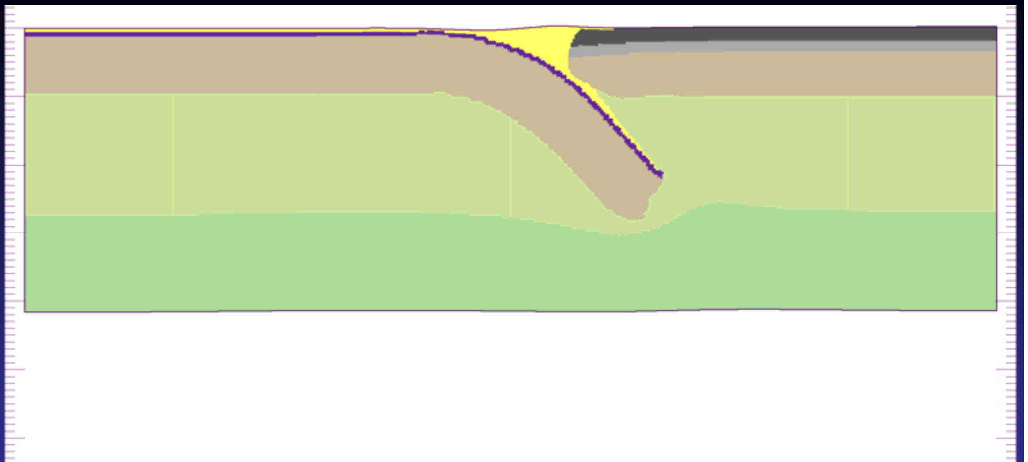

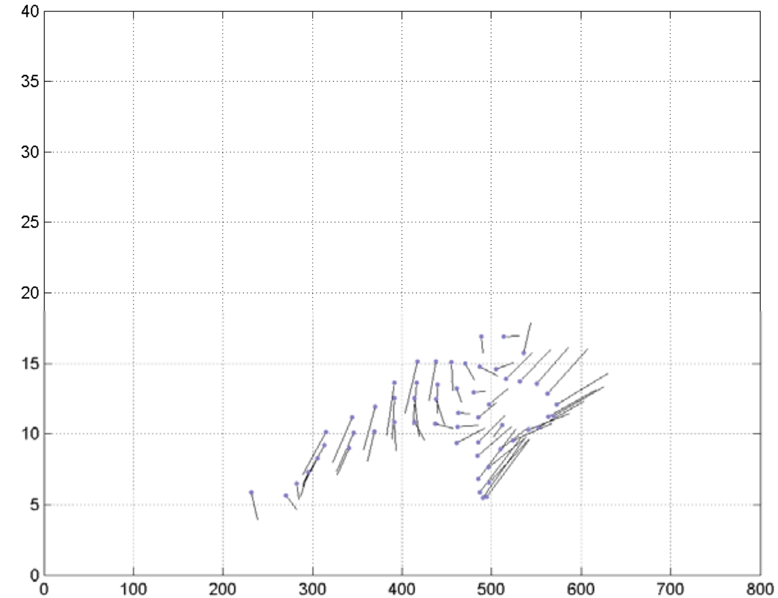

40
35
30
25
20
15
10
5
0
0
100
200
300
400
500
600
700
800

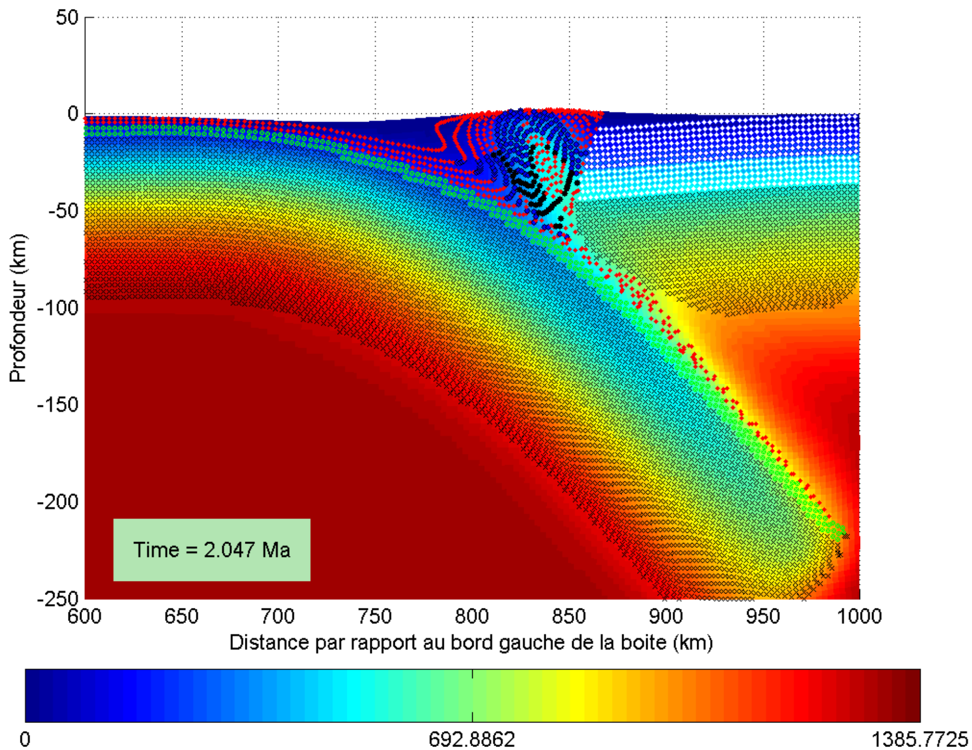

50
0
-50
-100
-150
-200
-250
Profondeur (km)
600
650
700
750
800
850
900
950
1000
Distance par rapport au bord gauche de la boite (km)
Time = 2.047 Ma
0
692.8862
1385.7725

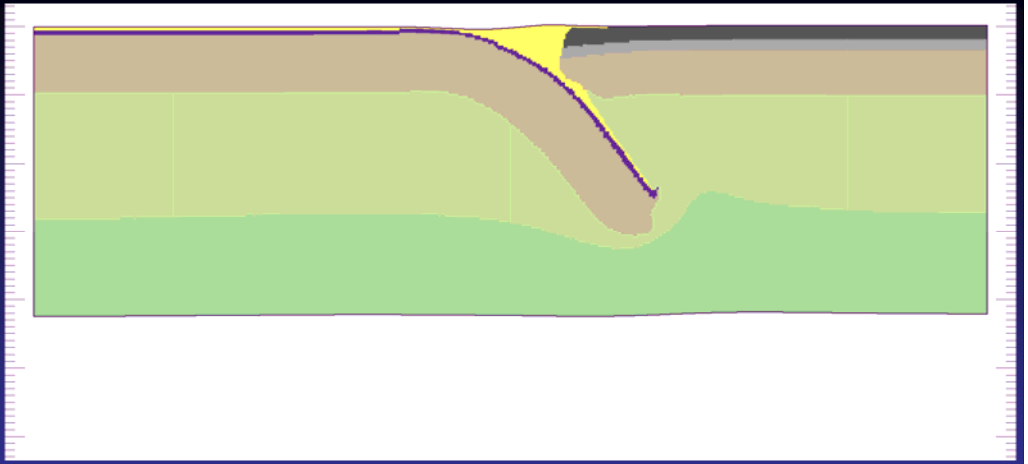

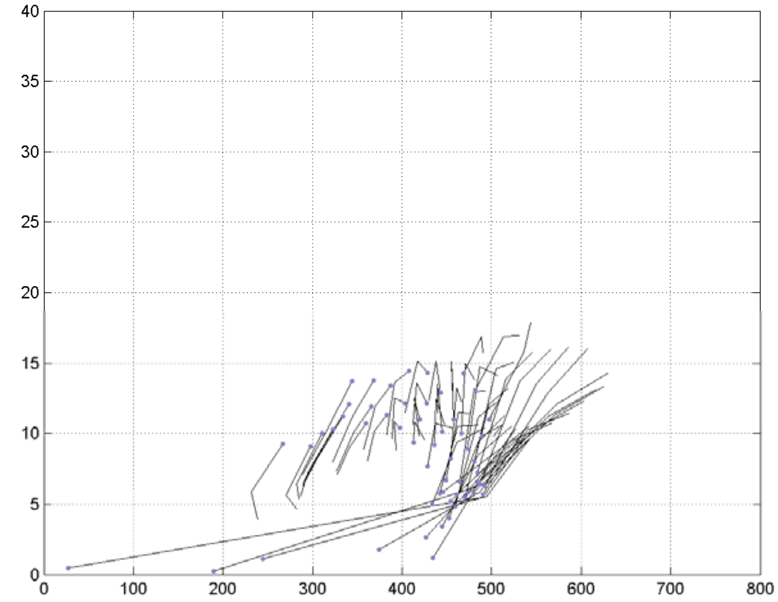

40
35
30
25
20
15
10
5
0
0
100
200
300
400
500
600
700
800

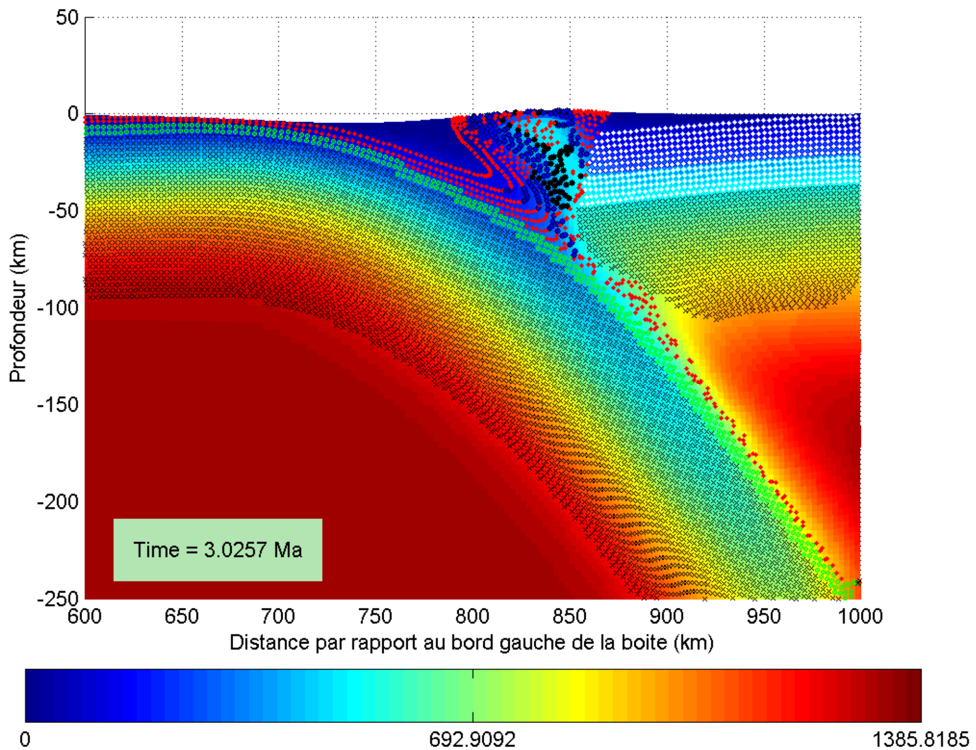

50
0
-50
-100
-150
-200
-250
Profondeur (km)
Time = 3.0257 Ma
600
650
700
750
800
850
900
950
1000
Distance par rapport au bord gauche de la boite (km)
0
692.9092
1385.8185

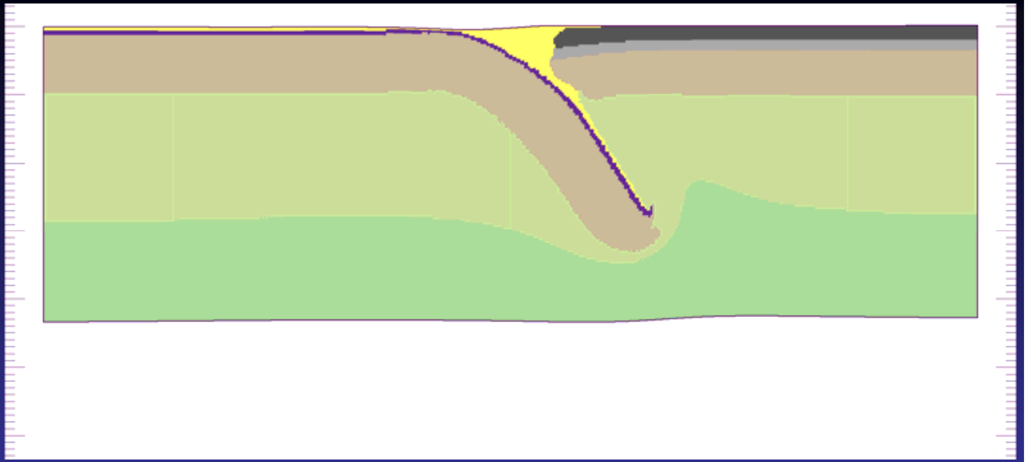

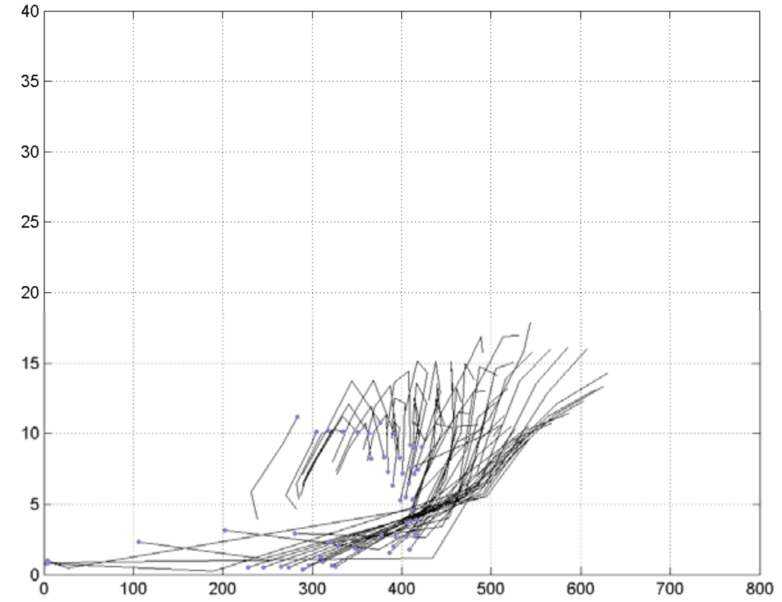

40
35
30
25
20
15
10
5
0
0
100
200
300
400
500
600
700
800

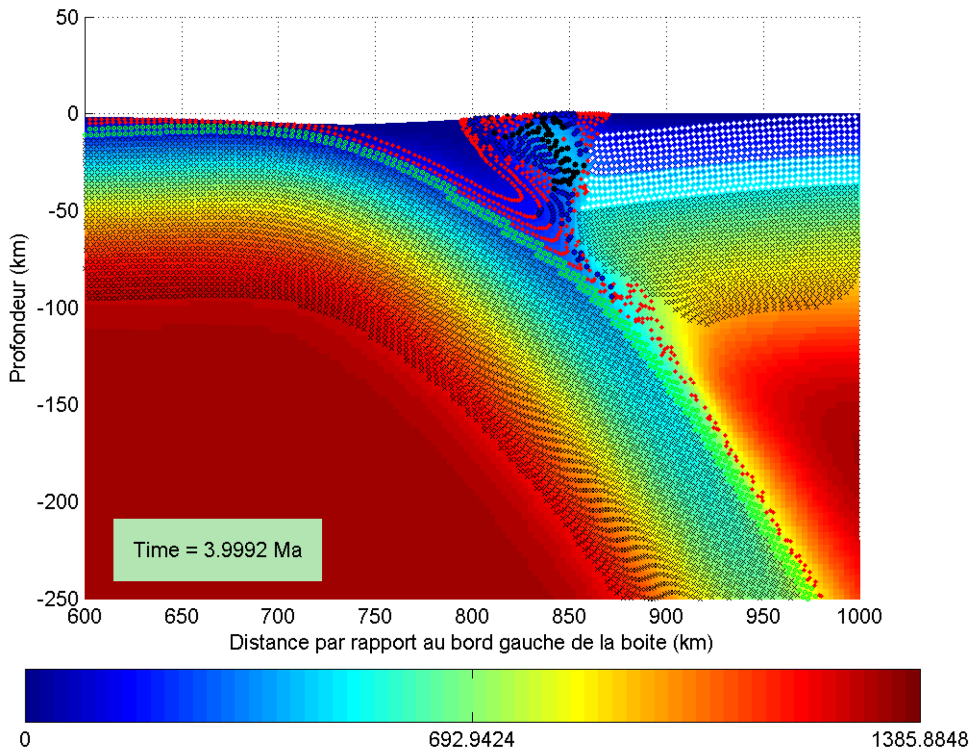

50
0
-50
-100
-150
-200
-250
Profondeur (km)
600
650
700
750
800
850
900
950
1000
Distance par rapport au bord gauche de la boite (km)
Time = 3.9992 Ma
0
692.9424
1385.8848

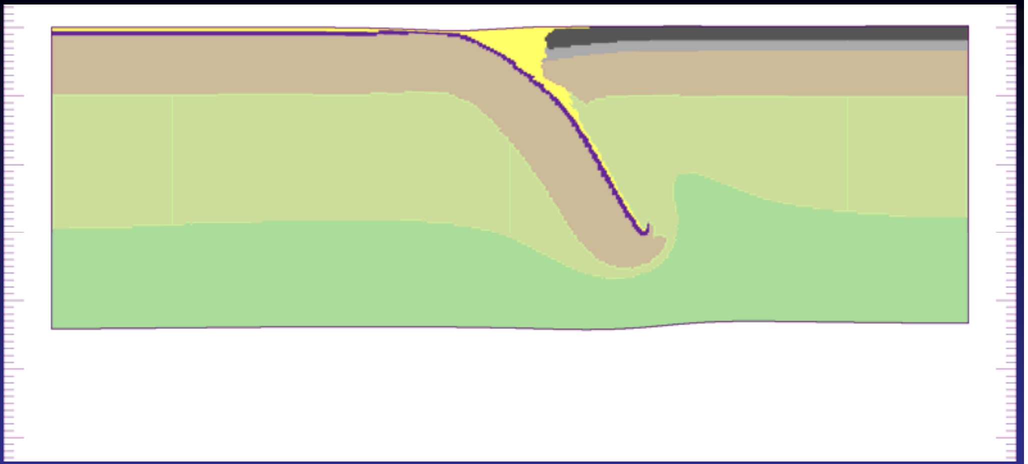

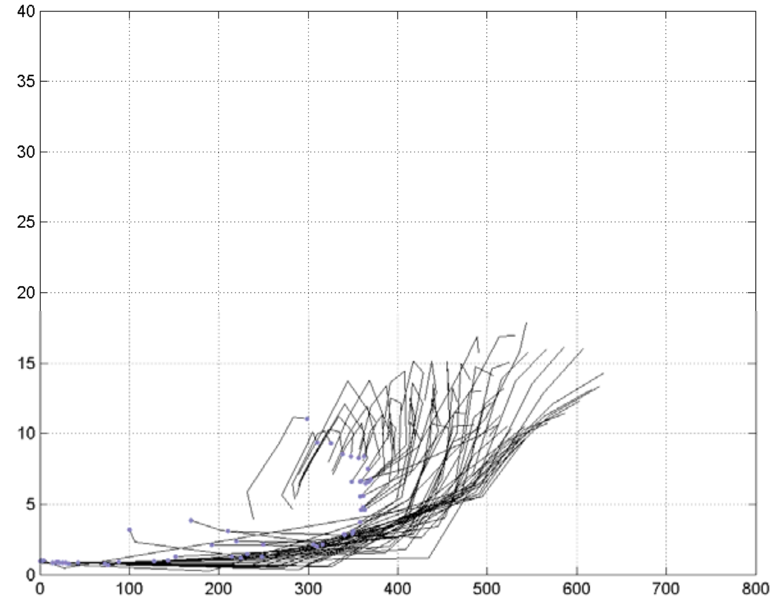

40
35
30
25
20
15
10
5
0
0
100
200
300
400
500
600
700
800

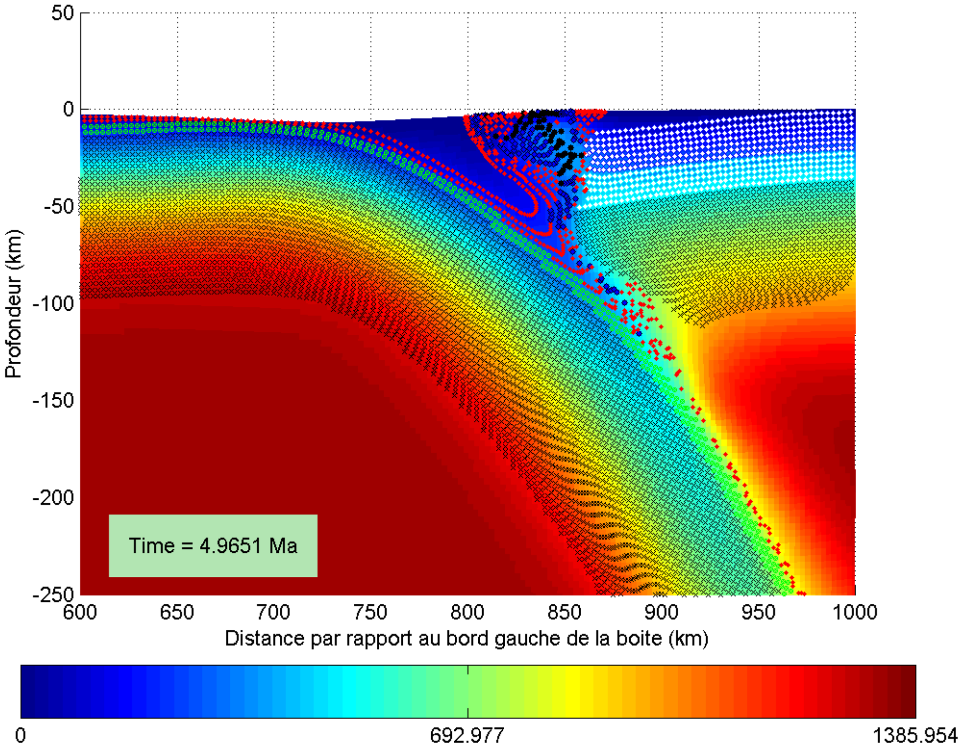

Time = 4.9651 Ma
Profondeur (km)
50
0
-50
-100
-150
-200
-250
600
650
700
750
800
850
900
950
1000
Distance par rapport au bord gauche de la boite (km)
0
692.977
1385.954

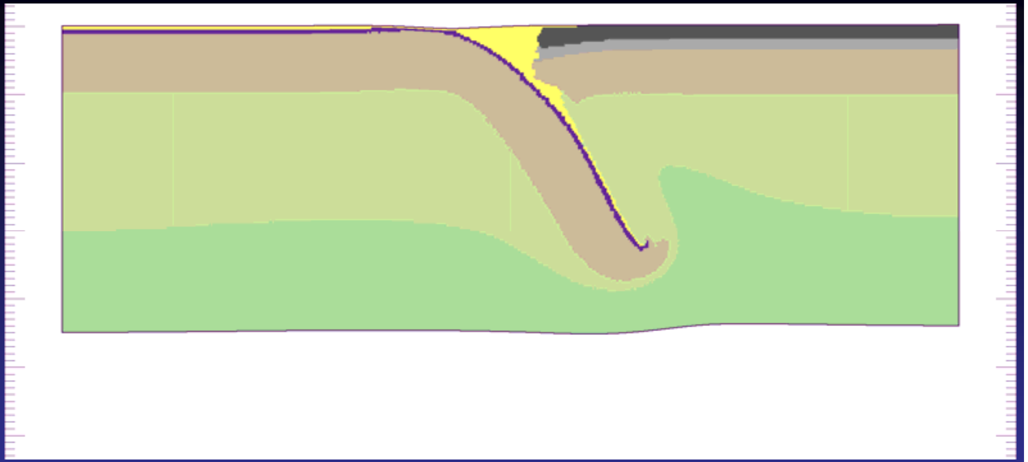

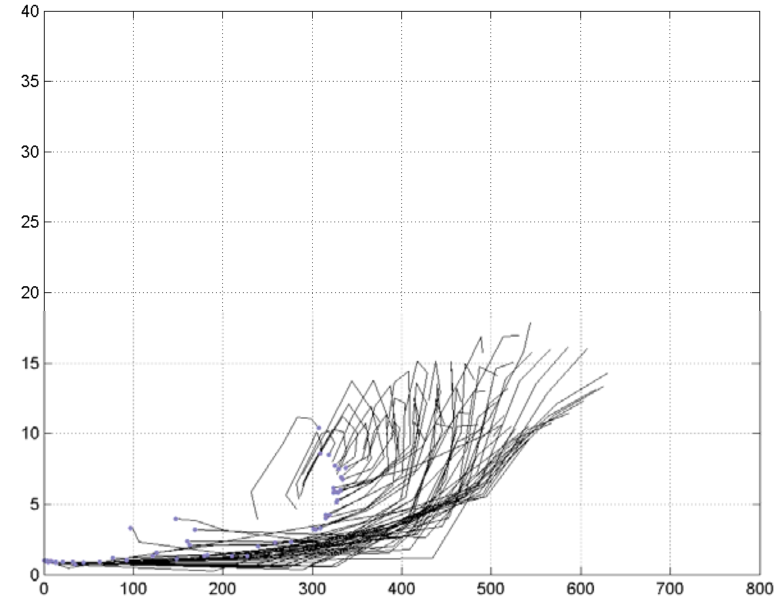

40
35
30
25
20
15
10
5
0
0
100
200
300
400
500
600
700
800

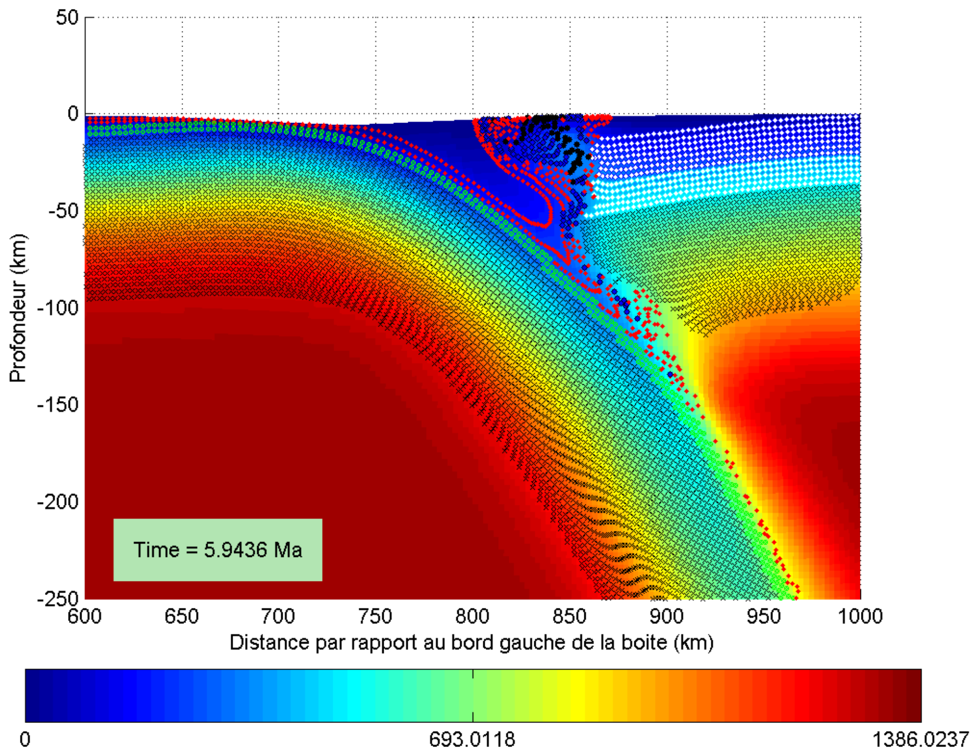

50
0
-50
-100
-150
-200
-250
Profondeur (km)
Time = 5.9436 Ma
600
650
700
750
800
850
900
950
1000
Distance par rapport au bord gauche de la boite (km)
0
693.0118
1386.0237

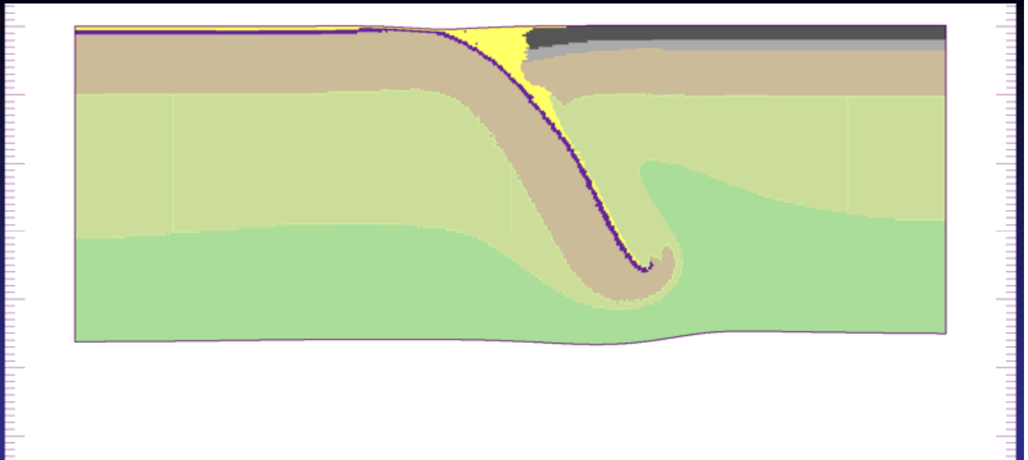

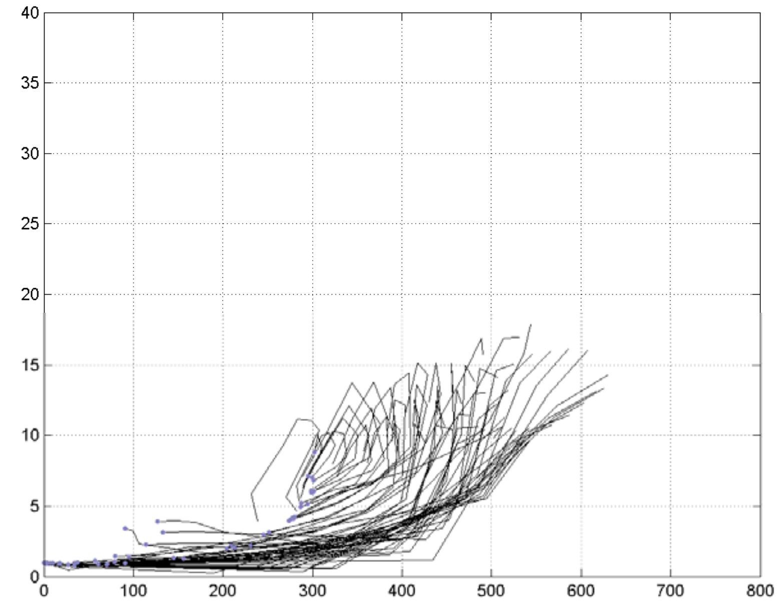
40
35
30
25
20
15
10
5
0
0
100
200
300
400
500
600
700
800

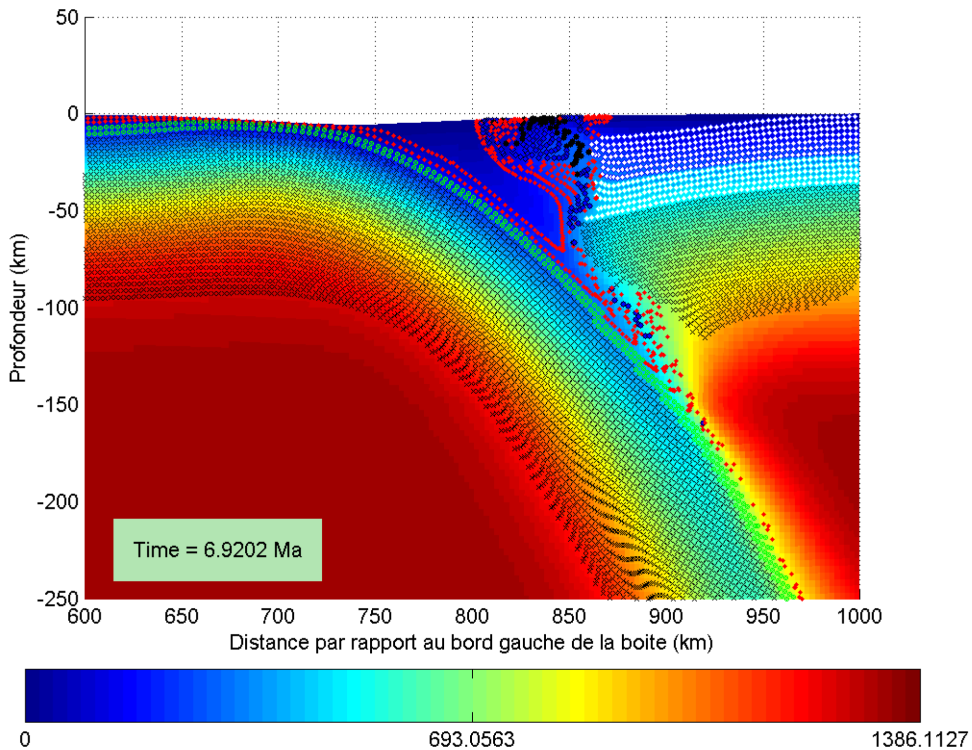
50
0
-50
-100
-150
-200
-250
Profondeur (km)
Time = 6.9202 Ma
600
650
700
750
800
850
900
950
1000
Distance par rapport au bord gauche de la boite (km)
0
693.0563
1386.1127

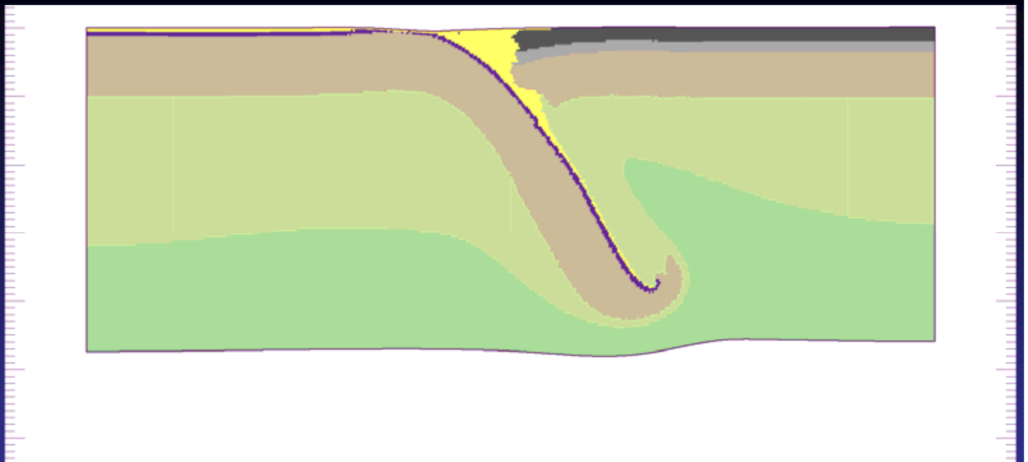

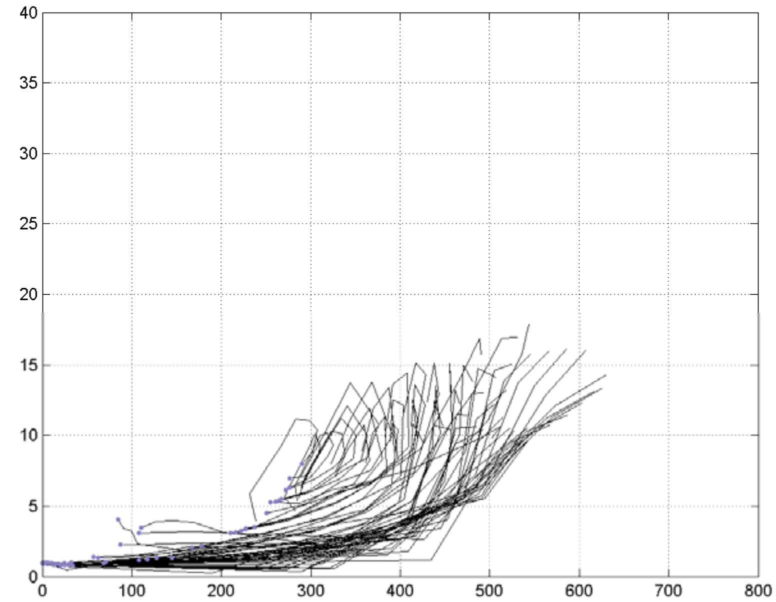

40
35
30
25
20
15
10
5
0
0
100
200
300
400
500
600
700
800

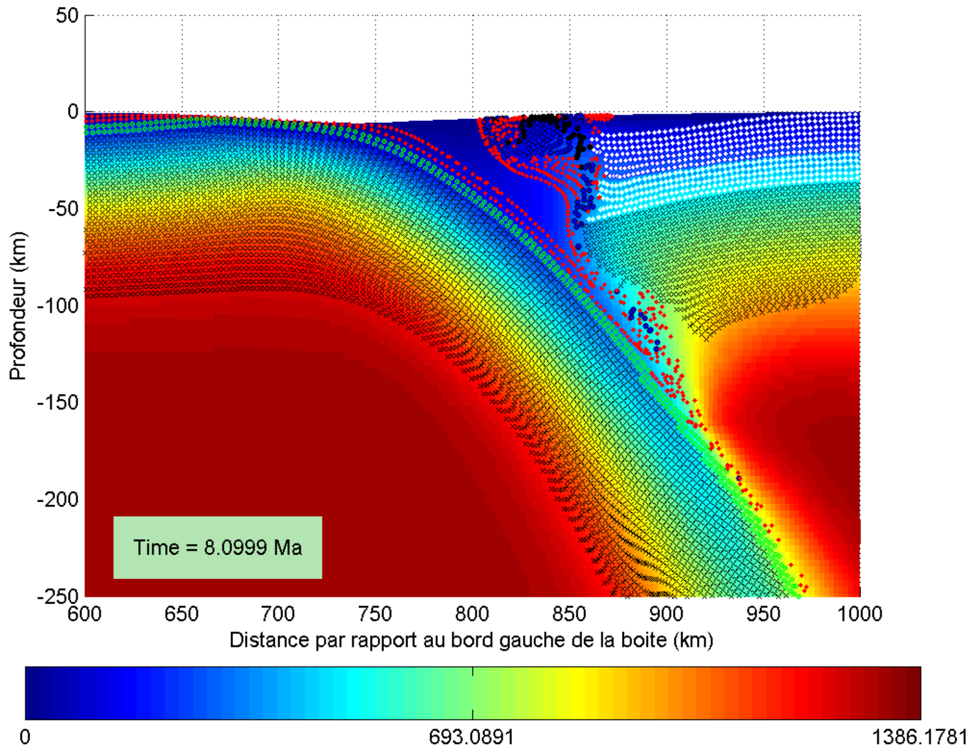

50
0
-50
-100
-150
-200
-250
Profondeur (km)
Time = 8.0999 Ma
600
650
700
750
800
850
900
950
1000
Distance par rapport au bord gauche de la boite (km)
0
693.0891
1386.1781

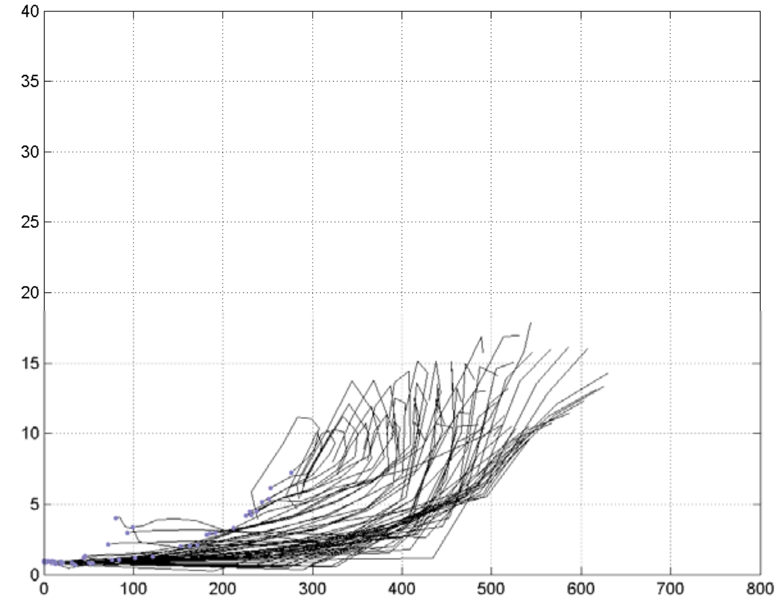

40
35
30
25
20
15
10
5
0
0
100
200
300
400
500
600
700
800

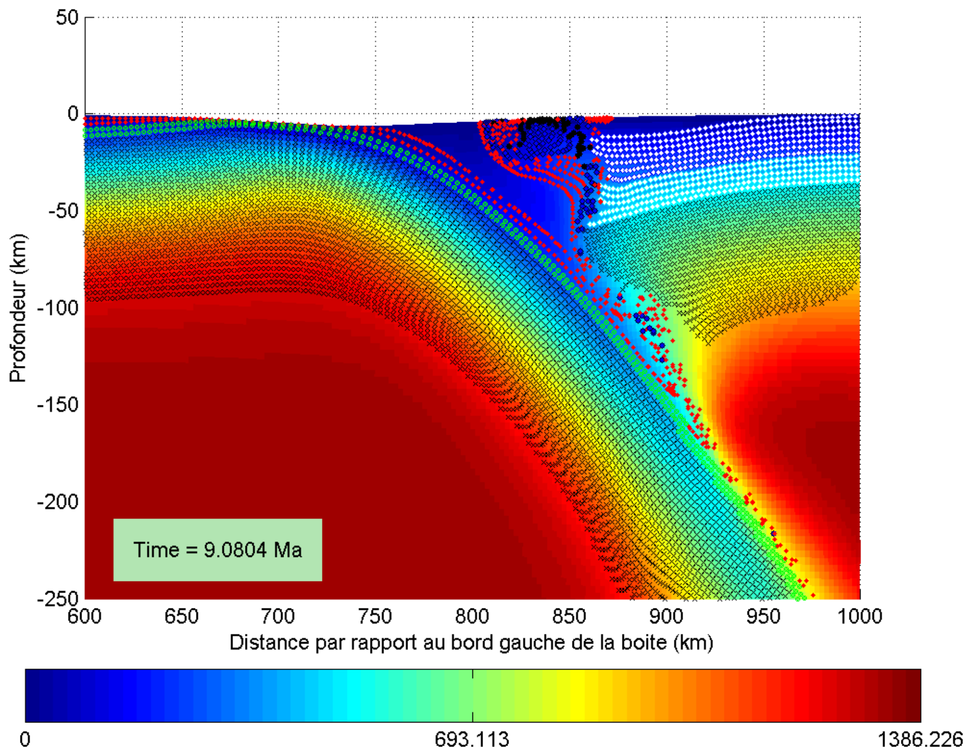

50
0
-50
-100
-150
-200
-250
Profondeur (km)
Time = 9.0804 Ma
600
650
700
750
800
850
900
950
1000
Distance par rapport au bord gauche de la boite (km)
0
693.113
1386.226

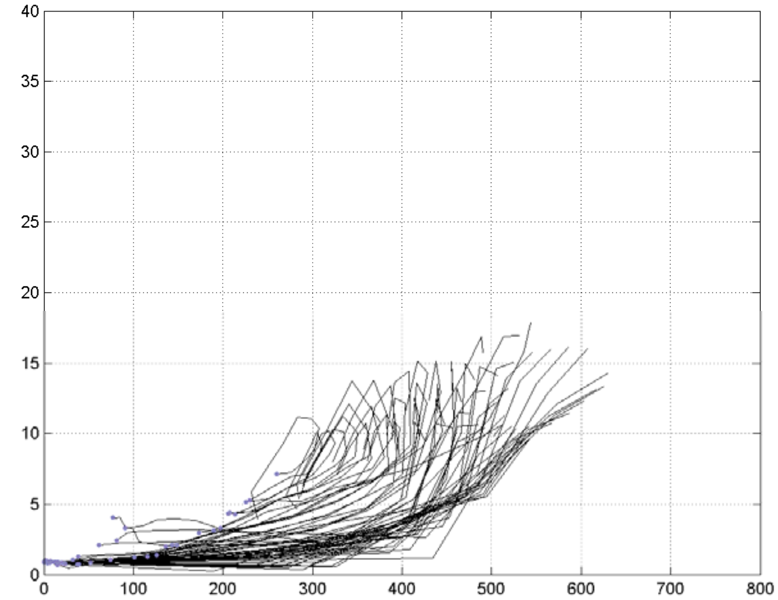

40
35
30
25
20
15
10
5
0
0
100
200
300
400
500
600
700
800

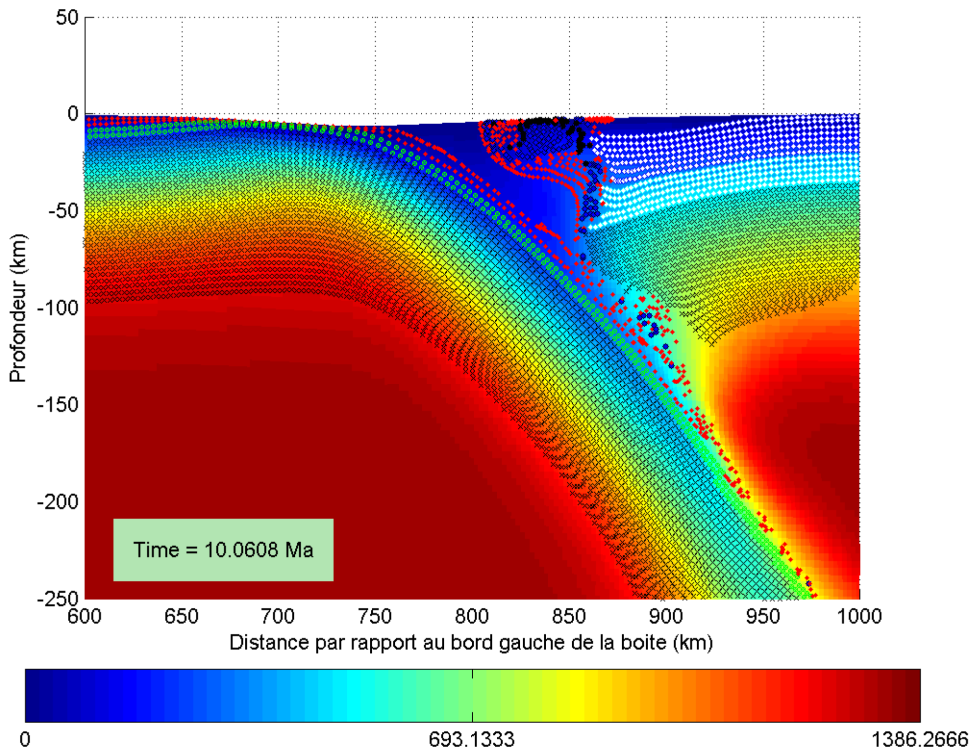

50
0
-50
-100
-150
-200
-250
Profondeur (km)
600
650
700
750
800
850
900
950
1000
Distance par rapport au bord gauche de la boite (km)
Time = 10.0608 Ma
0
693.1333
1386.2666

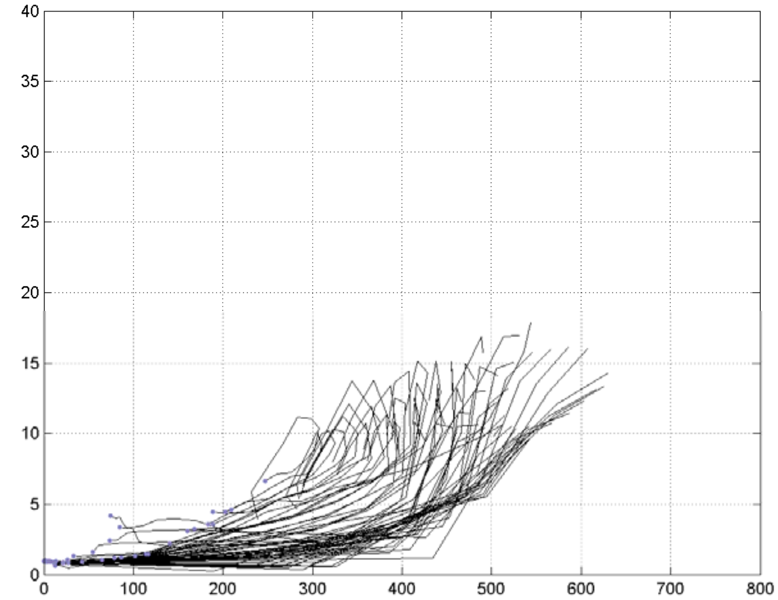

40
35
30
25
20
15
10
5
0
0 100 200 300 400 500 600 700 800

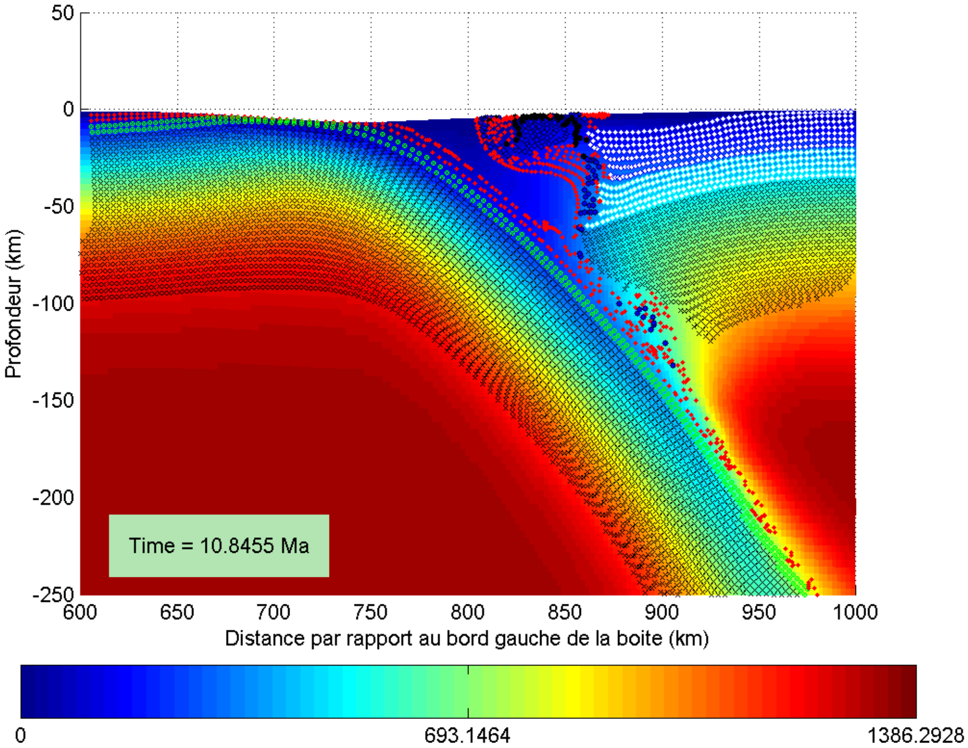

50
0
-50
-100
-150
-200
-250
Profondeur (km)
Time = 10.8455 Ma
600 650 700 750 800 850 900 950 1000
Distance par rapport au bord gauche de la boite (km)
0
693.1464
1386.2928

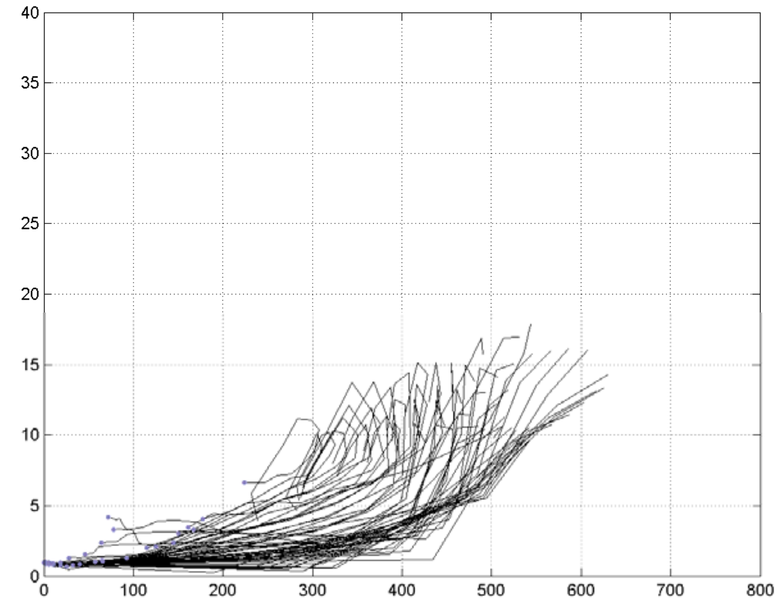

40
35
30
25
20
15
10
5
0
0
100
200
300
400
500
600
700
800

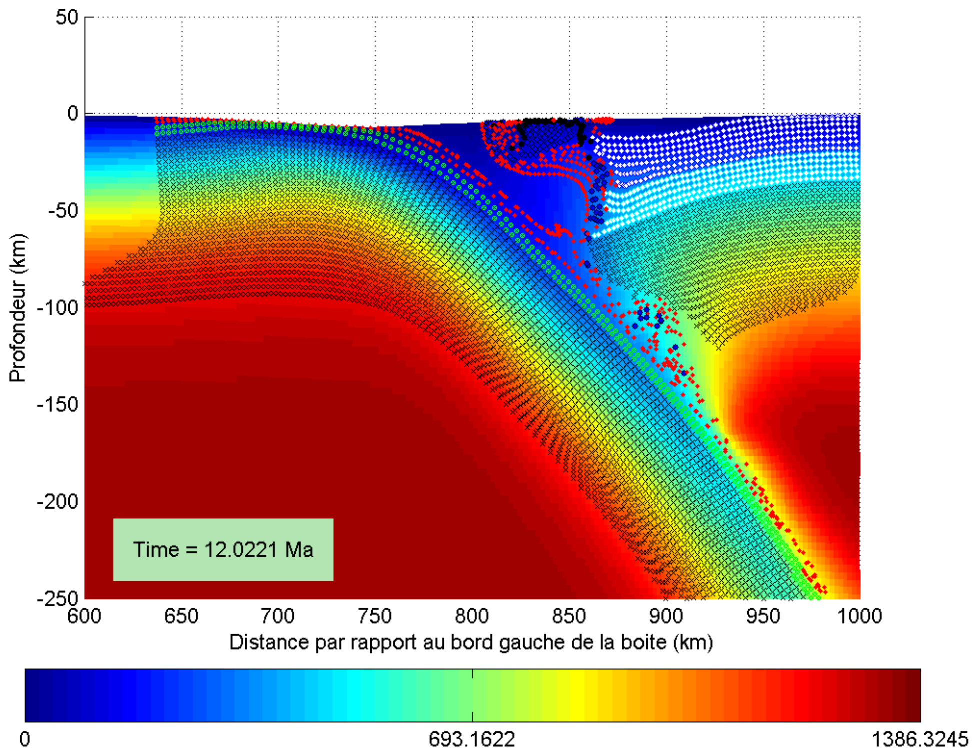

50
0
-50
-100
-150
-200
-250
Profondeur (km)
600
650
700
750
800
850
900
950
1000
Distance par rapport au bord gauche de la boite (km)
Time = 12.0221 Ma
0
693.1622
1386.3245

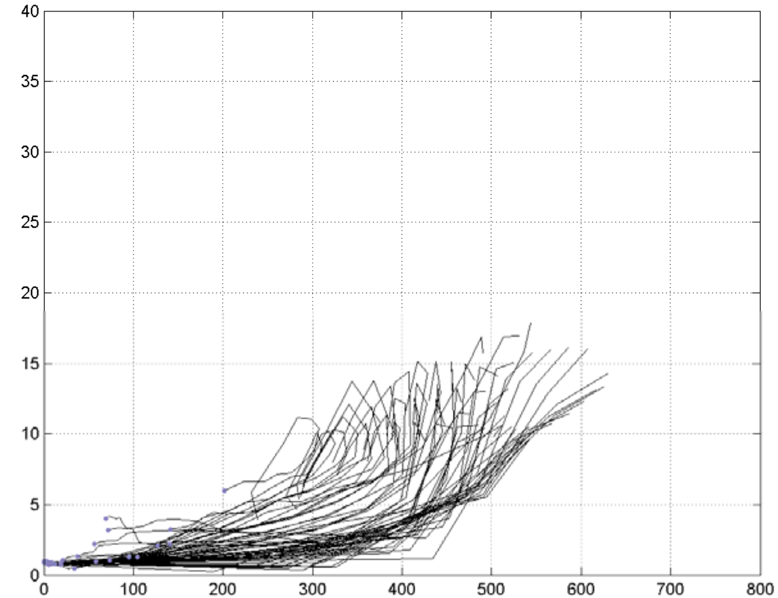
40
35
30
25
20
15
10
5
0
0
100
200
300
400
500
600
700
800

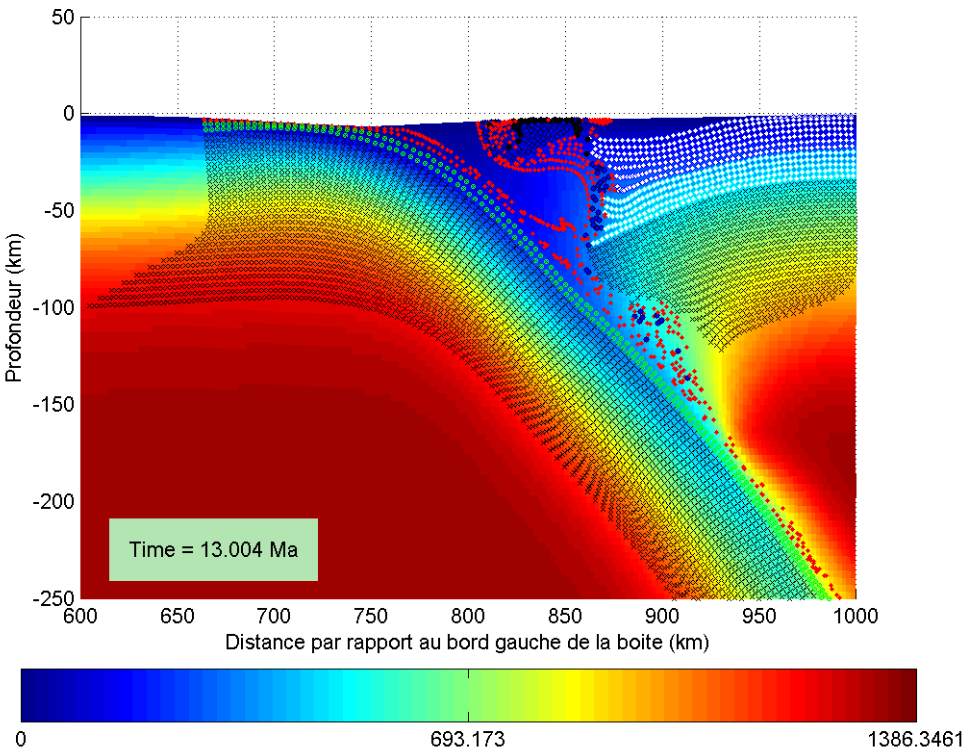
50
0
-50
-100
-150
-200
-250
Profondeur (km)
600
650
700
750
800
850
900
950
1000
Distance par rapport au bord gauche de la boite (km)
Time = 13.004 Ma
0
693.173
1386.3461

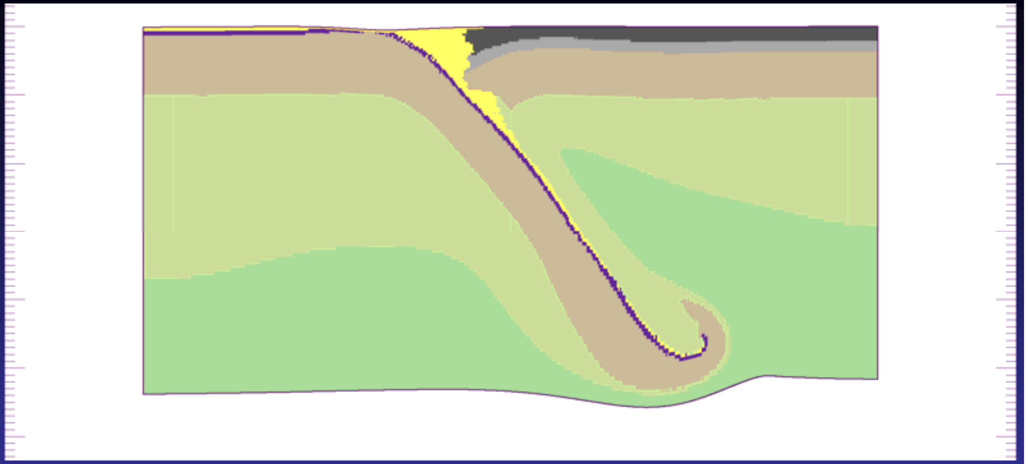

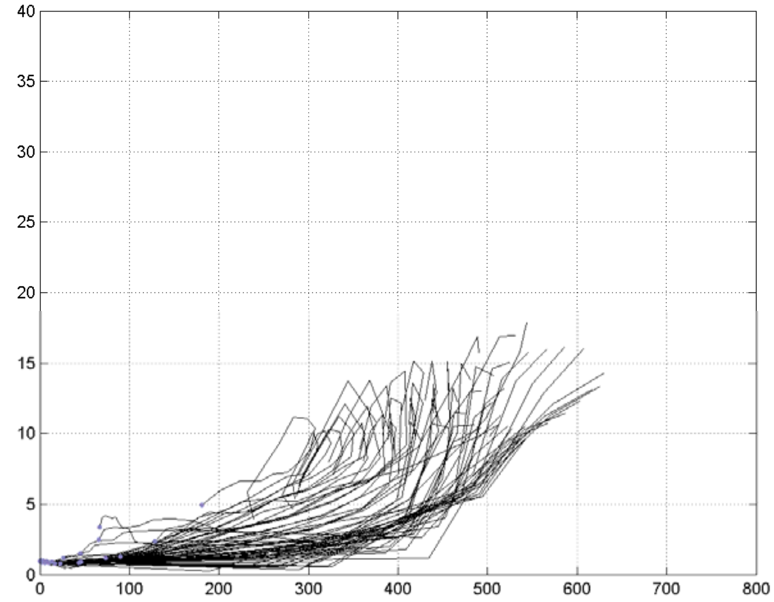

40
35
30
25
20
15
10
5
0
0
100
200
300
400
500
600
700
800

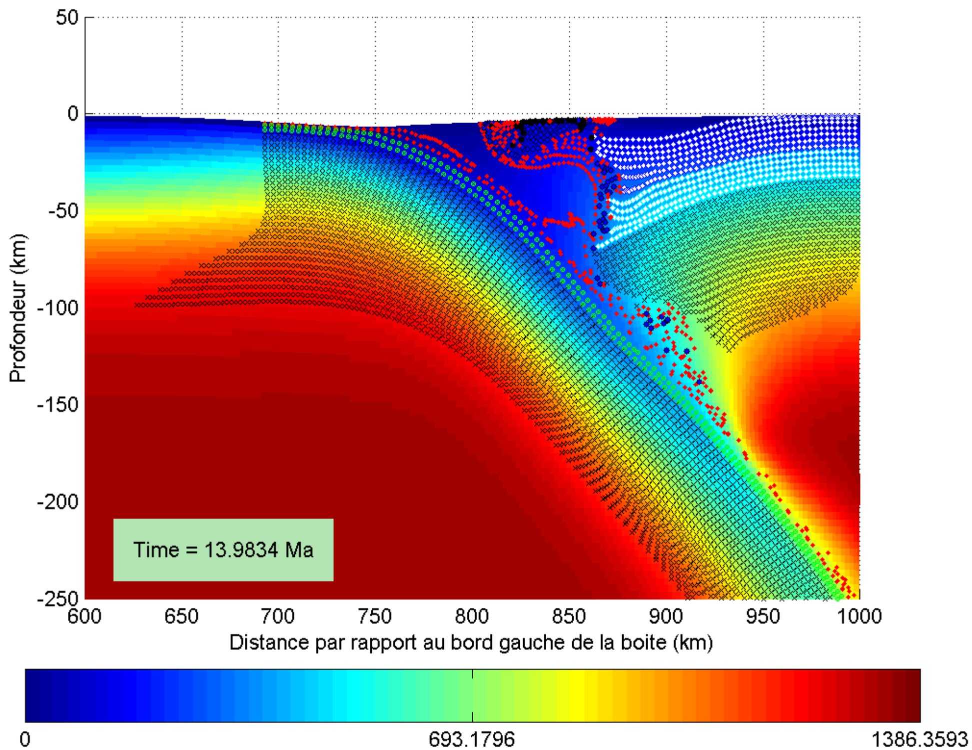

50
0
-50
-100
-150
-200
-250
Profondeur (km)
Time = 13.9834 Ma
600
650
700
750
800
850
900
950
1000
Distance par rapport au bord gauche de la boite (km)
0
693.1796
1386.3593

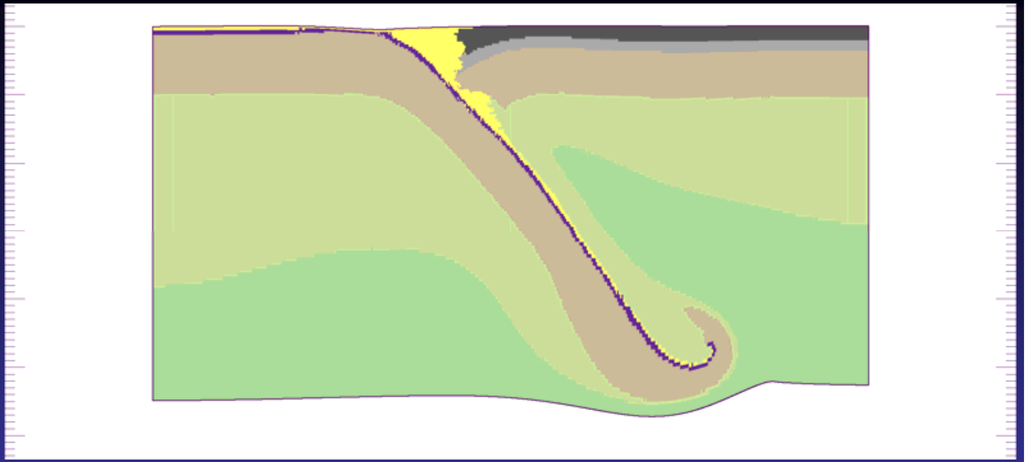

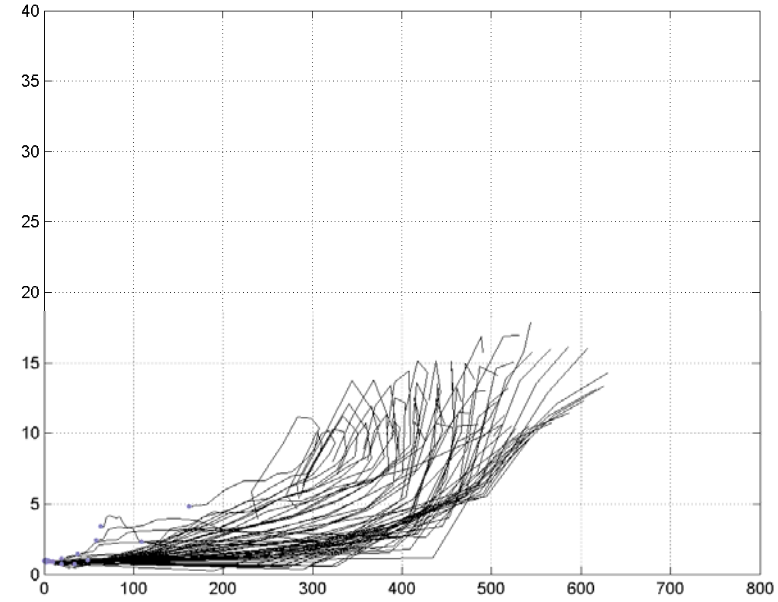

40
35
30
25
20
15
10
5
0
0
100
200
300
400
500
600
700
800

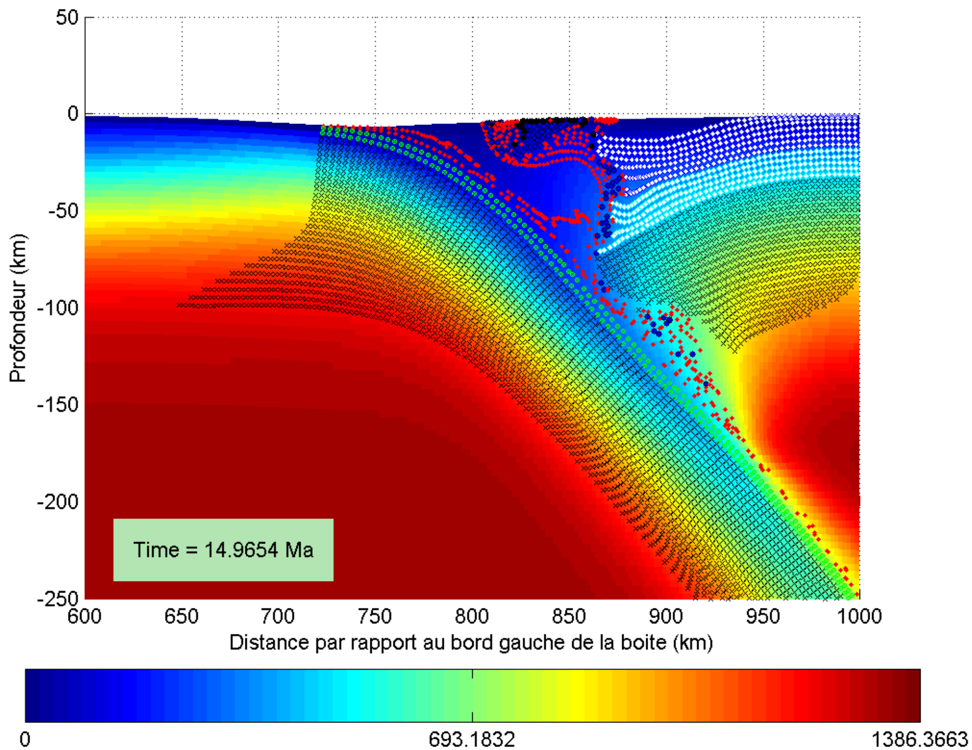

50
0
-50
-100
-150
-200
-250
Profondeur (km)
Time = 14.9654 Ma
600
650
700
750
800
850
900
950
1000
Distance par rapport au bord gauche de la boite (km)
0
693.1832
1386.3663

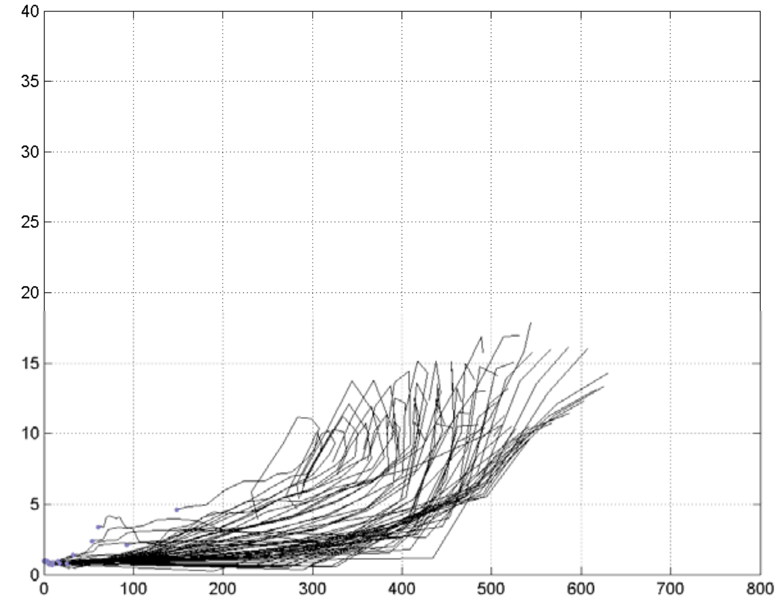

40
35
30
25
20
15
10
5
0
0
100
200
300
400
500
600
700
800

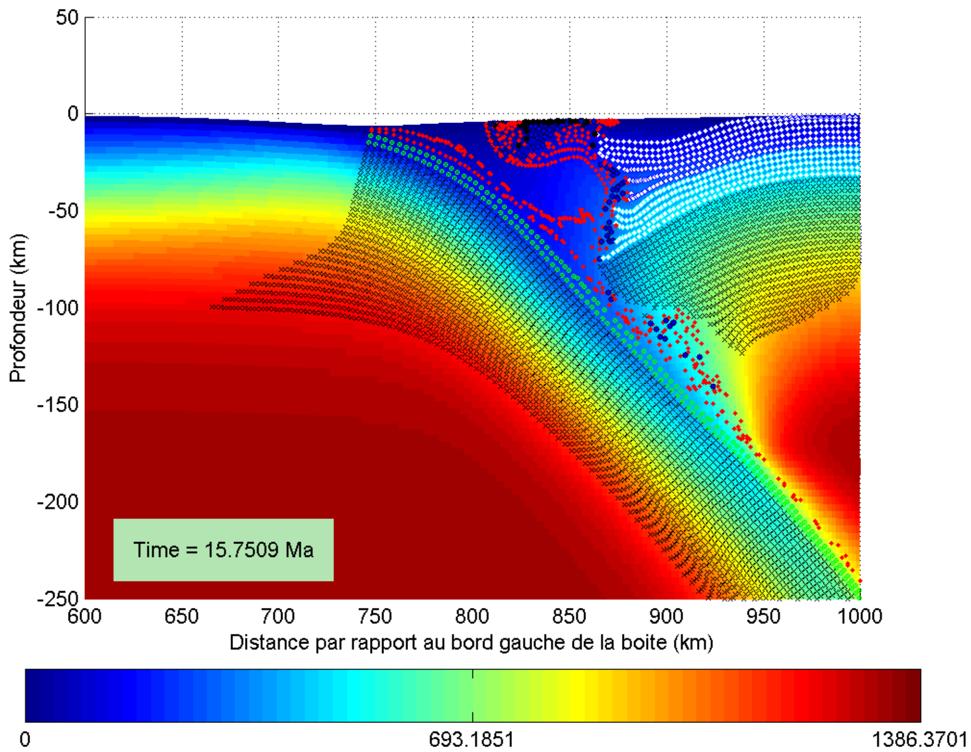

50
0
-50
-100
-150
-200
-250
Profondeur (km)
Time = 15.7509 Ma
600
650
700
750
800
850
900
950
1000
Distance par rapport au bord gauche de la boite (km)
0
693.1851
1386.3701

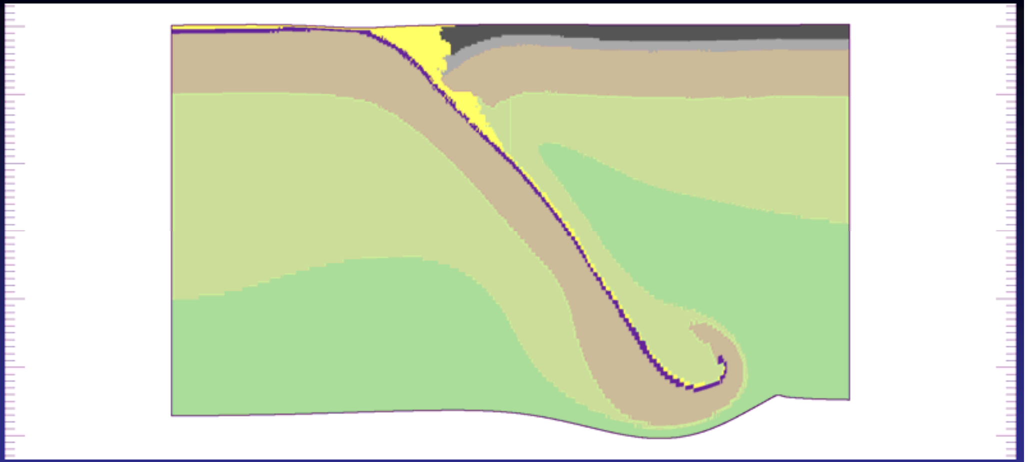

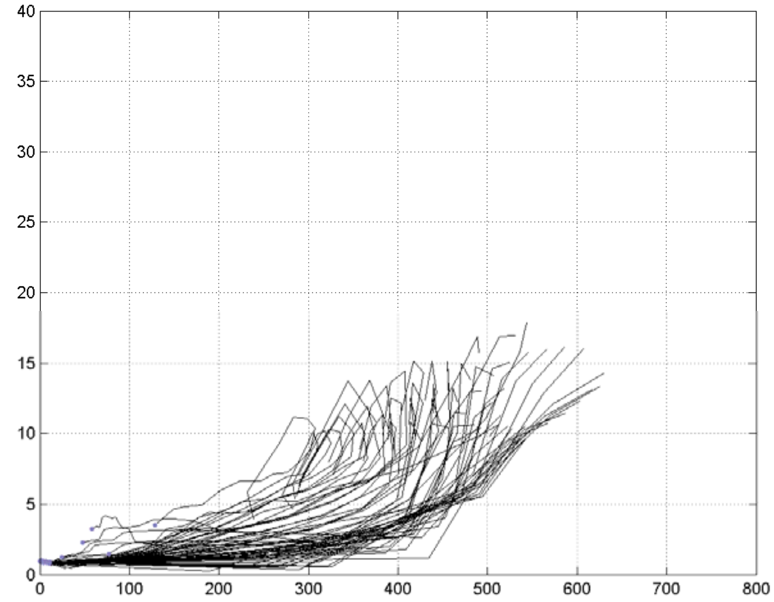

40
35
30
25
20
15
10
5
0
0
100
200
300
400
500
600
700
800

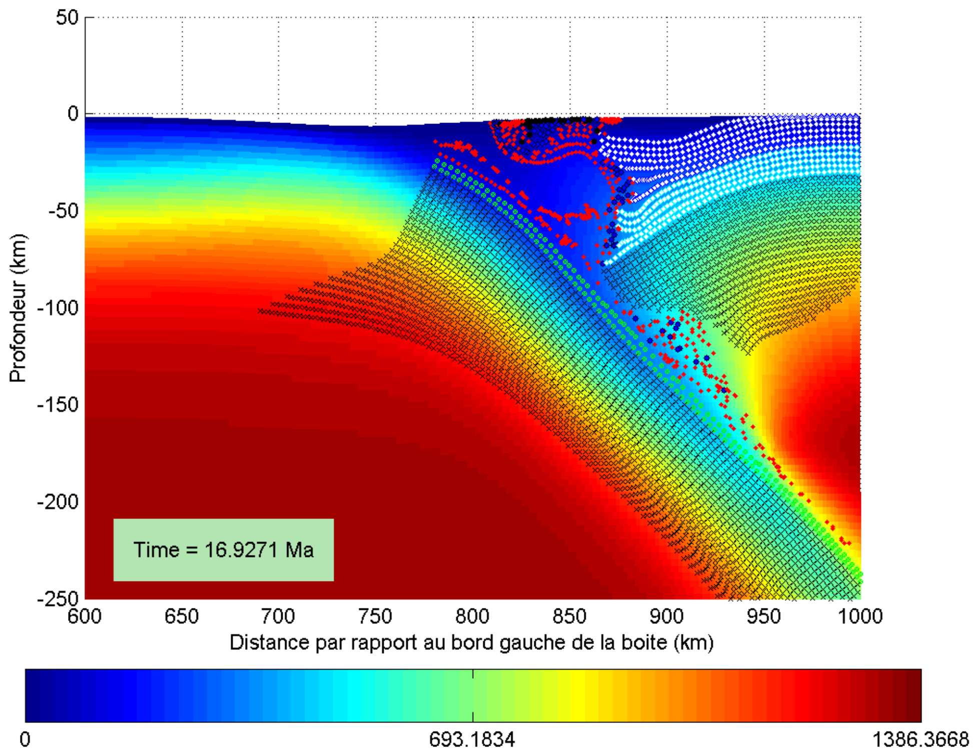

50
0
-50
-100
-150
-200
-250
Profondeur (km)
Time = 16.9271 Ma
600
650
700
750
800
850
900
950
1000
Distance par rapport au bord gauche de la boite (km)
0
693.1834
1386.3668

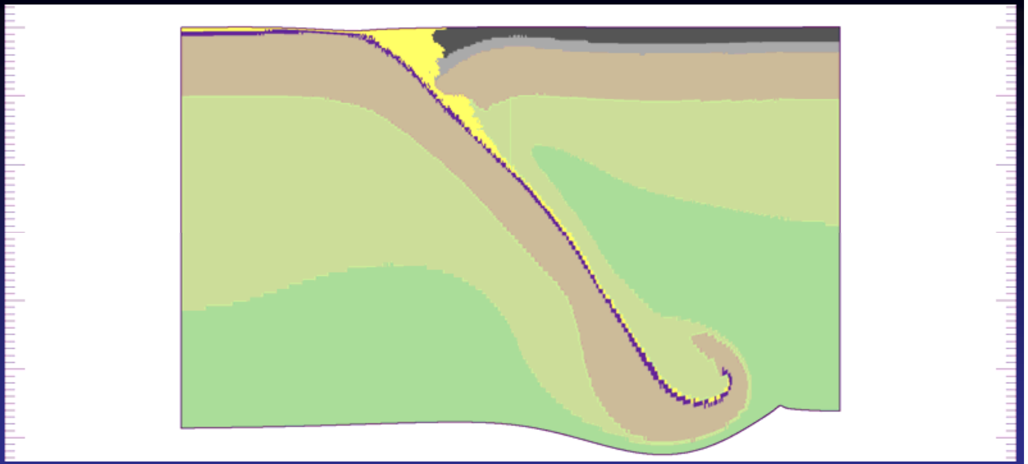

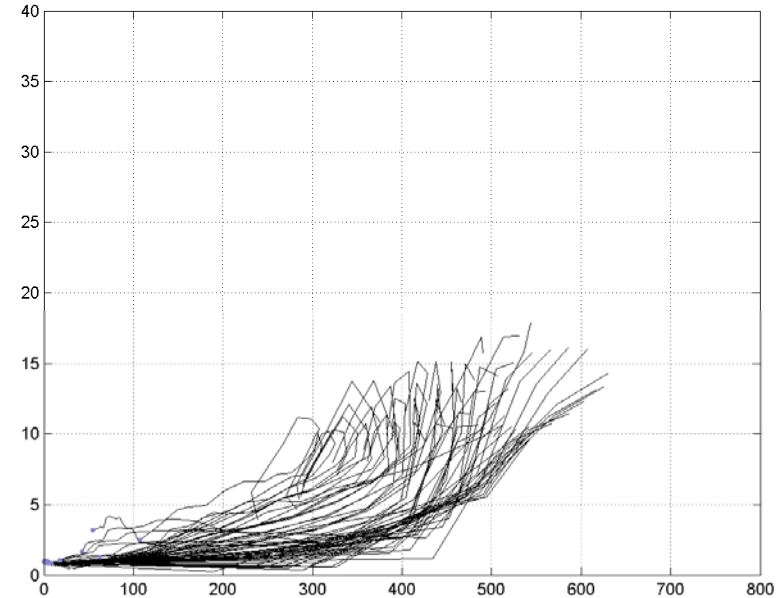

40
35
30
25
20
15
10
5
0
0
100
200
300
400
500
600
700
800

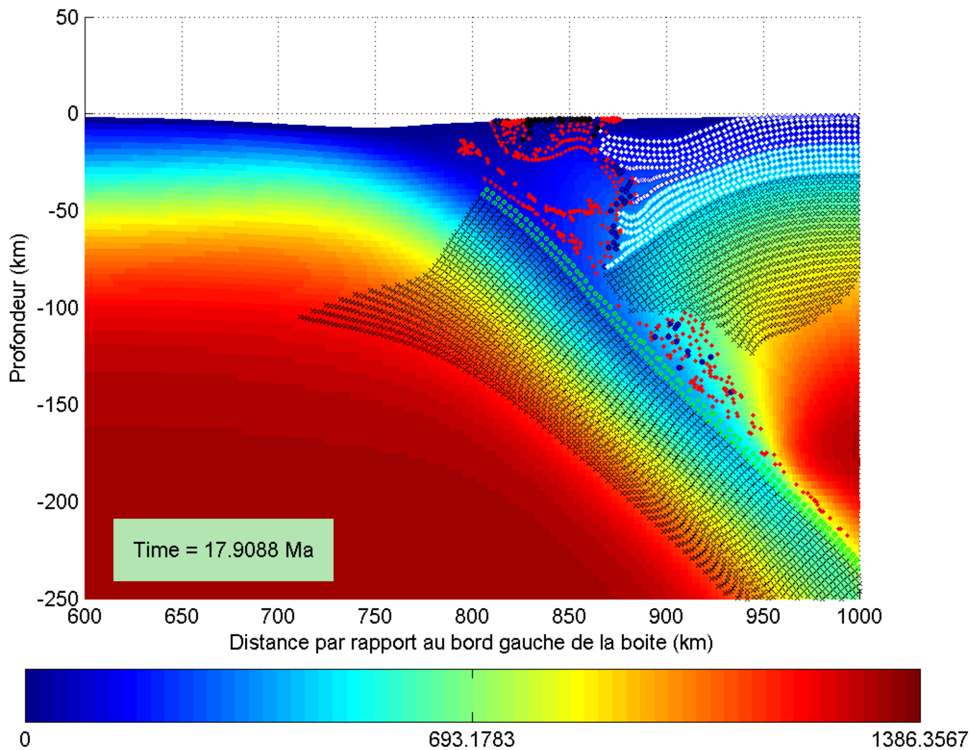

50
0
-50
-100
-150
-200
-250
600
650
700
750
800
850
900
950
1000
Profondeur (km)
Distance par rapport au bord gauche de la boite (km)
Time = 17.9088 Ma
0
693.1783
1386.3567

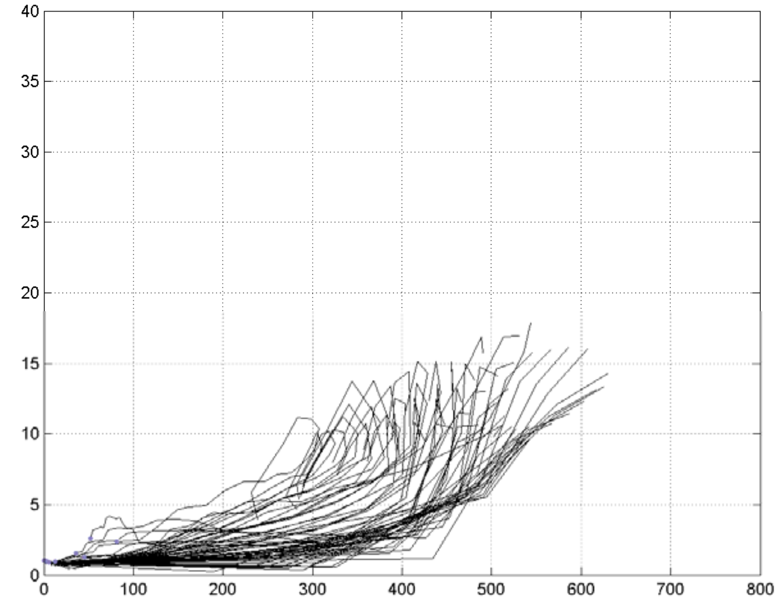
40
35
30
25
20
15
10
5
0
0
100
200
300
400
500
600
700
800

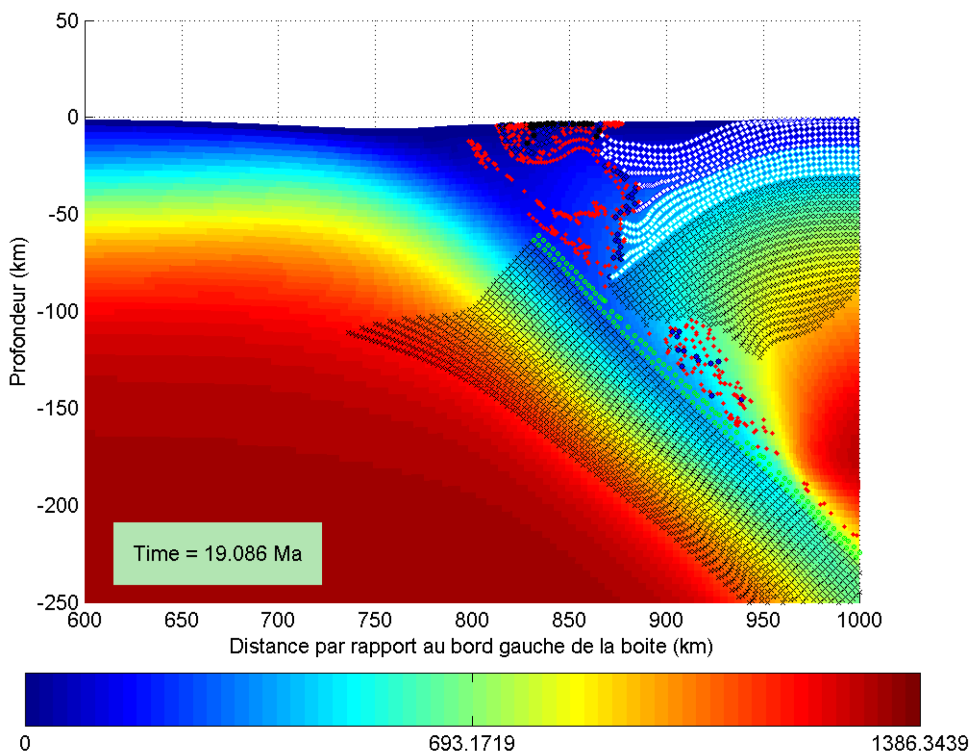
50
0
-50
-100
-150
-200
-250
Profondeur (km)
Time = 19.086 Ma
600
650
700
750
800
850
900
950
1000
Distance par rapport au bord gauche de la boite (km)
0
693.1719
1386.3439

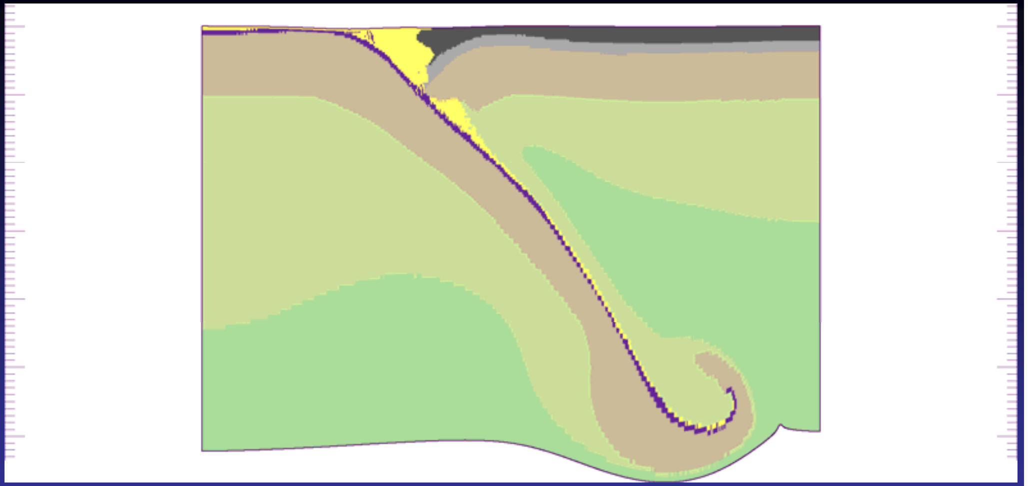

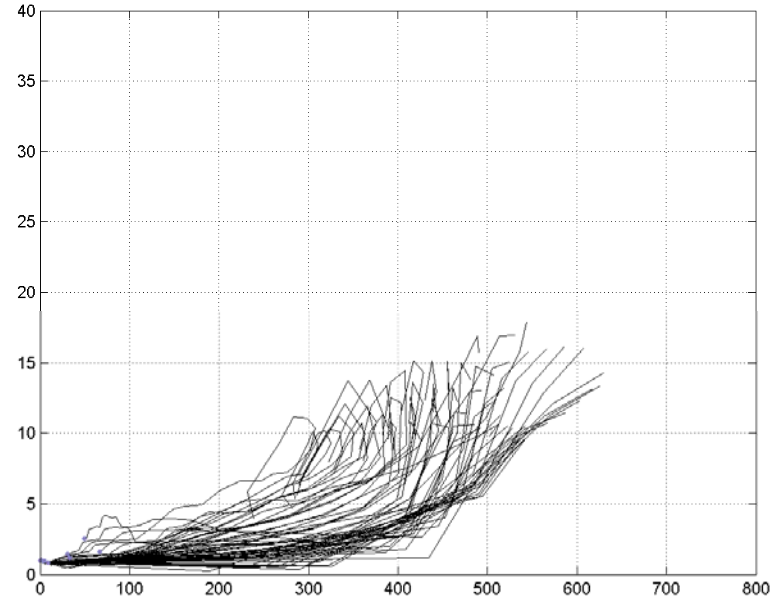

40
35
30
25
20
15
10
5
0
0
100
200
300
400
500
600
700
800

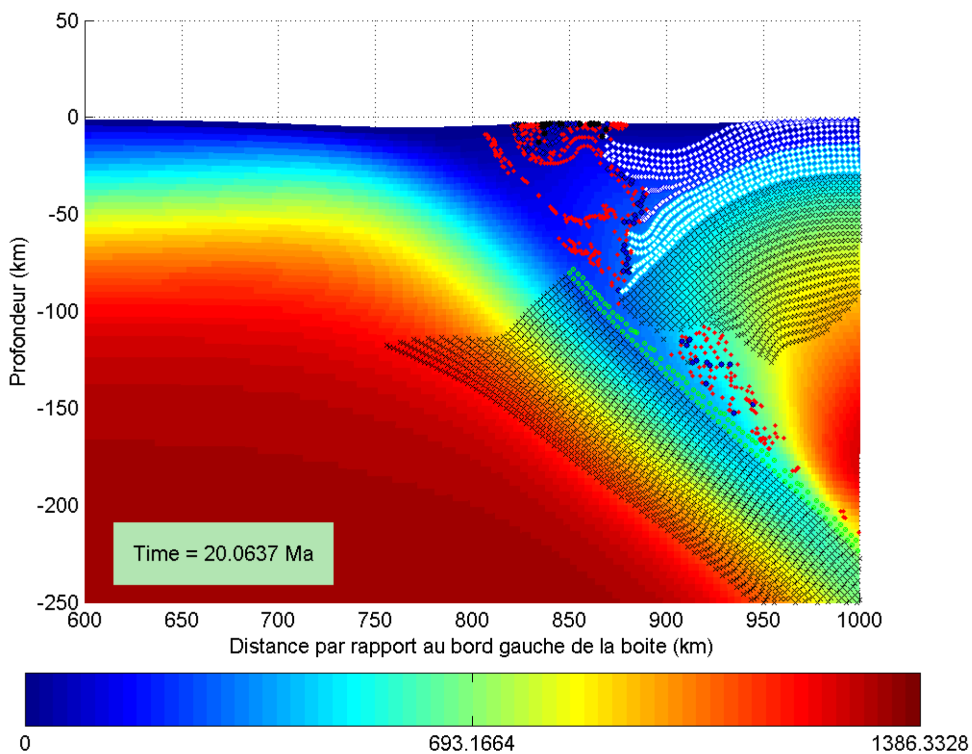

50
0
-50
-100
-150
-200
-250
Profondeur (km)
600
650
700
750
800
850
900
950
1000
Distance par rapport au bord gauche de la boite (km)
Time = 20.0637 Ma
0
693.1664
1386.3328

The Results:

Evolution of an accretion prism

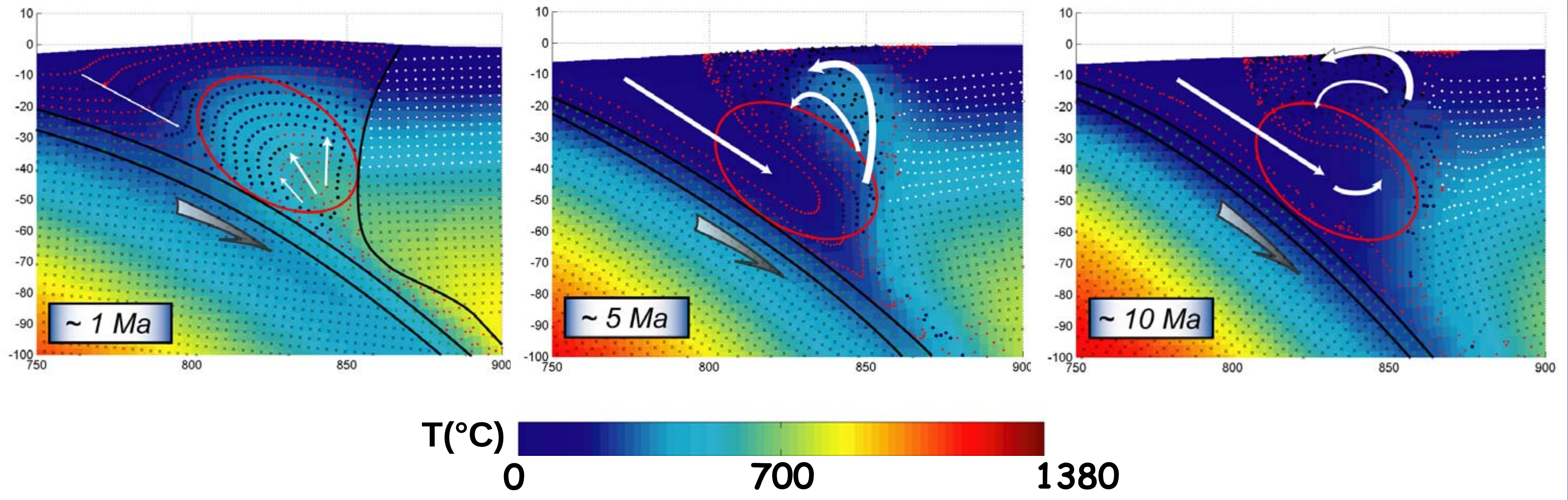

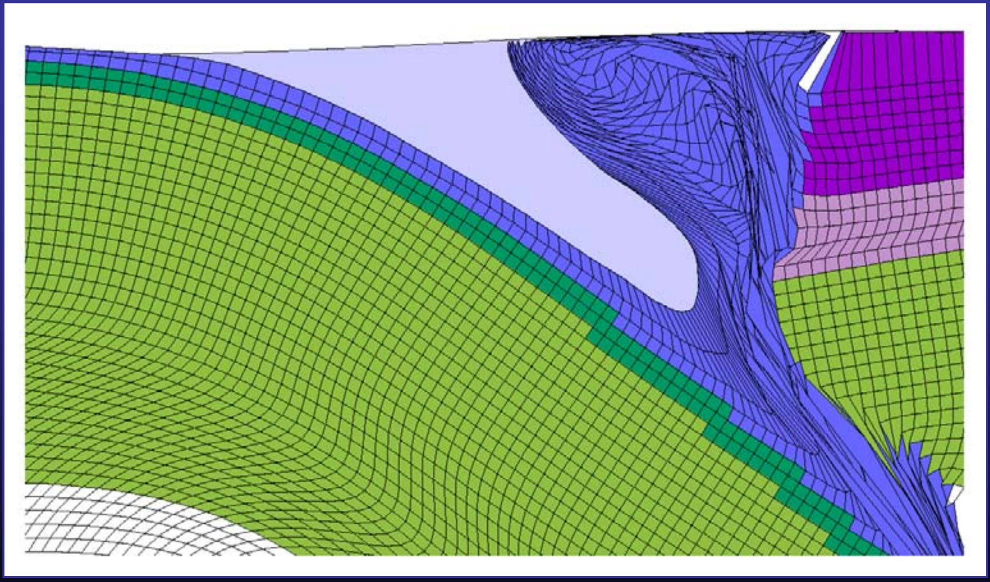

The Results

➡ Observed versus predicted P-T-t paths

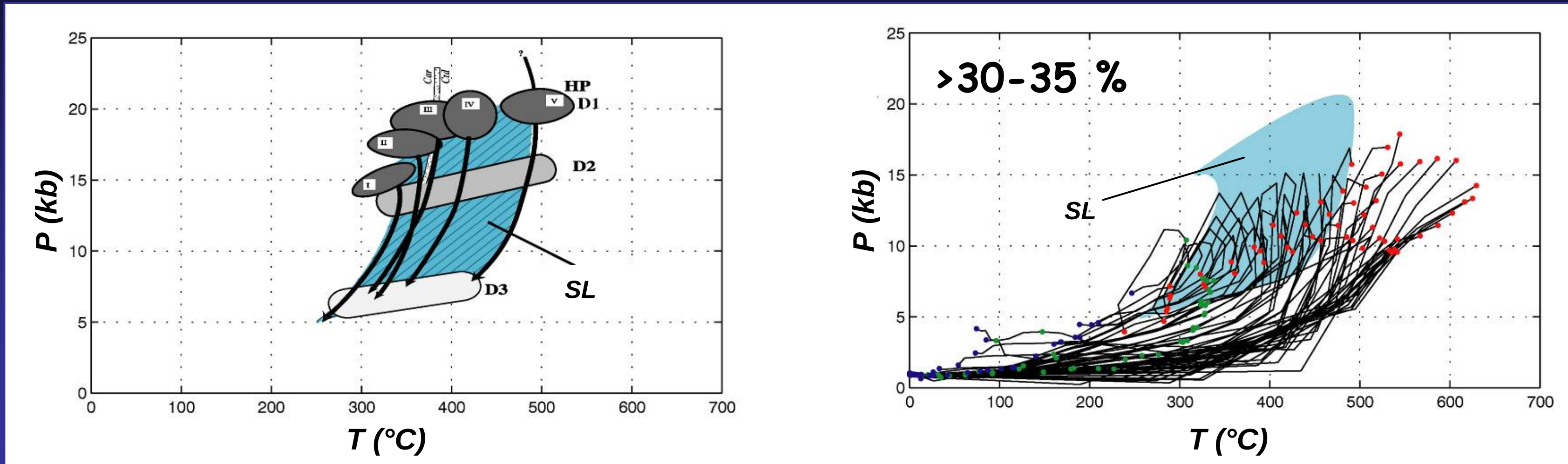

➡ Exhumation rates of sediments in the accretion prism

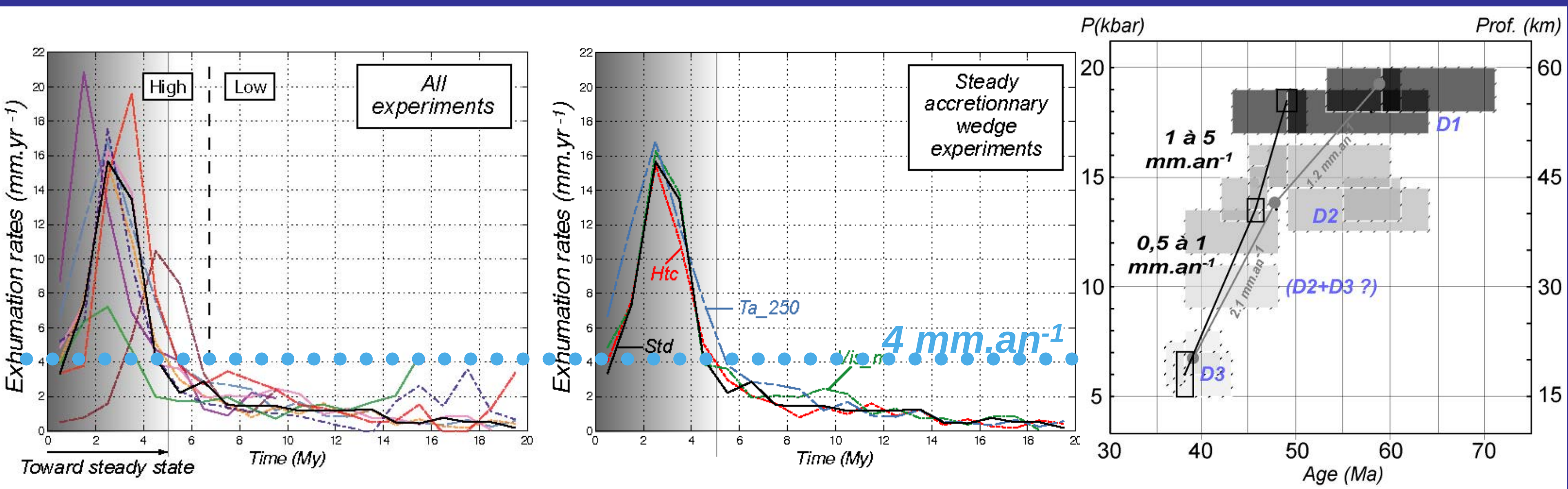

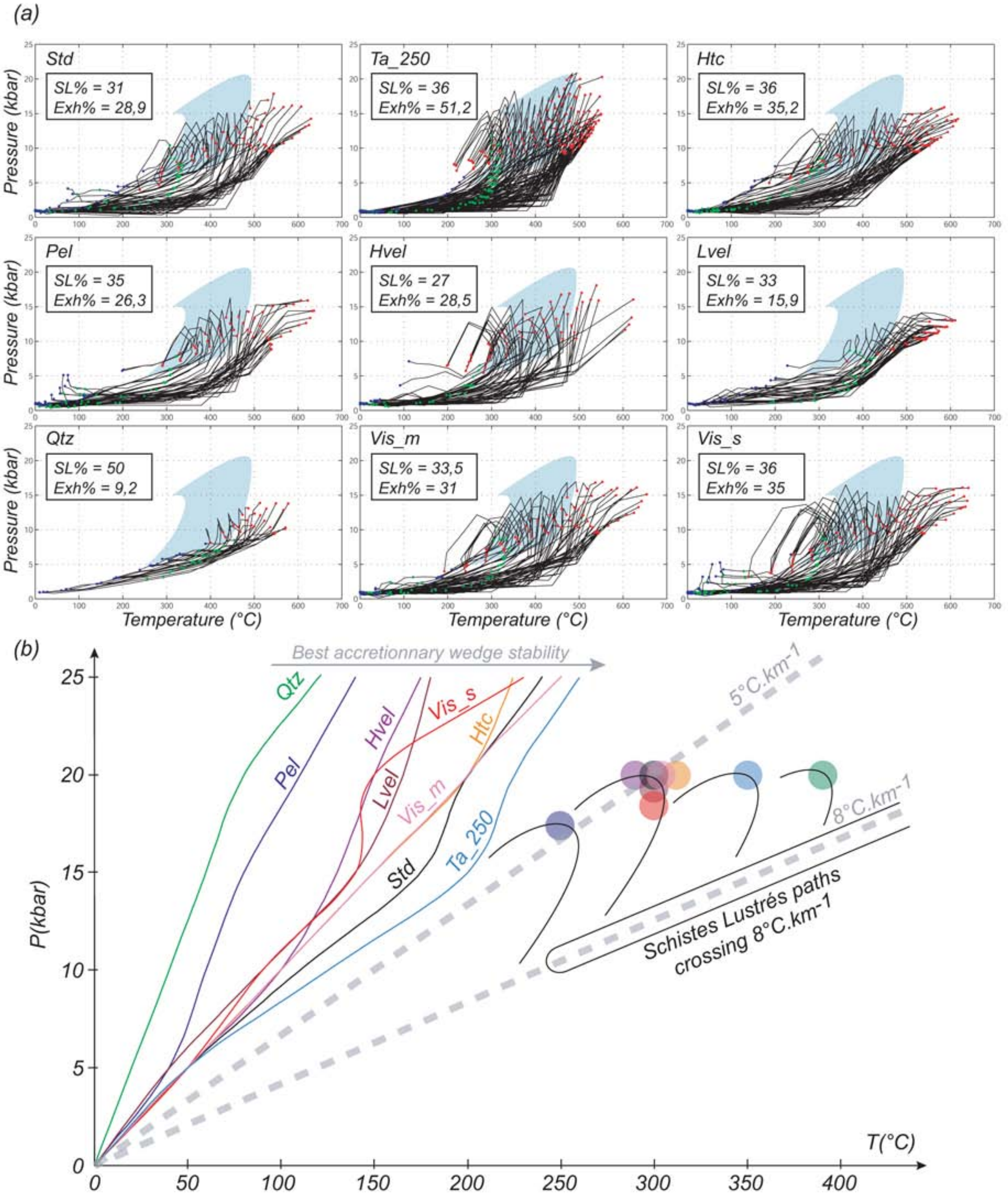
(a)
Std
SL% = 31
Exh% = 28,9
Ta_250
SL% = 36
Exh% = 51,2
Htc
SL% = 36
Exh% = 35,2
Pel
SL% = 35
Exh% = 26,3
Hvel
SL% = 27
Exh% = 28,5
Lvel
SL% = 33
Exh% = 15,9
Qtz
SL% = 50
Exh% = 9,2
Vis_m
SL% = 33,5
Exh% = 31
Vis_s
SL% = 36
Exh% = 35
Pressure (kbar)
Temperature (°C)
(b)
Best accretionnary wedge stability
Qtz
Pel
Hvel
Lvel
Vis_s
Htc
Vis_m
Std
Ta_250
5°C.km-1
8°C.km-1
Schistes Lustrés paths crossing 8°C.km-1
P(kbar)
T(°C)

Serpentinite layer (light, weak) below the oceanic crust: important condition for oceanic subduction

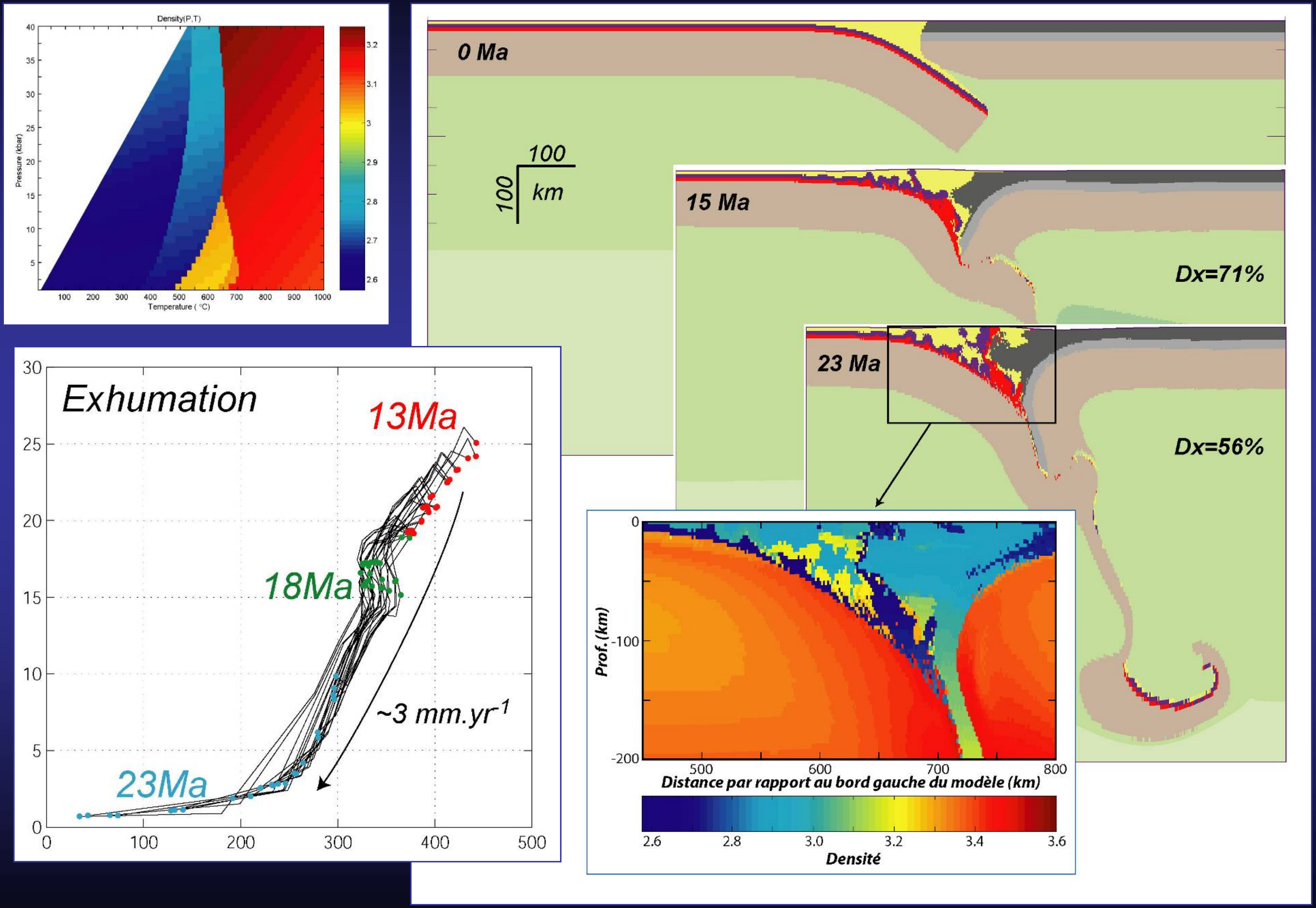

Slow Alpine Collision II:

continental phase

PhD thesis of Ph. Yamato;
Yamato et al., 2007

Alpine lithosphere-asthenosphere system

(*Courtesy of E. Kissling*)

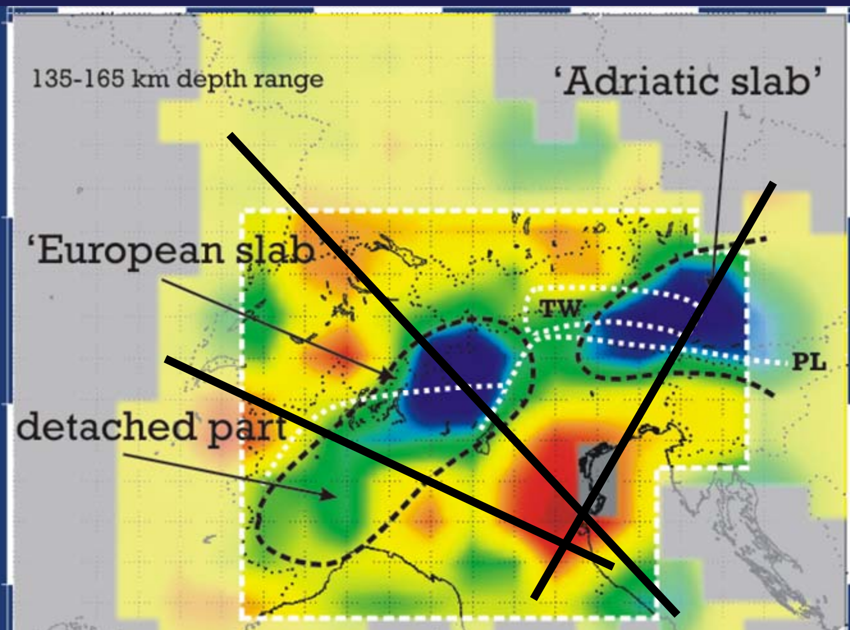

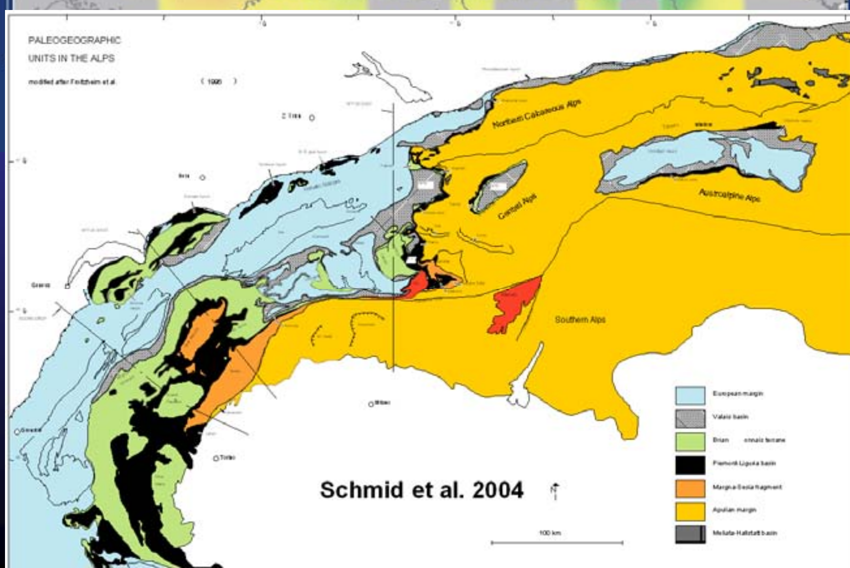

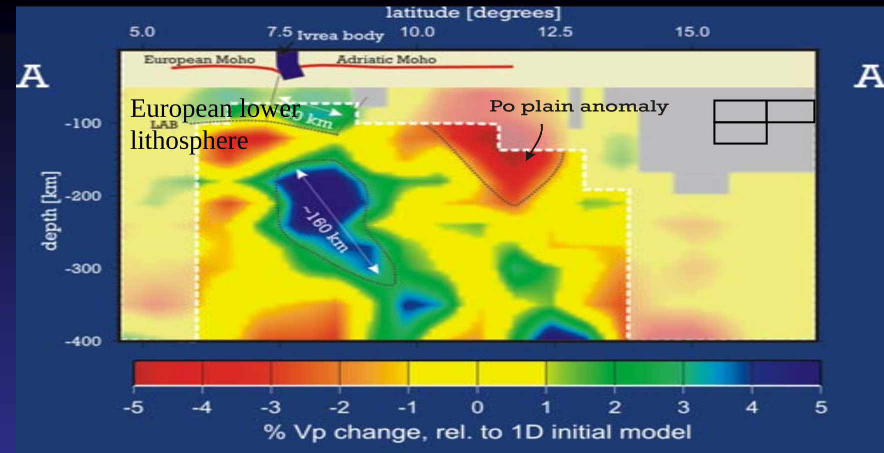

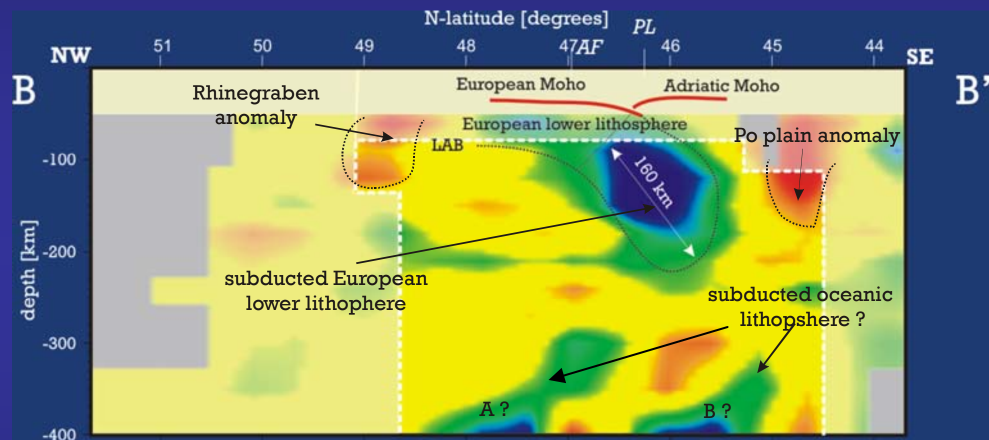

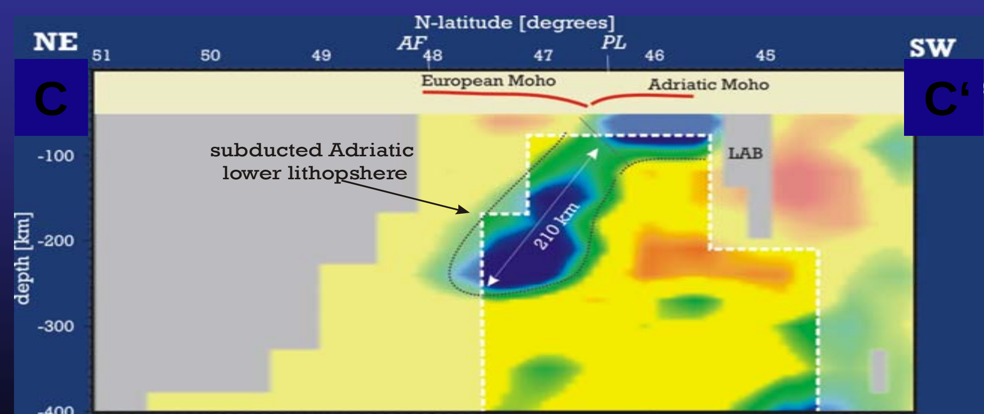

Lippitsch et al. 2003, JGR

SLOW collision, WEAK (Te<30 km) lithosphere

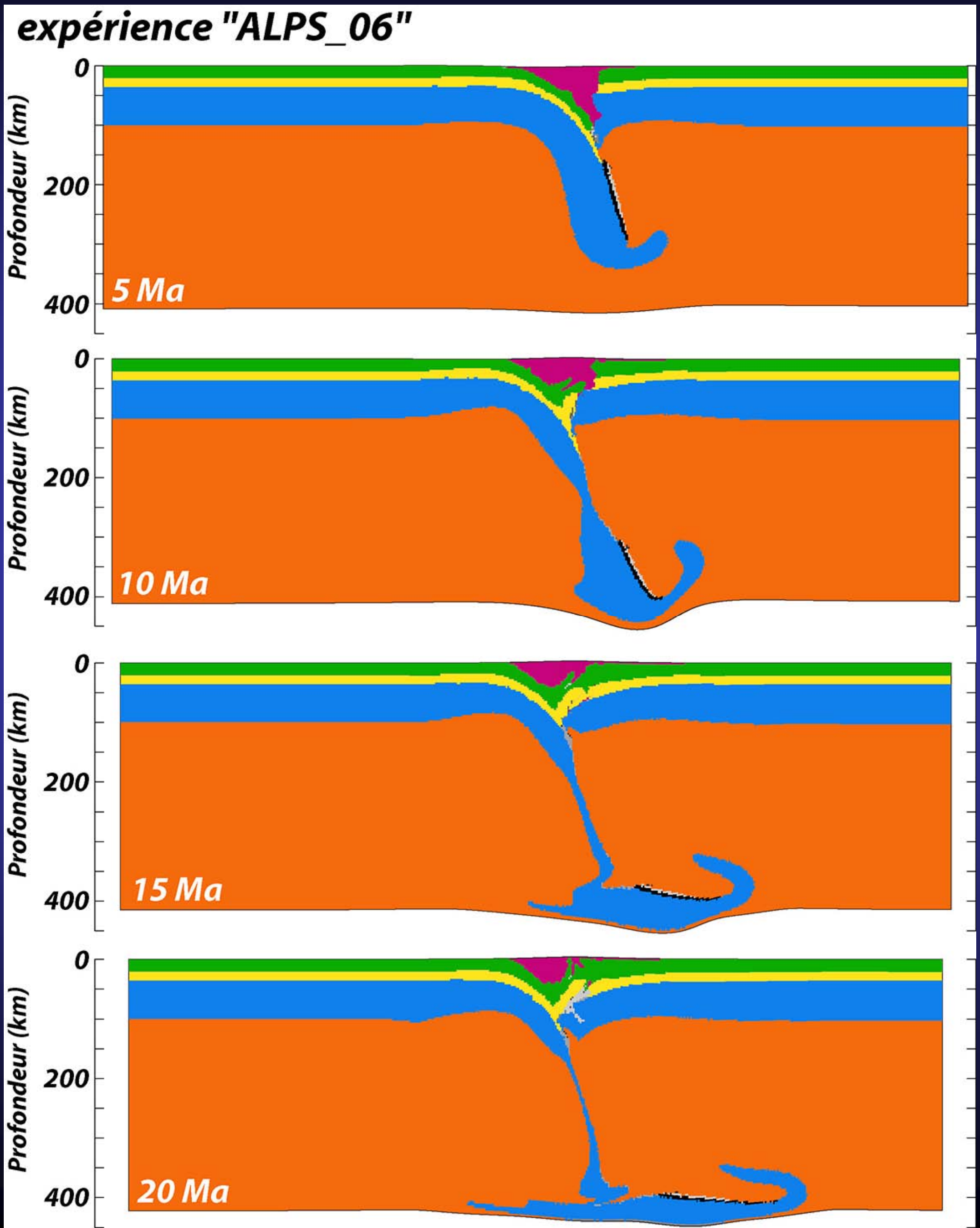

Influence of the crustal rheology

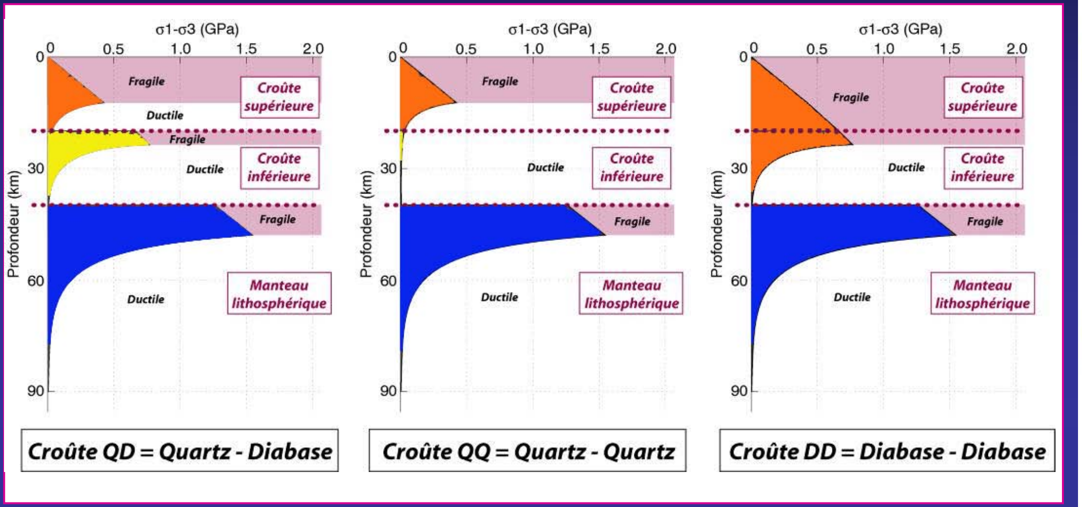

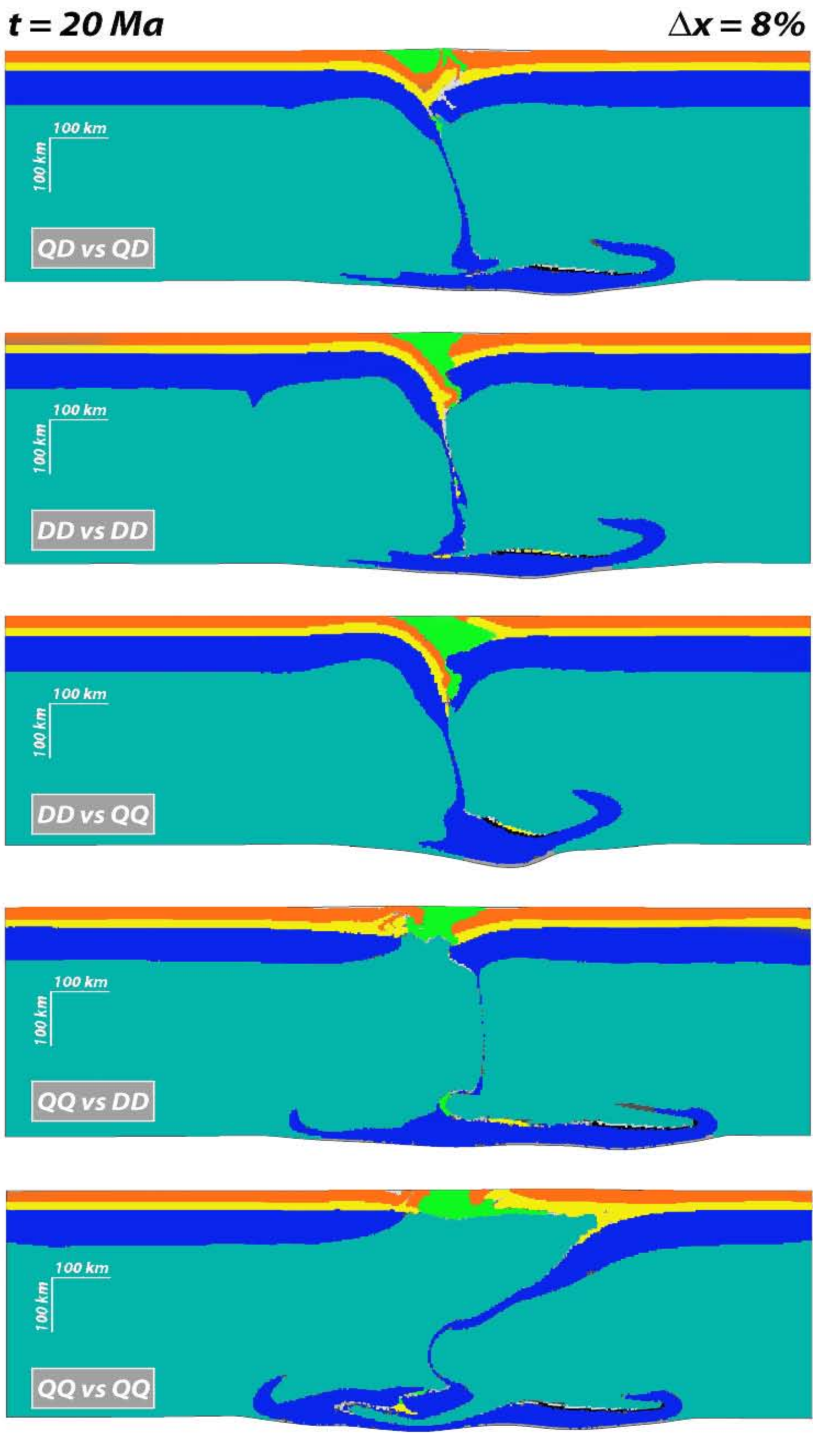

PhD Thesis
Yamato, 2007

Influence of convergence rate

at Δx = 5% **at t = 20 Myr**

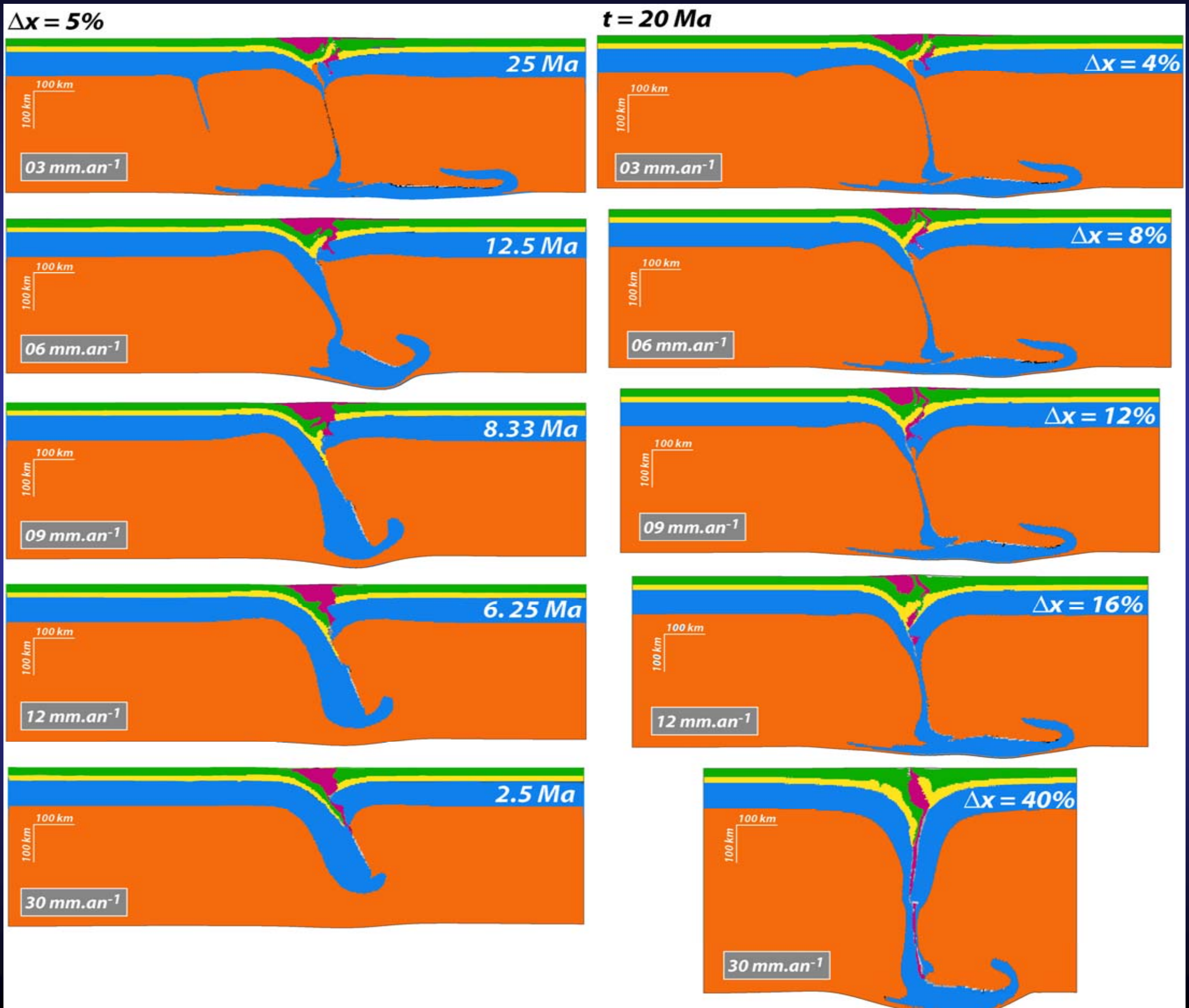

Influence of erosion (*k*) on collision mode

$k = 3000 m^2 y^{-1}$

$k = 1500 m^2 y^{-1}$

$k = 500 m^2 y^{-1}$

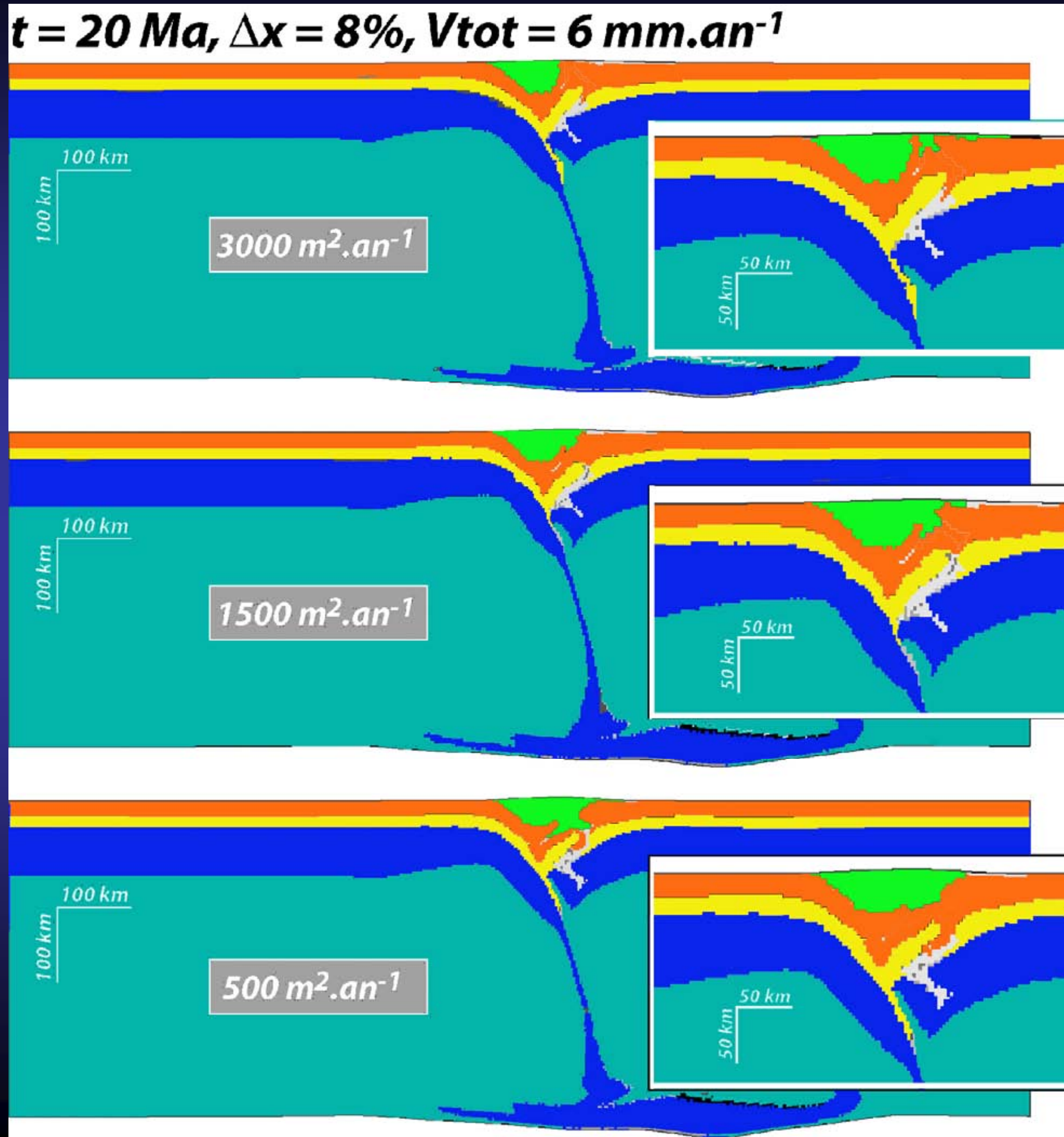

Reference case: evolution details

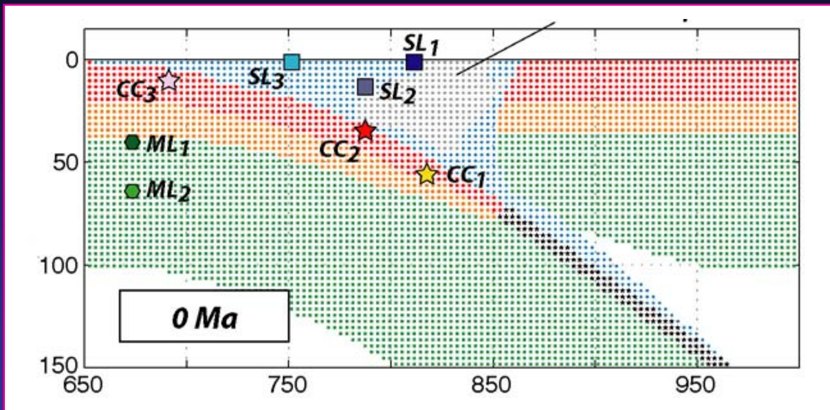

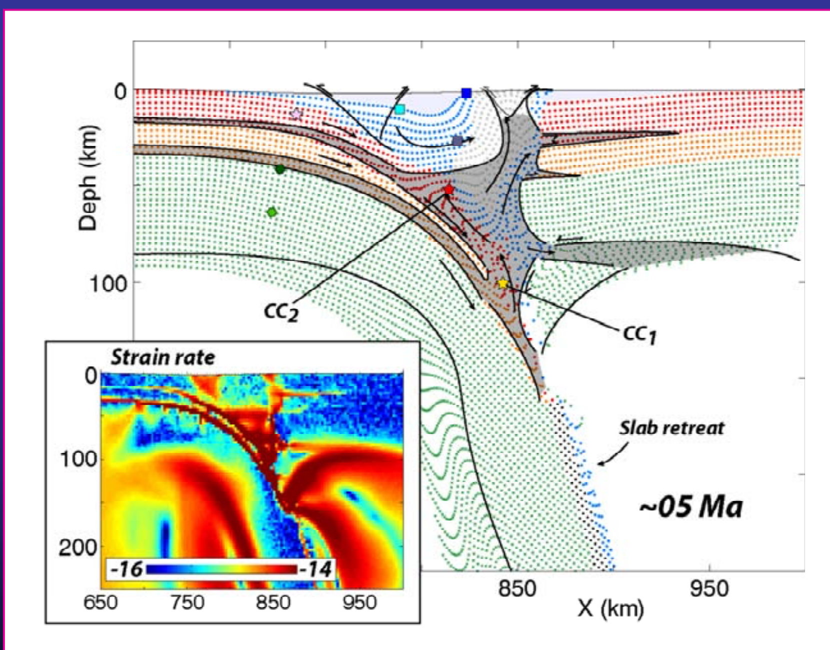

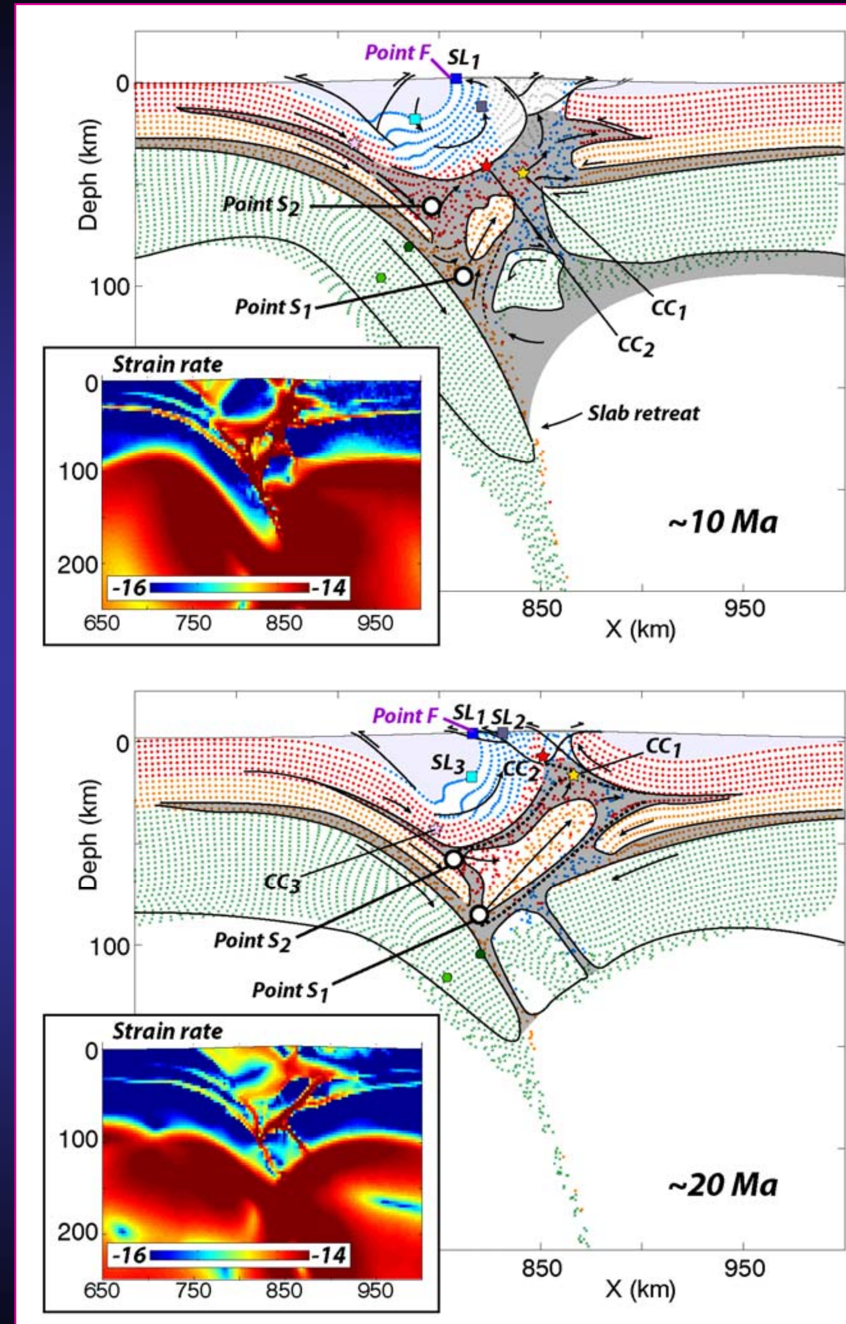

Reference case: predicted P-T-t paths

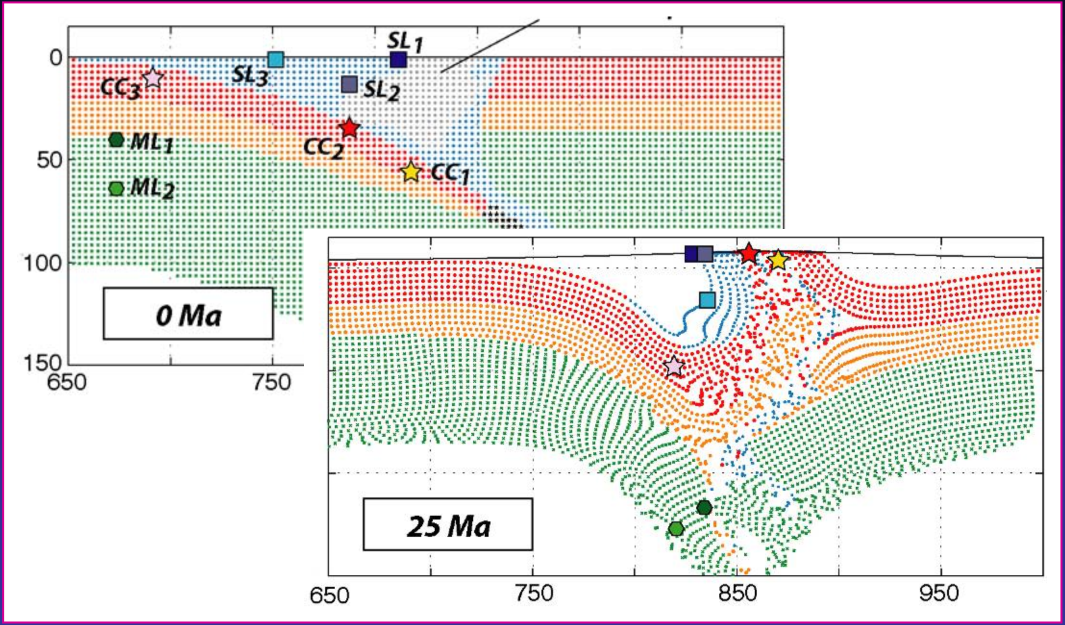

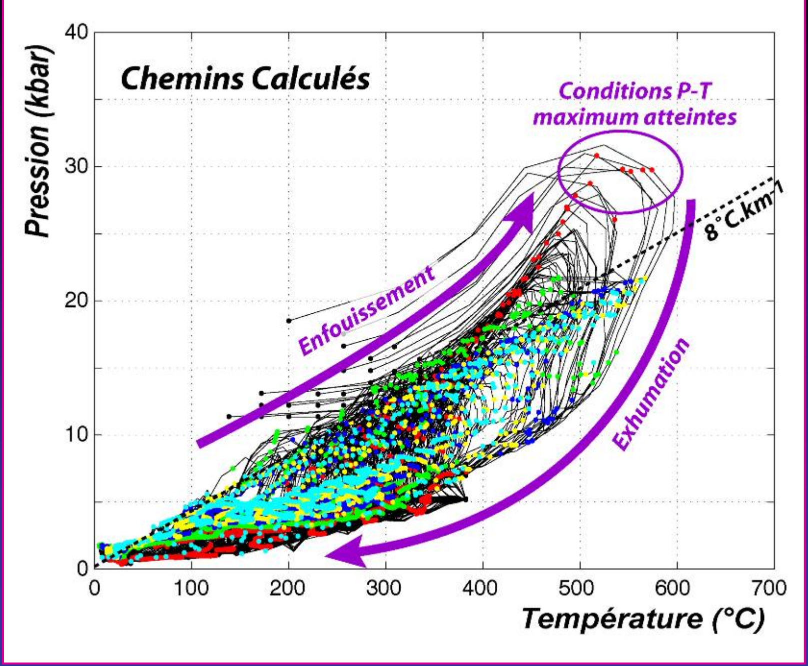

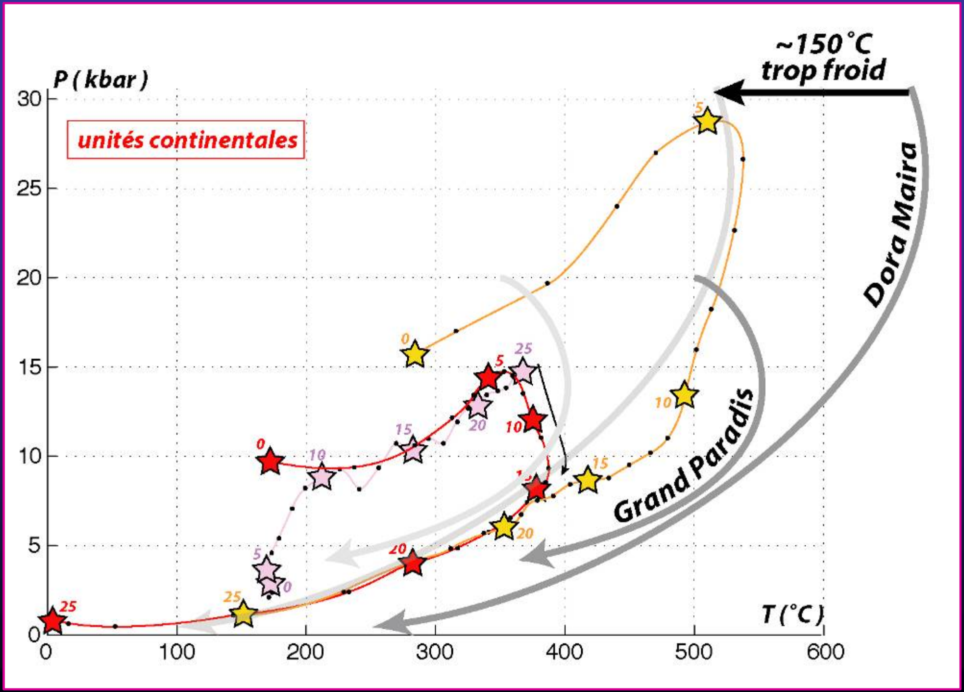

P-T-t Path

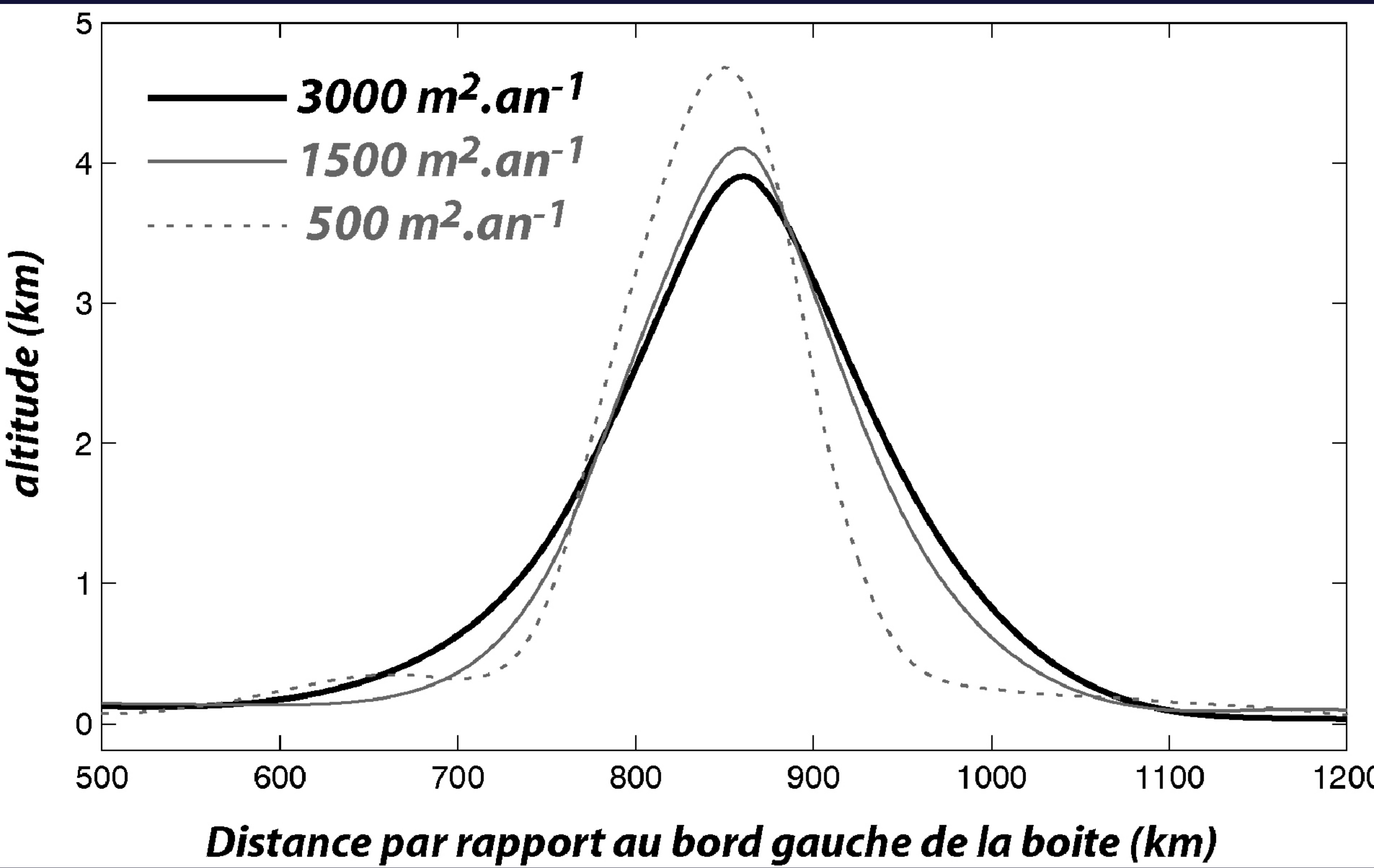

3000 m2.an-1
1500 m2.an-1
500 m2.an-1
altitude (km)
0
1
2
3
4
5
500
600
700
800
900
1000
1100
1200
Distance par rapport au bord gauche de la boite (km)

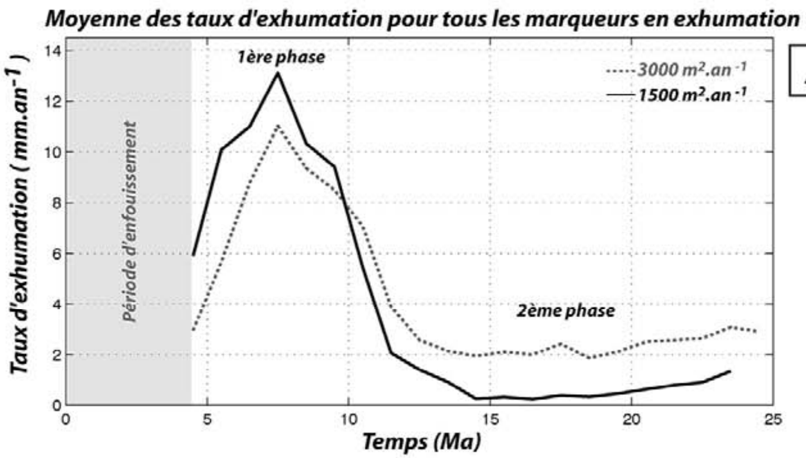

Exhumation rates as function of the erosion rate (first 20 Myr)

Top: markers that have achieved 20-40 kbar and 300-700°C

Bottom: markers that have achieved 10 kbar.

HP

LP

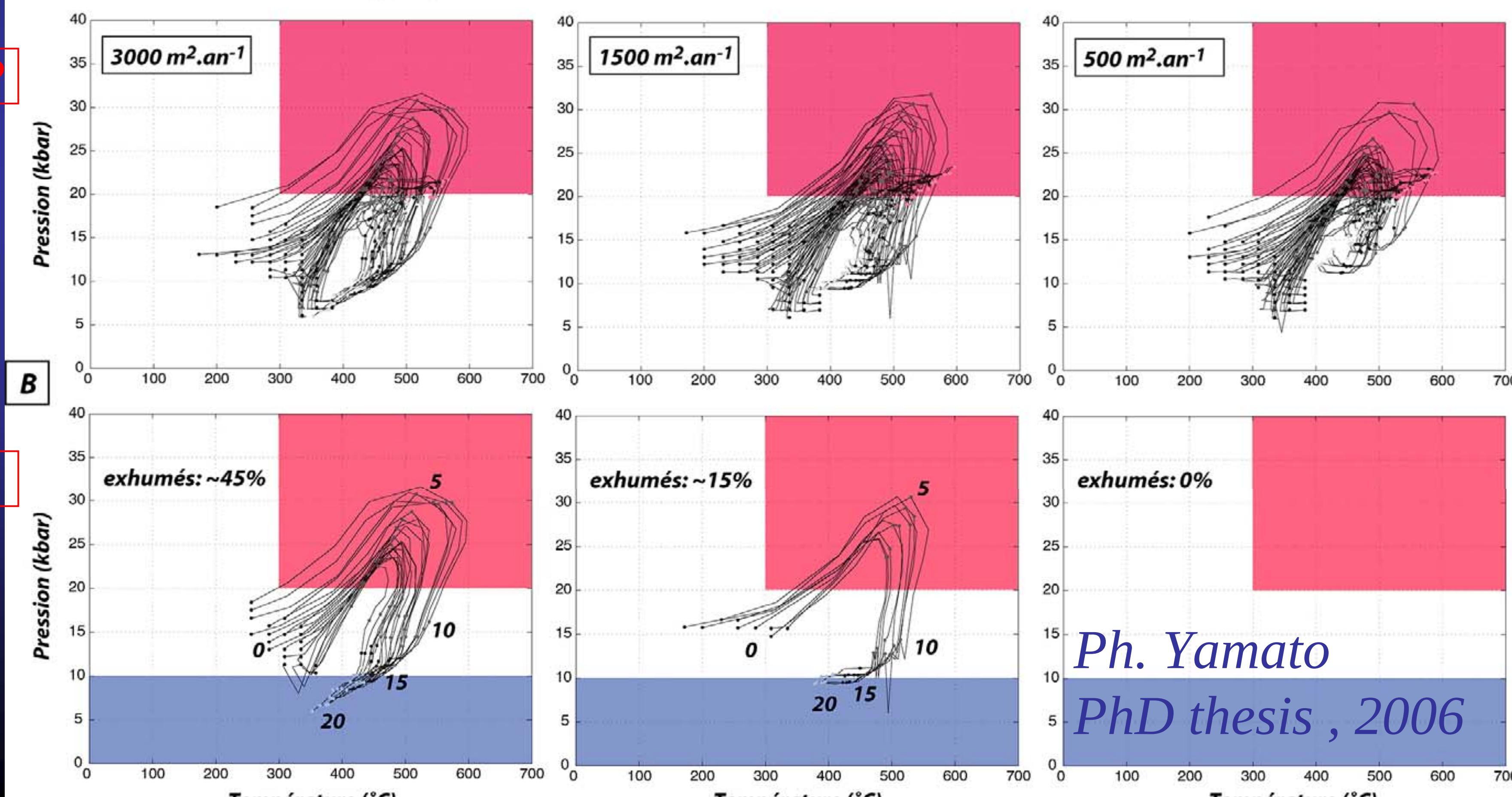

Ph. Yamato

PhD thesis , 2006

Summary of the parametric study of slow continental convergence

→ 3 major parameters

- Convergence rate
- Erosion
- Rheology of the continental crust

Effect of the convergence rate

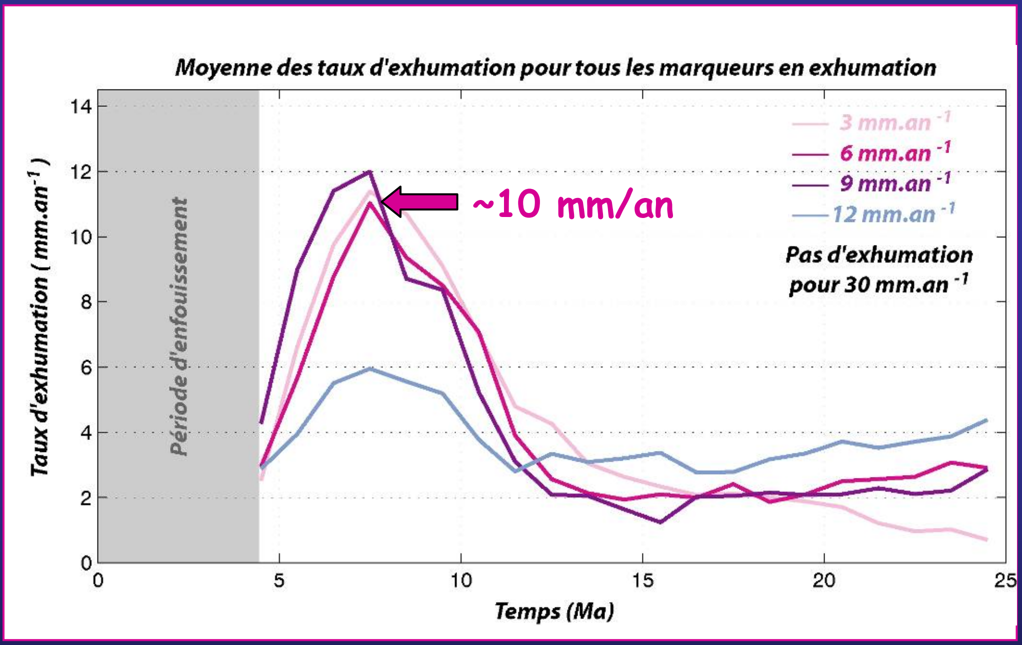

Effect of erosion

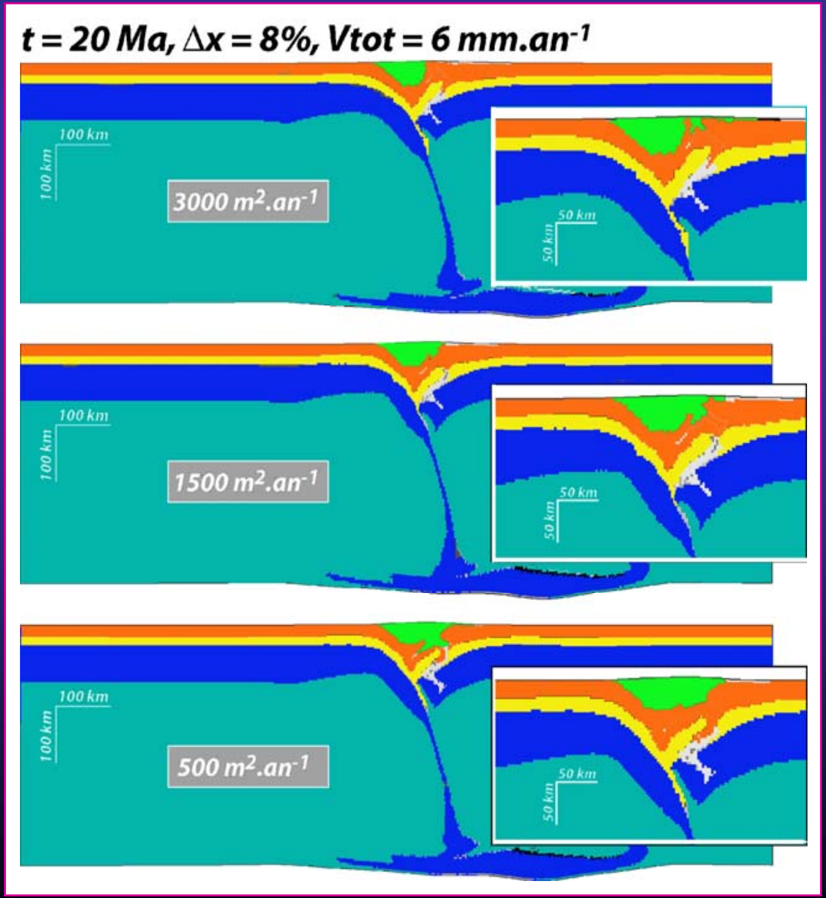

Yamato, 2007

Burov and Yamato, 2007

Oceanic versus continental subduction

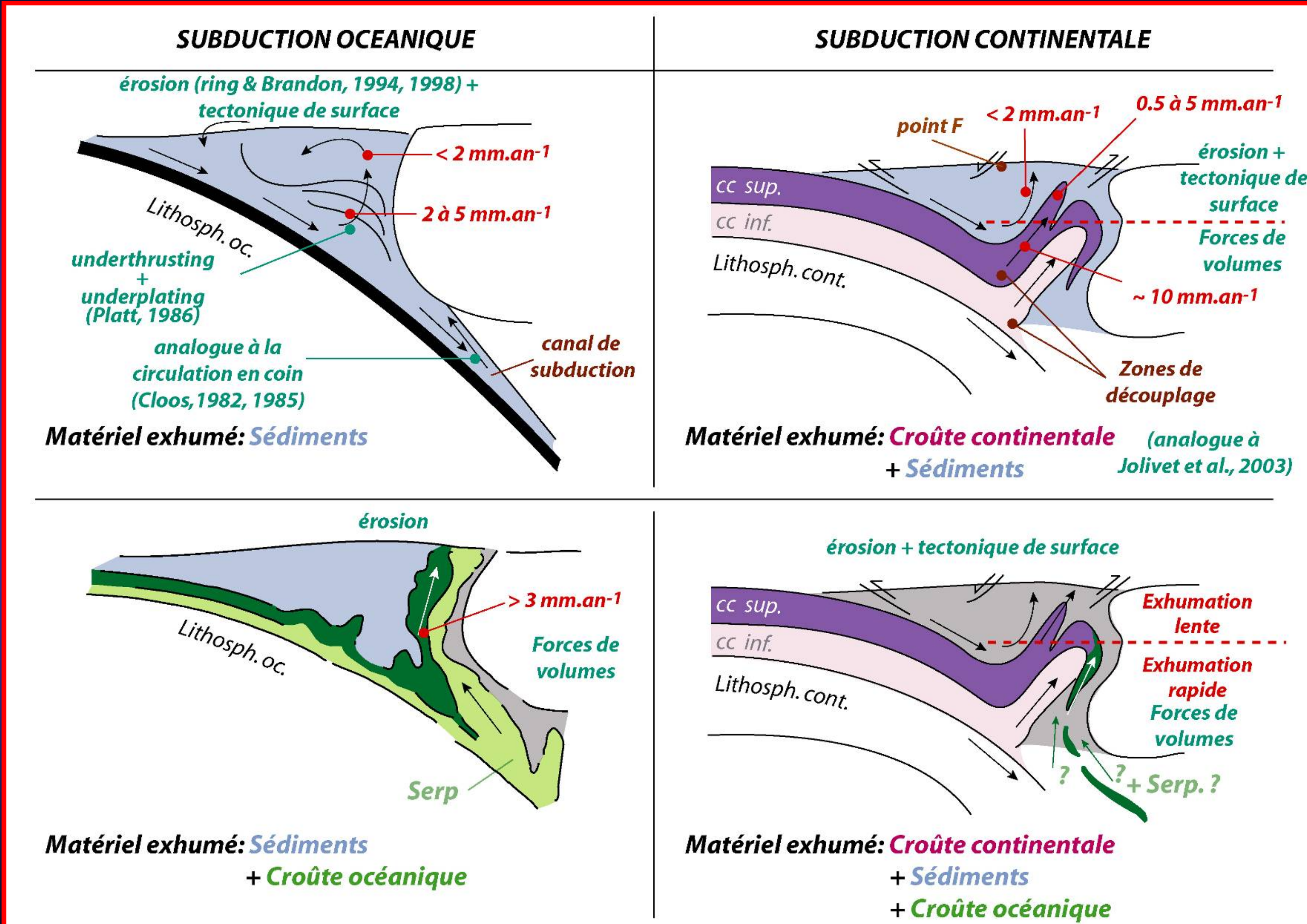

Some Perspectives

- Detailed study of impact of fluid circulation +
- P-T impact on rheology + melting + latent heat production.
- Parametrization of shear heating. Rheology of aggregates

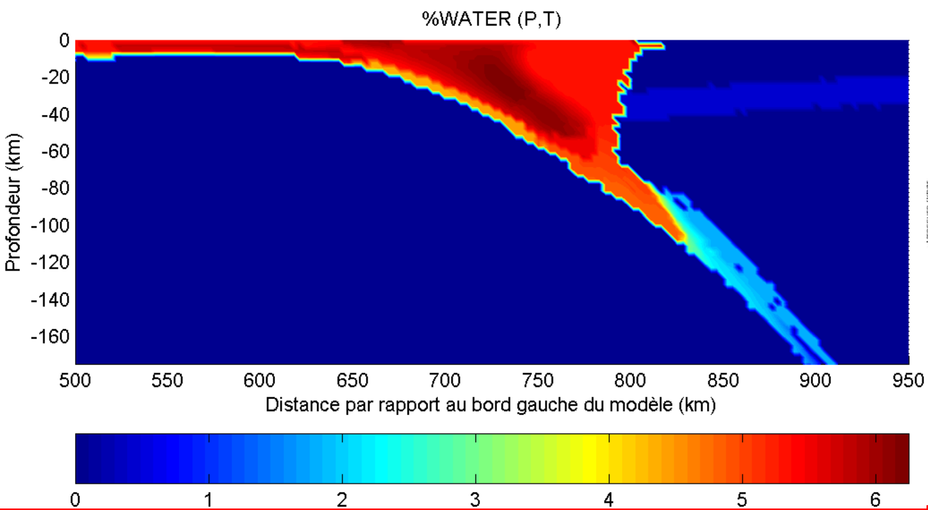

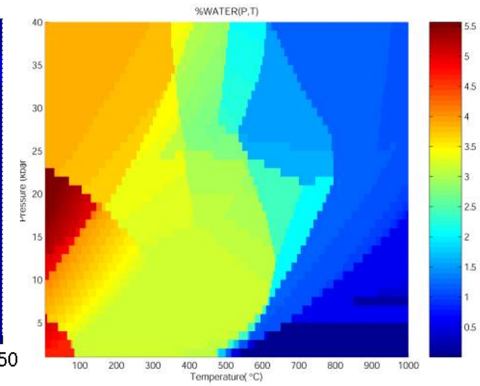

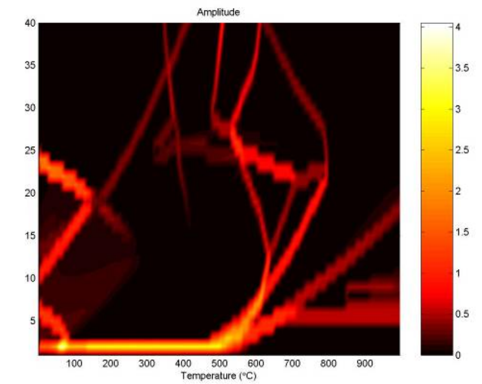

- Some new problems: obduction

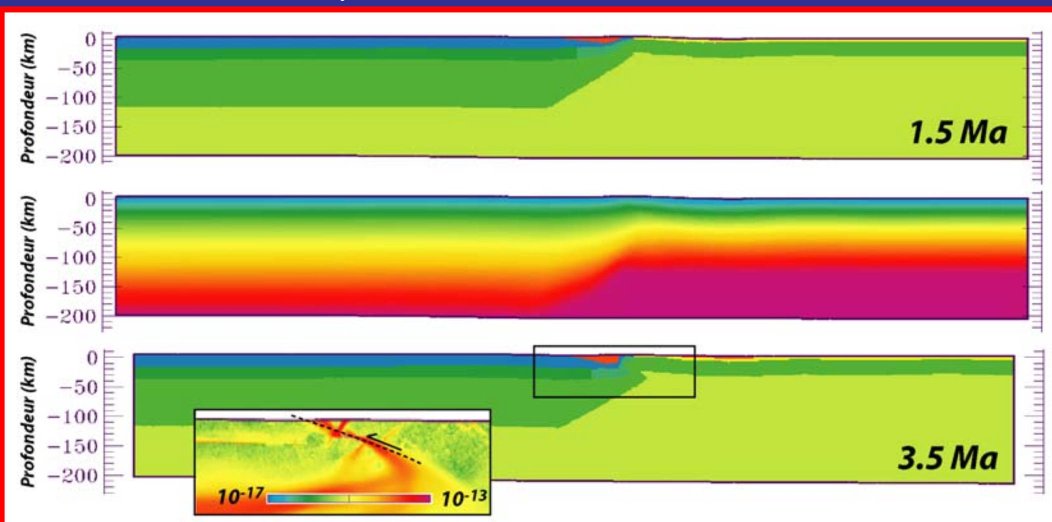

... and 'exhumation !

SUMMARY

- Viscous-elastic-plastic rheology and rheological structure (not simply integrated strength) of both convergent plates is of crucial importance. Some commonly inferred (from rock mechanics) rheological profiles are mechanically prohibited (e.g., CB): possibility to constrain rheology from models !

- Models need to reproduce in sufficient detail a wealth of the observed features such as accretion prism and topography evolution, fault distribution, sedimentary mass balance, P-T-t paths for the exhumed rock, surface heat flow, present day seismic velocity structures etc. Structural and P-T-t data become VERY important constraints on the models.

- Convergence rates < 1-2 cm/y or > 10 cm/y are incompatible with subduction mechanisms. Continental subduction is a short-lived stage (1-5 My for the Alpes, 15 My for India) of continental convergence. For oceanic subduction, fluids (serpentinization) condition stable asymmetric subduction.

- Topography, but also DEEP subsurface evolution strongly depend on dynamic interplays between subsurface and surface processes

- Need to account for deep mantle dynamic (and phase transitions) at list down to the depth of 650 km

- Phase transitions and evolution of the mechanical properties of rocks as function of P-T and fluid content need to be taken into account (next challenge !)

SUMMARY

- In difference from oceanic subduction, continental subduction requires far-field forcing and is strongly conditioned by rheological structure of the lithosphere. Strong mantle lithosphere and high initial convergence rate (> 2x1.5 cm/y) are the primary conditions for continental subduction.

- Evolution of collision zones depends on the rheology and crustal thickness of both, the upper and the lower plate.Crust-mantle decoupling in the subducting plate may drive crustal thickenining in the upper plate.

- Crustal material may be drawn to 100-150 km depths - the HP-UHP exhumation mechanisms are different for different convergence styles and rates - Structural and P-T-t data become important constraints on the models

- Fast convergence rates (e.g., 5 cm/y, Himalaya) favour polyphase evolution with *several episodes of crustal prism evolution and exhumation.*

- In real world, slow-down of the convergence rate during collision should play a primary role for exhumation and further evolution of collision

- Topography, but also DEEP subsurface evolution strongly depend on dynamic interplays between subsurface and surface processes